Past natural and anthropogenically altered sediment flux in the Spessart mountains – a central European landscape

Dissertation

zur Erlangung des Doktorgrades

der Mathematisch-Naturwissenschaftlichen Fakultät

der Christian-Albrechts-Universität zu Kiel

vorgelegt von

Annegret Larsen

Kiel, 2011

Dekan: Prof. Dr. Lutz Kipp

Referent: Prof. Dr. Hans-Rudolf Bork

Korreferent: Prof. Dr. Klaus Dierßen

Prüfer: Prof. Dr. Ulrich Müller

Tag der mündlichen Prüfung: 3.2.2012

Zum Druck genehmigt: 3.2.2012

EIDESSTATTLICHE ERKLÄRUNG

Die vorgelegte Arbeit ist nach Inhalt und Form meine eigene, abgesehen von der Beratung meiner Betreuerinnen und Betreuer. Der vorliegende Text wurde nicht und auch nicht zum Teil einer anderen Stelle im Rahmen eines Prüfungsverfahren vorgelegt, veröffentlicht oder zur Veröffentlichung eingereicht. Diese Arbeit wurde unter Einhaltung guter wissenschaftlicher Praxis nach den Regeln der Deutschen Forschungsgemeinschaft erstellt.

Annegret Larsen

ABSTRACT

The Late Quaternary surface processes of a steep gully system in Central Europe occur mainly as multiple gully erosion and sedimentation cycles. These cycles depend largely on the relation between sediment supply and sediment transport capacity. The gully thalweg was aggraded during the Younger Dryas as a result of high sediment supply from the slopes and a diminished transport capacity in the channel instigated by a reduction in vegetation during this time. For the majority of the Holocene time period phases of headward gully incision are the dominant process, which occurs as a result of internal hydrological and geomorphic thresholds under well vegetated conditions. During this time sediment was also deposited on the gully fan. The onset of intense human agricultural activity during medieval times led to large scale slope erosion due to vegetation removal and subsequent thalweg re-aggradation. In comparison with the natural hillslope sediment flux during the Younger Dryas, erosion from human driven slope instability was found to be at least ~2.3 time more efficient. More specifically, it is clear that different land-use techniques on the catchments slopes, as reconstructed from the analysis of soil charcoal analysis, are the dominant control on overall hillslope erosion rates. The lowest erosion rate was found in an area where only small agricultural fields were maintained.

The recovery of most of the catchment vegetation in the last ~ 500 years has re-stabilised the slopes and modified the internal threshold of sediment supply/sediment transport capacity, such that the gully has begun a new incision phase. Hence, sediment is again transported from the thalweg into the gully fan and floodplain of the adjacent trunk stream. The quantification of sediment fluxes reveals that the most recent and continuing phase of sediment export is also the most geomorphically significant for the trunk stream, since it is the only time in the last ~15 000 years that a large percentage of the thalweg erosion budget is able to be incorporated into the alluvium of trunk streams. Because the gully system itself has a large storage capacity, sediment delivery from small headwater catchments to trunk streams generally does not occur until vegetation has re-stabilised the slopes, and allows the sediment transport capacity to increase. The recent changes to high sediment delivery to the floodplain and adjacent stream is a possible explanation for the observed floodplain aggradation of trunk streams and the resulting changes to the rivers regime. However, it is also suggested that valley bottom damming for various purposes throughout this time is also a major factor controlling this large change in the rivers behaviour, and the investigation of this direct human impact on the river landscapes of central Europe is a critical avenue of further research.

Mehrere Erosions- und Sedimentationszyklen haben die spätquartären Oberflächenprozesse in einem Einzugsgebiet eines Gullys in der Mittelgebirgsregion von Mitteleuropa geprägt. Diese Zyklen sind im Wesentlichen vom Quotienten zwischen Sedimentzufuhr und Sedimenttransportkapazität abhängig. Der Thalweg fungierte während der Jüngeren Dryas als Folge der hohen Sedimentzufuhr von den Hängen als Sedimentfalle, da keine schützende Vegetationsdecke die Hänge mehr bedeckte. Während des weitaus größten Teils des Holozäns war das Einzugsgebiet bewaldet und die Hänge daher stabil. Daraus ergab sich eine hohe Erosions- und Transportkapazität des Oberflächenabfluss im Thalweg und die daraus folgende Rückverlagerung des Gully-Kopfes, was widerum eine Ablagerung von Sedimenten im Bereich des Schwemmfächers zur Folge hatte. Der Beginn intensiver ackerbaulicher Tätigkeiten im Mittelalter führte durch die großflächige Bewirtschaftung der Hänge zu Hangerosion und zu einem erneuten Anwachsen der Thalwegsedimente. Die Menge des im Mittelalter erodierten Hangmaterials überstieg den der Jüngeren Dryas um den Faktor 2.3. Detaillierte Analysen von Hangsedimenten und den darin enthaltenen Holzkohlen zeigt, dass verschiedene Formen der Landnutzung unterschiedlich hohe Erosionsraten verursachten, mit dem geringsten Hangabtrag in den Bereichen, in denen kleine Feldgrößen vorherrschten. Die Wiederbewaldung des größten Teils des Einzugsgebiets vor ca. 500 Jahren stabilisierte die Hänge und führte zu einer erneuten Einschneidungsphase des Gullies, was erneuten Sedimenttransport zum Schwemmfächer und in den Vorfluter und dessen Aue zur Folge hatte. Die Quantifizierung und Bilanzierung des Sedimentflusses zeigt, dass dies die einzige Phase in den letzten ~ 15000 Jahren war, die den Transport einer geomorpholgisch relevanten Menge von Sedimenten in den Vorfluter verursachte, welche vom Fluss aufgenommen und in die Auelehme eingearbeitet wurden. Dies ist ein möglicher Grund für das beobachtete Anwachsen der Auelehme, aber auch Talverbauungen wie Mühlwehre spielten vermutlich eine große Rolle. Die Erforschung dieses direkten Einflusses des Menschen auf die Flusslandschaften ist ein Forschungsprojekt, das aus der hier vorliegenden Arbeit hervorgehen kann.

KEYWORDS

gully, sediment transport, sediment flux, quantification, land-use, mill-dams
Gully, Sedimenttransport, Sedimentfluss, Quantifizierung, Landnutzung, Mühlwehre

ACKNOWLEDGEMENTS

The possibility that I got a scholarship to write a PhD-thesis in Kiel about the Spessart mountains, my beloved home area, in the framework of this new Graduate School, with so many PhDs that became good friends, was not only incredibly lucky, it was also governed by my supervisor, Hans-Rudolf Bork. I first of all have to thank him that he accepted my application and then turned the project that I proposed into one that was manageable, even though as a result I had to spent three years on 42 ha. This was not always fun, especially for the poor catchment, which is now basically perforated like swiss cheese, and for which I herewith apologise. After these three years, I am convinced that in terms of understanding the processes, this was the best education one can get as a geomorphologist. Hans-Rudolfs enormous knowledge and his endurance in field work and his talent to motivate makes him an excellent teacher, thank you very much. Furthermore, there are all the people who helped me in the months of field work and beyond: Mathias Bahns, thank you for your flexibility, constant good mood, taking over the root-cutting and just forget when I was a stressed and didn't strike the right note. The same thank goes to my RISE-student Nicole Bilsley, an incredibly enduring person - you were a huge enrichment for the team, and thank you for constantly calling me "boss", which was very euphemistic. Thank you also to Sophia Dazert, Markus Schütz, Isabell Raschke and Lauren Herwehe in supporting the lab and also field work. A very special thank you goes to my charcoal trainers: first of all the Ingelise Stuijts, Oliver Nelle, Doris Jansen and Vincent Robin, I apologise for my thick-wittedness. Vincent is also thanked for being such a good colleague and friend, I hope we can continue cooperation. Christoph and Markus Steffen have been helping with GIS, and also Rouven Schneider, whom I also want to thank for his friendship. Annika Mertens dated the ceramic fragments, thank you for that, and Wiebke Kirleis for the analysis of the macro-remains! To have a reliable person who dates your OSL-samples is worth more than gold in such a work, and this was done by Alexander Fülling, who also helped with field work and brought a bunch of Berlin students to the rainy and cold Spessart. The Archaeological Spessart Project is thanked for the possibility to let me dig three trenches in their excavation area. My co-authors Tobias Heckmann, Alexander Fülling, Vincent Robin and Markus Fuchs are thanked for their valuable comments and support with the data analysis. From an organisational point of view the Graduate School team must get a big award, especially Mara Weinelt and Rhina Colunge, for their professional and personal support during these years of exploring the university structure and the forms being related to it. I know it must be hard to understand why one always fails to put all signatures on a Dienstreiseantrag. A very big thanks goes to the village Heimbuchenthal, which supported me so much with labour and machines. In particular, Christoph Brand (the best excavator-driver in the world), Rüdiger Stenger and

Wolfgang Bauer, without whom this research like it is presented here, would have been never so detailed. And also, it would have been not possible without the support and patience of my family and Heinz Schädle, who besides of all other things, gave me their clean cars and got them back dirty, had to move soil samples in the shed to reach their own things and even suffered from a medieval latrine sample in their freezer for a few months. I cannot thank Uta Lungershausen enough at that place, for all the little and big things she did for me, she is just the living evidence that basically all you need is a real friend. And then, finally, there was the help of Josh Larsen, who supported patiently the whole process of data analysis and writing, was never tired of trying to understand what I mean, and deleted all my precious details (and corrected my germenglish) to make it (hopefully) readable and understandable for the rest of the world, and tortured my brain with constant questioning about the relevance of my research. Josh, without you this would have really been never possible. Thank you so much for all your help – and for making this world and life a much, much better place, at least for me.

TABLE OF CONTENTS

LIST OF FIGURES

the gully thalweg, black circles the approximate location of the gully head at distinct time period based on the chrono-stratigraphic evidence. Details of each phase are discussed in the text.

Figure 12: (a) Assumed ratio between sediment supply (SS) and sediment transport capacity (ST) in the gully thalweg during the Late Quaternary. The light grey line shows an idealised stochastic variation of this ratio about the mean (blue line). Black circles indicate gully head retreat events, and the star marks the timing of the only recorded Holocene debris flow event. Numbers indicate five phases in which the ratio shows a particular pattern: 1 = effective sediment transport connectivity; 2 = 1st fill-phase; 3 = 1st incision-phase; 4 = 2nd fill-phase; 5 = 2nd incision-phase, and correspond with phases to those in Figure 11.
(b) River erosion and deposition phases in Central Europe after Schirmer (1991) and Schirmer (2007). Phases dominated by deposition are interpreted by Schirmer (1991) as periods of relative morphological stability, whereas those dominated by erosion, also described as "breaks", are interpreted as active phases.
(c): Lake levels from Southern central Europe (French and Swiss Jura mountains) after Magny (2004). High lake levels are interpreted as wet climatic phases, and low lake levels as dry climatic phases.

Figure 13: Location and map of the research area projected on the 1 m digital elevation model (DEM) (© by Bavarian Survey office Munich, 2011)

Figure 14: Predicted thickness of the Holocene colluvial layer in the Kirschgraben catchment area. The points at the locations of corings and excavations (n=183) indicate under- and overprediction by the UK model as calculated using leave-one-out cross-validation.

Figure 15: (a) boxplots of the distributions of measured (n=183 data points) and predicted (n=6254 raster cells) thickness of the Holocene colluvial layer. (b) The box forms the interquartile range (q75-q25), with the thick lines indicateing the median value. The whiskers extend 1.5 times the interquartile range, and data exceeding this range (outliers) are plotted as single points. (b) Measured vs. predicted thickness at 183 data points (corings, excavation sites) produced by leave-one-out cross-validation. The continuous line represents a 1:1 fit of predicted and measured data, the dotted shows the simple linear regression.

Figure 16: Cross-section through the gully thalweg sediments (modified from chapter 6)

Figure 17: DEM extracted cross-sections through gully thalweg showing remnant deposits

(upper graph). Field investigations (lower picture) showing those sediments on the left side of the photo to have been influenced by Late Pleistocene solifluction, and typical Holocene colluvial type deposits on the right. The bolder in the foreground indicates the erosional base of this part of the gully.

Figure 18: (a) Cross-section through the gully fan (modified from chapter 6). Dashed lines indicate the estimated prediction of the sedimentary layers based on a regression of the existing topographic surface. (b) Schematic illustration of the quantification procedure of the fan based on an idealised geometry

Figure 19: Schematic Holocene sediment budget for the Kirchgraben catchment in Central Europe. Numbers represent the phases detailed in Table 5. The solid line indicates approximate changes in the talweg sediment storage.

Figure 20: (a) Map of the Kirschgraben catchment within the Spessart mountains of Central Germany (inset). (b) Historical map of the research area from 1850 AD.

Figure 21: Exposures of hillslope sediments (a,b,c). Longitudinal and valley cross-sections extracted from the DEM. Locations are shown in Figure 20a.

Figure 22: Percentage (wt %) of wood species from the charcoals fragments in each layer. The labels refer to the segments in Figure 21.

Figure 23: The birch-forest cultivation technique. Modified from Walentowski (2001)

Figure 24: (a) Percentage of sand in sediment < 2mm. Labels refer to Figure 21. (b) percentage by weight of all pioneer wood species from the analysed charcoal fragments

Figure 25: Left: Map of Spessart Mountains; right**:** Map of Central Europe (with rough location of the research area)

Figure 26: “Pfinzing” Spessart-map from 1594 (map is orientated with west to the top). The enlarged window shows the details of the mapped riverscapes: M2 describes a mill site (and subsequent valley bottom damming in that area).

Figure 27: Extract from the Bavarian “Urkatasteraufnahme“ referring to a part of the Elsava River floodplain. It shows a detailed mapping of dams (indicated by blue arrows). These maps

are available for the whole research area and provide the location of all dams existent around 1840 AD (depending on the year of mapping of the individual map). Scale: 1:25000.

Figure 28: Geomorphometric analysis based on a DEM of the Elsava River (catchment area and curvature analysis).

Figure 29: Excavation site HB SIII_N. The blue line indicates the channel deposits. The yellow line shows the lower border of the wetland soil. The OSL sample was taken from a sand lens in the angular gravel fan deposit that intersects with rounded gravel channel deposits. We have evidence from stratigraphic analysis that legacy sediments are common in this region and that the flow regime of the Elsava River has changed substantially. Approximatly 30 m upstream of a medieval mill site we excavated a 35 m long and 4 m deep trench in the gully fan and floodplain sediments. We chose an area where the riverbed is confined by the fan sediments on one side and a valley with steep slopes on the other side. The site has been stratigraphically logged and analysed in detail (see Appendix 4). In the alluvial sediments, enlarged in the figure above, we find a partially stripped black wetland soil unconformably overlying sandy-gravely river bed sediments. The next phase of deposition was river channel sands and gravels and associated silty overbank deposits. The hydromorphic superimposition (orange/black colours) is due to rsing ground water levels, most probably as a result of subsequent damming. This sequence is topped by an accumulation of gravel (presumably from the gully fan), and was closely followed by a fine layered flood loam deposit that intersects with the fan sediments, and forms the focus of this study.

LIST OF TABLES

1. INTRODUCTION

Agriculture is the spatially largest land-use on the planet and the most important in terms that it provides the base of all human living. Unfortunately, its influence on the soil on which it depends is high and it is obviously crucial to investigate these influences, because the world still feeds on food, not oil. Besides influences on the soil chemistry, a major problem in terms of sustainability caused by agricultural is an acceleration of soil erosion – and has been a problem since agricultural techniques spread widely in Neolithic times. Additionally, soil erosion is in most of the cases a slow process and difficult to observe in a life span of a human being, and therefore often beyond our perception. Hence, to investigate this topic and to finally create and define a sustainable agriculture, longer time periods must be analysed.
Soil erosion influences not only the hillslopes on which agricultural land-use causes erosion, the eroded sediment also accumulates in the geomorphic system, and causes feedbacks and changes internal thresholds. The results of this change are very hard to assess or predict and have long-term effects on the environment, even when agriculture was already abandoned for a long time. These off-site damages are often studied in floodplains, where additional sediment load originating in deforestation and agriculture, its deposition and hence the change in sheer stress might have caused a fundamental change of the rivers regime. After thousands of years of agricultural land-use, the question arises, if at least in the mid-latitudes, human influence has already completely masked historically distinctive river forms? Besides the academic interest, the reconstruction of "natural" rivers is the basis of river restoration and management. The Water Framework Directive, a river restoration program from the EU, is designed to result in a European-wide restoration of mainly low-order streams. The landscapes in the headwaters of big river systems are especially sensitive to human impact, mainly because they can be more easily re-engineered to suit industrial or agricultural needs. Besides intensive soil erosion on the slopes delivering sediment to the main channel, streams were also commonly altered by the construction of mill-dams probably from medieval times onwards. Astonishingly enough, these landscapes are today considered to be "natural" and one example of this being the streams of the Spessart mountains. This thesis examines these problems in greater detail within the context of results from a small catchment while also contributing to the broader issues surrounding the impact of humans within the landscapes they occupy.

2. AIMS AND OBJECTIVES

This thesis investigates sediment fluxes through the detailed analysis of a single catchment. The rational for this approach is that the interpretation and analysis of sediment flux from hillslopes to the floodplains requires fundamental research on the relevant geomorphic processes and their interactions. Therefore, this research seeks to understand the timing, causes, effects, and quantity of sediment transport from the headwaters of a first order catchment to the floodplain of the adjacent trunk stream. In order to understand these processes, a range of related questions concerning vegetation cover and composition, and land cultivation techniques also need to be investigated. Generally, the transfer of sediments from the catchment headwaters to the floodplain of trunk streams or their termination in lake systems also determine exactly what is available to be recorded in environmental archives. This study therefore also compares catchment and floodplain records with those available environmental archives in order to assess how they are related, and if general trends in climate or human impact can be discerned.

The structure of this thesis is designed so that major questions concerning the topics discussed above are presented in chapter 3. Chapter 4 focuses on the detailed description of the research area in focus, and chapter 5 considers the analysis of landscapes within the general concept and framework of the research presented in the later chapters.

Chapter 6 aims to understand the transfer of sediment from the slopes to the floodplain in a small first order catchment, and has been submitted to the journal *Geomorphology* for peer-review. It also investigates how humans have influenced erosion and what role changes in vegetation cover played in the development of the surface and their broad impact upon the natural dynamics in the system. A final consideration of this chapter is also to ask how reliable commonly used sedimentary archives are as consistent indicators of change in climate or land use given the large potential lags in the sedimentary system.

In order to enable the comparison of sediment flux between catchments, actual quantification of eroded and deposited sediments is necessary. The objective in chapter 7, which is submitted to the journal *Geomorphology*, is to determine the sediment mass balance between inputs and outputs to the gully thalweg channel system. This mass balance, or sediment budget, provides interesting contrasts over the Holocene, and allows a direct comparison between climatically driven slope instability phases with those driven by human impact. Finally, this chapter aims to determine which gully erosion phases contributed significant sediment to the adjacent trunk stream and its floodplain.

Chapter 8, a manuscript soon to be submitted to *The Holocene*, aims to find out how land-use changed in time in the research area and how these changes affected past hillslope erosion processes. This interdisciplinary study aims to combine the reconstruction of past vegetation cover by wood species analysis from sediment charcoal fragments with the reconstruction of past sediment flux using the same sedimentary archive. This study also addresses the question of sustainable land-use techniques in the past

The research presented in the previous chapters build the base for the research outline in chapter 9. This future project aims to analyse and quantify human influence on low order streams and their floodplains. Besides the increased sediment flux caused by deforestation and agricultural land-use, it focuses on the influence of medieval and modern valley bottom damming in the Spessart mountains. This study proposes this damming was also a critical mechanism for the effective trapping of this increased sediment load, and that not only the increased sediment delivery from deforestation and agricultural land-use was not the only cause. It also aims to determine the onset and magnitude of this first impact of humans on riverscapes as a result of valley bottom damming, and examines the management implications.

3. STATE OF THE ART

3.1 Soil erosion under human influence: deforestation and agriculture

According to the Food and Agriculture Organization (FAO) of the United Nations, croplands cover 1.53 billion hectares (about 12% of Earth's ice-free land), while pastures cover another 3.38 billion hectares (about 26% of Earth's ice-free land). Altogether, agriculture occupies about 38% of Earth's terrestrial surface, the largest use of land on the planet. These areas are located on the land best suited for farming, with much of the rest is covered by deserts, mountains, tundra, cities, ecological reserves and other lands unsuitable for agriculture (Foley et al., 2011). Spatially, agriculture is therefore the most important economic factor in the world.

Unfortunately, its influence on the soil on which it depends can also be detrimentally high. Besides influences on the soil chemistry, a major problem resulting from agricultural land-use is soil erosion – and has most likely been the case since agricultural techniques spread widely in Neolithic times. The earliest soil erosion rates were measured in the US in the 1930s, which subsequently decreased due to soil conservation methods and then are supposed to have increased again since the 1970s (Trimble and Crosson, 2000). On this topic almost all studies have suggested that soil erosion is an extremely serious environmental problem, if not a crisis (Pimentel et al., 1995). Billions of dollars have been spent for conservation methods, often without sufficient field evidence, because most of the studies are based on generalised models. Soil erosion models have been largely developed on basis of the USLE (Universal Soil Loss Equation) or SDR (Sediment Delivery Ratio) (Trimble and Crosson, 2000). While models based on the USLE estimate the movement of sediment on the fields (and not the loss of soil), those based on the SDR estimate in a simple empirical way sediment yield as a function of catchment area. The processes behind these empirical relationships are poorly understood and its validity questioned (de Vente et al., 2007). This is most likely because we lack the necessary field data, and the possibility that much of the sediment stays close to its source and is not transported further downstream, is very often not recognised. Therefore, studies suggesting high sedimentation rates downstream from anthropogenic accelerated soil erosion in upland areas remain difficult to justify (Montgomery, 2007). The investigation of the set of processes linking erosion in upland areas with sediment delivery downstream ideally requires the construction of a sediment budget (Trimble and Crosson, 2000). This budget accounts for the input, transport, storage, and export of sediment from a geomorphic system, and also strongly depends on the timescales of investigation. Since the 1960's sediment budgets have become an established method of investigation, and are used to address the landscape-scale effects of land-use (Reid and Dunne, 2003). Sediment budgets

over a Holocene time span have become increasingly important within geomorphic studies in Central Europe (Fuchs et al., 2011; Houben et al., 2006; Stolz, 2011), especially since advances in dating methods which have enabled the absolute dating of sediment layers in catchments (Brown et al., 2009). Trimble's study in the US-american Coon Creek catchment remains the standard for research on past sediment budgets (Trimble, 2008). Trimble (2008) was able to use past channel measurements, observations and historic photographs in a detailed geomorphologic analysis with excellent chronological control, unfortunately such data is rarely available for most of the world-wide catchments. In order to extend the times scales addressed by Trimble (2008), an alternative approach to utilises all available sources of information about past land-use and surface processes contained within the sedimentary record. Previous non-quantitative studies which examine past soil erosion in Central Europe date back to the 1930s and were carried out predominately by historians and historical geographers. Bork (1983) established a quantitative approach towards past soil erosion analysis. Since this work, numerous studies have been carried out, also in combination with archaeological and historical research (Bork, 1998; Dotterweich, 2008; Niller, 1998). Following these studies, Bork (1998) developed a conceptual model about the long-term interaction between past soil erosion and land-use change (Figure 1). The model assumes

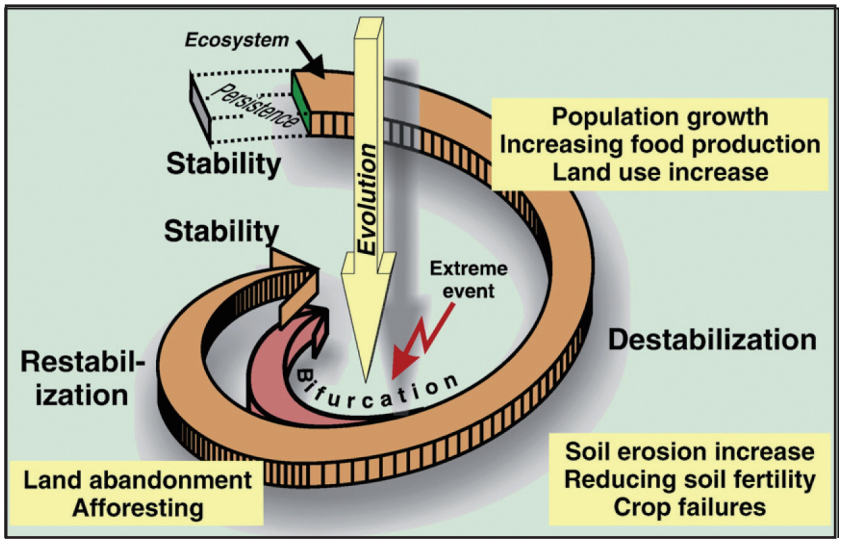

Figure 1
A conceptual model for the long-term interaction between soil erosion and land-use change (Dotterweich, 2008 based on Bork, 1998)

that under natural conditions many rates of geomorphic processes are slowed by vegetation, with the exceptions of riparian systems, coastlines, and alpine systems. The majority of Central Europe maintained relatively stable natural catchment processes since the beginning of the Holocene, and were therefore ideal conditions for land-use. With the subsequent deforestation and onset of agricultural land-use, water, nutrient, and sediment fluxes in most catchments changed, soil development modified, and the risk of soil erosion increased. Due to these increased fluxes, the catchments, and in particular hillslopes, become more unstable until a certain threshold is reached, and from which erosion events can have a catastrophic

effect. After such an event a new equilibrium is established, land is sometimes abandoned due to its loss in fertility, and more or less naturally driven processes return to dominate the system (Dotterweich, 2008).

3. 2 Investigating past soil erosion

To investigate past earth surface processes, three main archives are available: 1. sediment archives (geo-bio-archives), 2. written and painted sources, and 3. historical measurements (Bork, 2006). For this study, old maps and written sources were first consulted, however, the bulk of the analysis resides within sedimentary archives, including bio-archives (soil charcoal fragments), since they preserve a local Holocene vegetation record. The analysis and material methods used in this study vary between chapters and so are described separately in each chapter. An overview of typical sedimentary archives preserved in a cascade system are shown in Figure 2, and from which truncated soils, colluvial sediments (including gullies and their fans) and floodplains, form the focus of the this study and are reviewed in the following section in the context of the research questions relevant to this thesis.

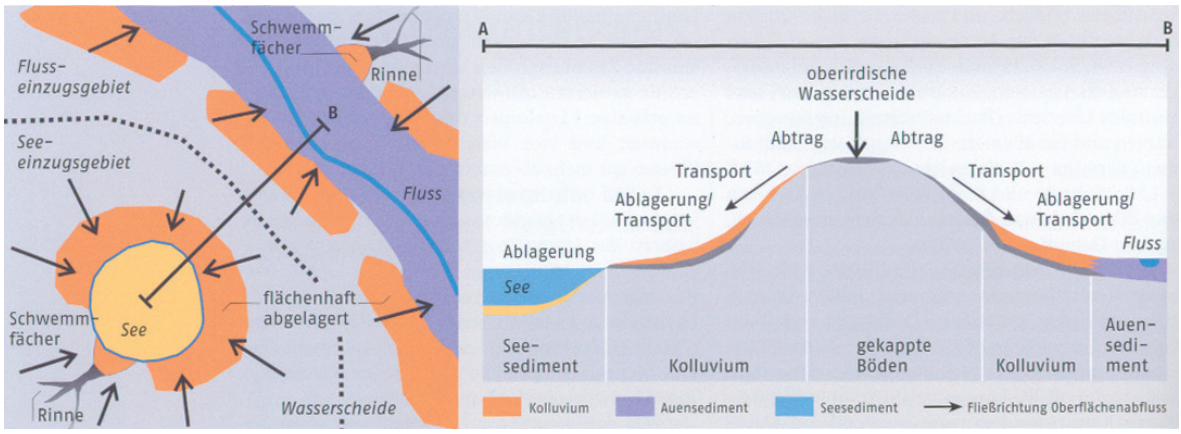

Figure 2: Schematic illustration of gio-bio-archives (Bork, 2006)

3.2.1 Hillslopes

3.2.1.1 Natural hillslope erosion

Despite intense debate surrounding soil erosion, it is not until recently that natural rates of soil erosion and their quantification have become a focus of research. One gain in this new research effort to quantify mainly human induced soil erosion has been to establish which

soil erosion rates might be sustainable over long time periods (i.e soil production = soil erosion) (Montgomery, 2007). In vegetated areas, soil erosion on slopes is closely linked to bioturbation, a phenomena first observed and researched by Darwin (Darwin, 1899), the implication being that flora and fauna are the major drivers facilitating erosion in these areas. Research on this topic was reviewed by Dietrich and Perron (2006), and specific treatments by Roering (2002) and Hughes (2009) have established hillslope soil erosion rates under natural, vegetated conditions. Agricultural ploughing and the resulting accelerated soil erosion can easily destroy the sedimentary record of natural soil erosion, especially in smaller catchments with limited sediment storage areas. To the authors knowledge, no natural hillslope erosion rates have been published for Central Europe, and therefore these natural rates remain unknown to this study. Nevertheless, in order to fully address the impact of human induced hillslope erosion, the estimation of natural hillslope erosion rates is critical, and should therefore be considered as a part of future research agendas.

3.2.1.2 Hillslope erosion from agriculture

As already discussed, hillslope erosion is a complex process that depends on soil properties, ground slope, vegetation cover, as well as rainfall amount and intensity. Changes in land-use are widely recognised as being able to accelerate soil erosion rates, which in turn is considered unsustainable if soil erosion exceeds soil production (Montgomery, 2007). This is relatively well understood at the plot scale, and is often quantified using the USLE equation, but is often criticised as being inappropriate for extrapolation across larger spatial scales. Over the long-term, hillslope erosion processes typically result in soil loss on the upper and middle slope segmenta, and storage on the lower slope segments, with very low percentages of the total hillslope sediments exported to trunk streams (Trimble and Crosson, 2000). This process can also lead to positive feedback and growth of the lower slope storage area, since the runoff is slowed upon reaching the less inclined lower slope segments, and the production of a convex lower slope shape in turn reduces its storage capacity. These colluvial sediments are the main archive for the examination of Holocene hillslope erosion processes, and their development is generally attributed to deforestation and agricultural practices, with climatic fluctuations generally considered of only minor importance (Lang, 2003). Since these agricultural practices began to spread at the Neolithic, the earliest colluvial layers in the Holocene record from Central Europe can therefore be found from this time period onwards (Dreibrodt et al., 2010; Lang, 2003). However, colluvial layers are not continuous archives, potentially suffer from reworking (Lang and Hönscheidt, 1999), and are therefore difficult to quantify. The quantification of hillslope erosion from these sediments is further complicated by the creation of artificial obstacles on slopes, which in turn can develop into field terraces.

If the position or integrity of these structures change over time then attempts to construct past sediment fluxes find a random distribution of colluvial layer thickness (Houben, 2008). Despite this, many studies have successfully quantifying past hillslope erosion (Bork, 1988; de Moor and Verstraeten, 2008) and have therefore been able to calculate erosion rates. Any upscaling of these results from the plot scale to river basins usually suffers from the absence of knowledge about changes in land-use (Macklin et al., 2006) both spatially and temporally, and is perhaps most obvious in the apparent contrast in erosion rates due Neolithic and medieval agricultural practices (Lang, 2003). This study aims to contribute to this discussion through the construction of a sediment budget and by calculating erosion rates due to different cultivation techniques (chapter 7, 8).

3.2.2 Gullies

Gullies are an important landscape component in the sediment transport system within catchments. This is because they can be an important sediment source, and are also effective links in the transfer of runoff and sediment from uplands to the valley talweg (Poesen et al., 2003). Conceptually, this means that gullies increase the sediment transport connectivity in the landscape, and must therefore be incorporated into studies investigating soil erosion, because they enhance sediment transport from fields into trunk stream and potentially destroy arable land by gully head retreat. In addition, understanding the factors controlling gully erosion becomes increasingly important under the observation that erosion due to agriculture is the most severe in semi-arid landscapes. This combination of circumstances is unfortunately most prevelant in 3rd world nations, which are already vulnerable and often depend solely on agriculture for income. An understanding of gully erosion processes and their rates is also critical for determining the sediment delivery to fresh water reservoirs (dams), from which some studies have found that gully erosion is responsible for ~ 70 % of the sediments in these contemporary sediment traps (Valentin et al., 2005).

Gully erosion has often been neglected in catchment studies because it is difficult to study and even harder to predict. This difficulty is derived from their threshold-driven and event-based nature, and an often complicated antecendent history (Valentin et al., 2005). Studies which have investigated the history of these landforms were often conducted in old and largely permanent gullies, with their presence depended on the deforestation and agricultural land-use and also upon heavy precipitation events necessary as a trigger for gully head retreat (Dotterweich, 2005; Dreibrodt, 2005; Stankoviansky, 2003; Vanwalleghem et al., 2005b). However, studies which seek to investigate the sediments derived from gully and gully fan activity within popular archives such as lake deposits, often find no clear coincidence in timing between deforestation or agricultural land-use and gully incision. Instead, it is commonly found

that gullies develop during phases in which archaeological and historical sources indicate abandonment of agricultural practices and the catchment begins reforestation (Anselmetti et al., 2007; Belyaev et al., 2004; Smolska, 2007). In terms of processes, Vanwalleghem (2008) found the only significant parameters in gully evolution and development to be slope and area. These two factors in combination with other topographic thresholds are also underlined in the channel initiation model of Montgomery and Dietrich (1992), and from this point of view implies that land-use has less of an effect on gully erosion than is otherwise regarded in the interpretation of sedimentary archives. However, these same studies demonstrate that changes in vegetation cover are also critical in gully development. Therefore, it is likely that changes in vegetation cover alter the thresholds of gully head retreat, however, determining the extent of this influence remains largely unexplained, and forms part of the motivation for the work presented in chapter 6.

3.2.3 Floodplains

Since the 1960s silty overbank deposits in floodplains have generally been regarded as the product of catchment slope instability from human driven soil erosion and/or climatic increases in flood frequency, especially those studied in the large river systems of Central Europe e. g: (Luettig, 1960; Wildhagen and Meyer, 1972). The deposition of these flood loams probably began ~ 11000 years ago (Schirmer, 1991), and are highly variable in thickness throughout Central Europe in the early – middle Holocene (Notebaert and Verstraeten, 2010). The rate at which these silty flood loams are deposited has been found to increase at the beginning of the Roman Period (de Moor and Verstraeten, 2008; Macklin and Lewin, 2008; Notebaert and Verstraeten, 2010; Schirmer, 2007) and peak in Medieval times (de Moor and Verstraeten, 2008; Fuchs et al., 2011; Hoffmann et al., 2008; Macklin and Lewin, 2008; Notebaert and Verstraeten, 2010; Starkel, 2002). High sediment delivery as a result of deforestation and agricultural harvesting of slopes, and the clearing of riparian vegetation have all been given as possible mechanisms (Becker and Schirmer, 1977; Lang et al., 2003; Rommens et al., 2006; Szmanda et al., 2004). The same reasoning is also invoked in the interpretation of sediment proxies within lake deposits (Gale and Haworth, 2005; Zolitschka, 1998). Nonetheless, studies which attempt to interpret the combination of timing, source, and the origin of these deposits still remain largely speculative. One possible reason for this is that most research has been conducted within very large floodplains (> 4th order streams), and largely neglect the possible record contained within the slopes, gullies, and small streams which drain to them. This study aims in part to address this problem, as well as larger questions concerning sediment delivery from headwaters to trunk streams in Central Europe (chapter 6, 7). Furthermore, a project for further research is also presented as chapter

9, the basis of which is to study valley bottom damming upon human arrival, and the effects of the subsequent retardation of the flow regime. This effect may in turn be responsible for fundamental changes to river regimes and possibly floodplain aggradation within many Central European rivers.

3.2.4 Lake sediments

Lake sediments from Central Europe can potentially provide a high-resolution and often continuous sedimentary archive, which have been commonly used for the construction of pollen records (Anselmetti et al., 2007; Dreibrodt, 2005; Enters et al., 2008; Zolitschka, 1998). Lake sediments themselves largely originate as suspended load within surface runoff, although in very small catchments can be derived directly from slumping or other mass failures. Holocene increases in sedimentation rate are typically interpreted to be the result of higher sediment delivery from catchments following deforestation and the agricultural harvesting upon slopes. However, lake shore erosion and perturbations in the lake sediments must be taken into consideration and potentially complicate this archive. The problems and legitimacy of catchment erosion reconstruction from lake sediments is discussed in further detail in chapter 6, and it is suggested that such reconstructions are likely to suffer from insufficient knowledge concerning the sediment delivery process.

3.3 The importance of vegetation for surface processes and its investigation

Vegetation is known to generally dictate the rate and pattern of surface wash and therefore strongly limits its efficiency (Dietrich and Perron, 2006). This general understanding largely originated witin plot-scale hillslope studies and was transferred to the larger gully and fluvial systems, and such a scaling necessarily requires some generalisations and simplifications. Recent studies have found that vegetation cover can actually facilitate gully erosion and subsequent deposition in floodplains and deltaic systems (Belyaev et al., 2004; de Vente et al., 2007; Temmerman et al., 2007). That gully incsision can occur under vegetated catchment conditions was explained by Belyeav et al (2004) as being determined by internal thresholds. These are possibly facilitated by preferential flow via root zones which lead to higher infiltration rates and an increase in the groundwater gradient, which in turn allows easier stormflow generation, and finally may cause gully incision (Steenhuis et al., 2011). This study attempts to determine whether or not vegetation is a major factor for gully initiation and gully head retreat through chronological comparisons and vegetation reconstruction using charcoal fragments in chapter 6 and 7 (Dreibrodt et al., 2009; Touflan et al., 2010).

It also explores what role changes in vegetation cover as a result of different cultivation techniques may have in changing the estimated gully erosion rates during the period of human influence using detailed comparisions of forest compositions within different parts of the landscape (chapter 8).

4. THE SETTING

The Spessart mountains (Figure 3) are generally considered to be a natural landscape, covered by dense forest and only sparsely settled. Historically, this low mountain range

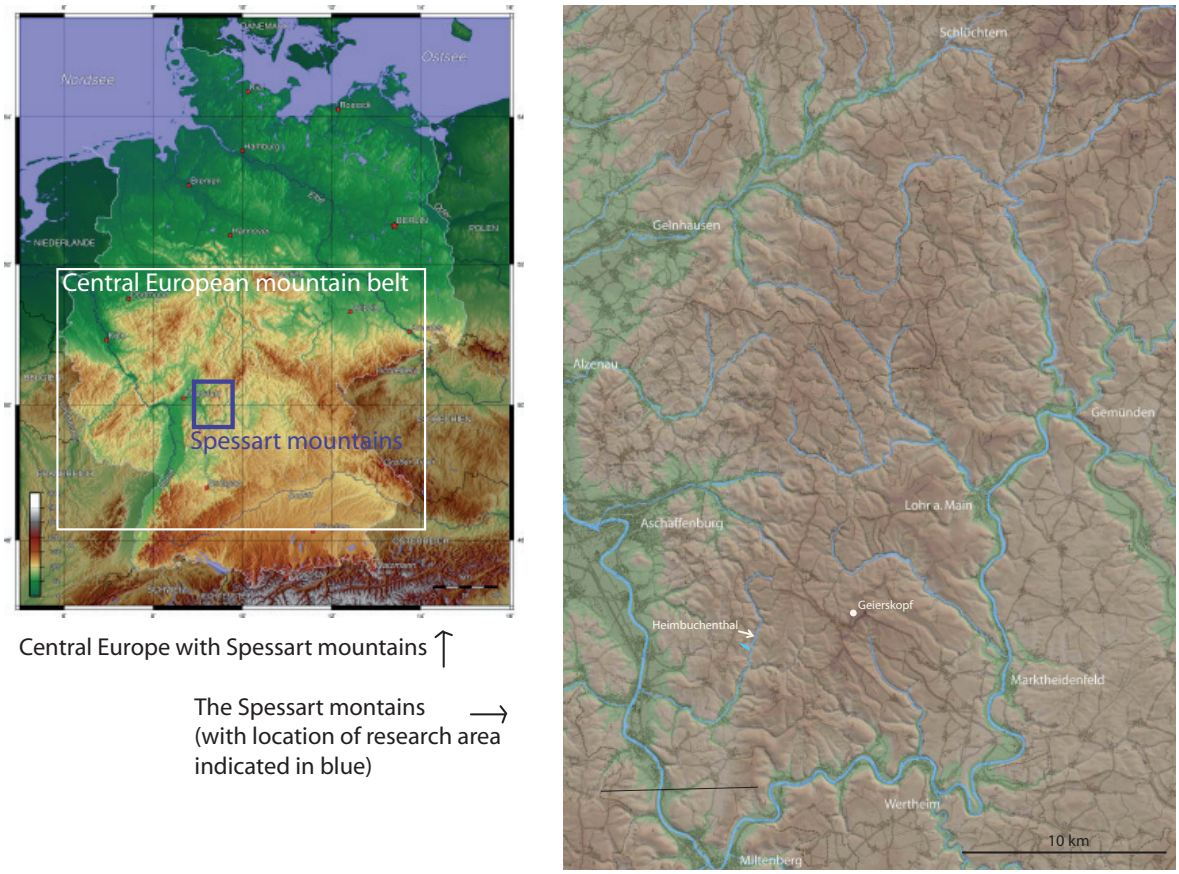

Figure 3: Location of research area in Central Europe (left) and in the Spessart mountains (right)

is known as an economically poor region in Germany, whose people suffered in the 1850s from overpopulation and famine largely because the soils were sandy, with steep slopes and relatively remote, resulting in what has been charitable despcribed as “moral degradation” (Virchow, 1852). From research conducted in other regions of Central Europe we know that enhanced soil erosion, especially in medieval times, follows a cycle which begins with intense soil degradation, a reduction in soil fertility, and famine in the following generations (Bork, 1998; Dotterweich, 2008), and finally reforestation of the degraded area if agriculture is abandoned. To test if this is the case in the Spessart mountains, a typical gully catchment was selected (the Kirchgraben catchment) and from which the settlement history is relatively well known as a result of archaeological excavations within the fan sediments of this catchment. The Kirchgraben catchment ranges from 203 to 401 m (asl) in relief and receives an annual rainfall of ~ 900 mm a year. The catchment exhibits a well incised gully system developed in

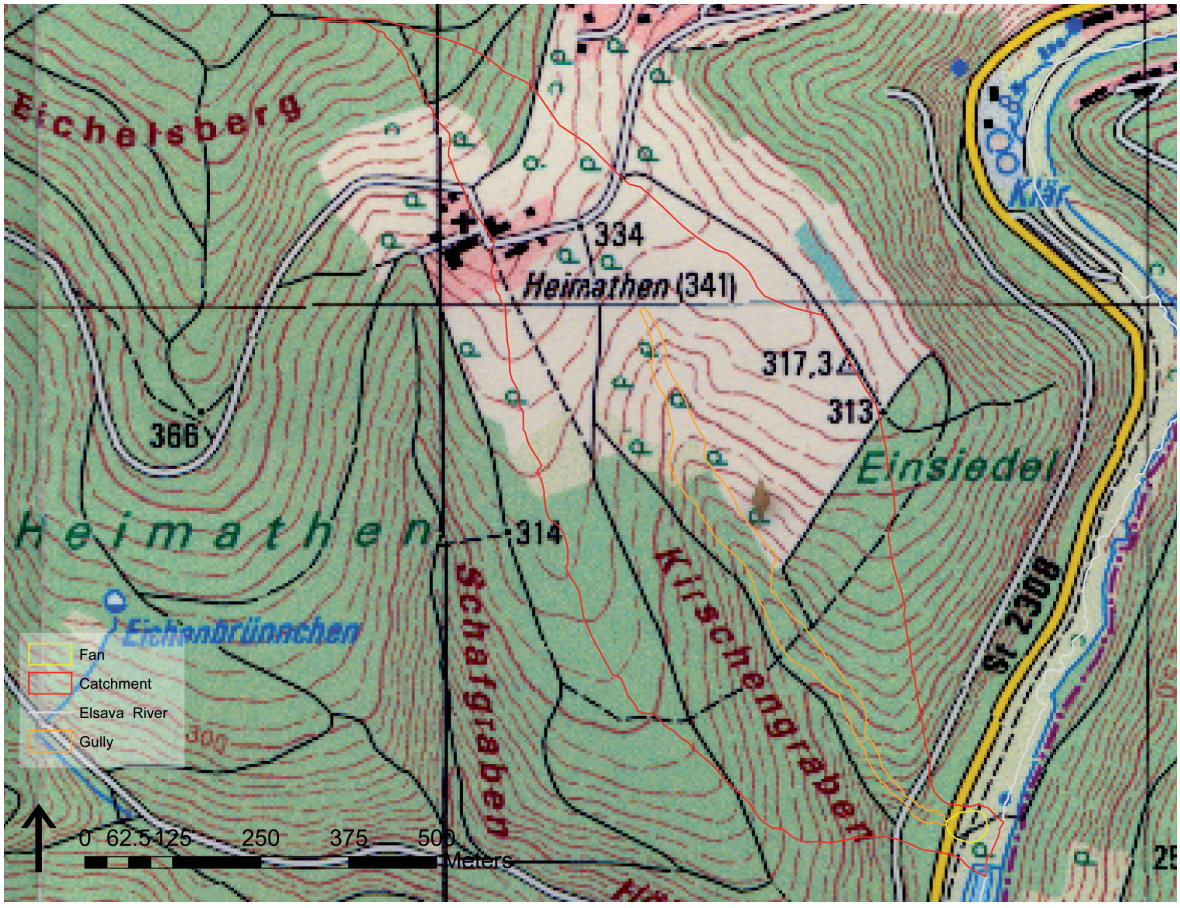

Figure 4: The topography oft he research ares at 1:50000 scale (© Bayrische Vermessungsverwaltung)

steep slopes below a smooth plateau surface (Figure 4), a morphology most likely inherited from repeated glacial cycles of periglacial processes. These cycles are evident from two main solifluction layers, which can be found in all exposures in the slope and thalweg sediments. These layers were in detail described by Mueller (2011) for the Spessart mountains. Figure 5 shows that the lower basal layer 1 is composed out of weathered mesozoic Bunter Sandstone, and includes some unweathered boulder clasts up to 1 m in length within a mostly sandy matrix, however, more clay rich layers are also present (Figure 6). The stratigraphy also features “pockets”, or clasts which are imbricated and twisted, which is typical for solifluidal transport under periglacial conditions. Because the bulk density of these layers is very high, this layer often forms outcrops or knickpoints (Figure 5), within the gully thalweg. These outcrops are also likely responsible for the limits to headward gully incision, and are therefore potentially an important buffer in gully erosion.

The basal layer then grades into a loess-derived silt dominated layer (Figure 5 and 6), which can be only 0.05 m thick on the slopes, and up to 3 m on the plateau surface, and indicates strong aeolian silt deposition during periglacial conditions which peaked during the Last glacial maximum (LGM). The oldest age for this layer was ~ 30000 a, and the youngest

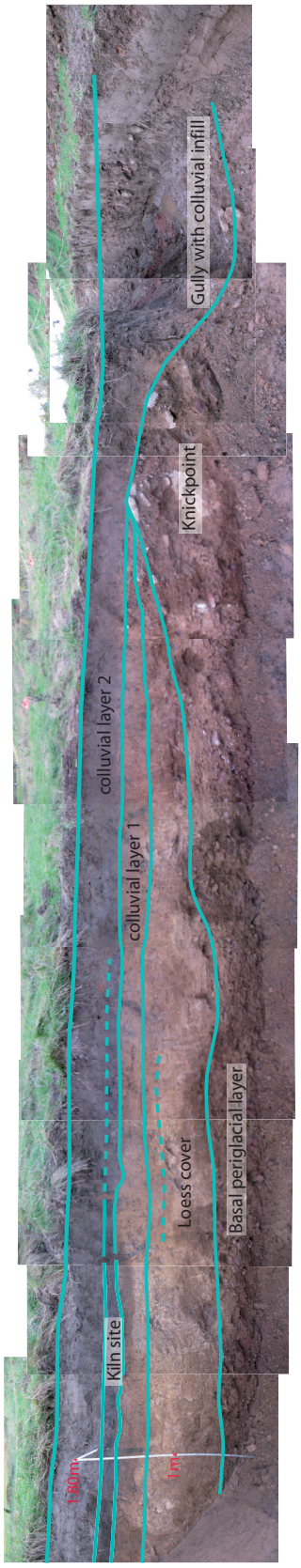

~ 11500 a (see appendix Table 1). This layer is subject to the development of a Luvisol, whose thickness is largely controlled by the thickness of the loessic parent material. In all cases simple grain size analysis revealed that mixing of loessic silt with the sandy weathered bedrock must have also taken place. The lack of imbricated clasts and the Luvisol masking sedimentary structures makes it difficult to determine which process lead to the mixing, and bioturbation was most likely also an important factor. The observed combination of mainly solifluidal and slopewash erosion in this layer is in broad agreement with Mueller (2011) and Semmel (e.g. 1976; 2002), which have argued for the Younger Dryas to be a major deglacial erosional phase. This layer is also of ecological of importance, because it is the parent material of the soil which has supported the Holocene development of vegetation. It is also the soil which was subject to ploughing through different phases of agriculture, as well as hillslope sheetwash.

In terms of human influence, all modern settlements in the area were more or less established by ~ 1300 AD. However, the analysis of settlement types of the area suggests early medieval settlement activity began from ~ 800 AD onwards (Denzer, 1996). The area is located at the border between the sphere of control of the county of Rieneck and monastery of Kurmainz, and was therefore a matter of conflict in medieval times. A hamlet is located on the plateau of the research area, first mentioned historically in 1383 AD (Bachmann, 1982) (Figure 7). At the mouth of the gully, where fan and floodplain of the Elsava River trunk stream intersect, a medieval moated site (~ 1200 – 1420 AD) was recently found and excavated (Figure 7). The inhabitants of this castle were owner of an estate that most probable included the Kirschgraben catchment. The owner's income was mainly based on agriculture, but a mill-stone has also been found, which suggets a medieval mill-site close to the castle. Mills were important pre-industrial businesses from which farmers were dependant and therefore important to control.

Figure 5: A typical excavation site as an example for the Pleistocene development of the research area

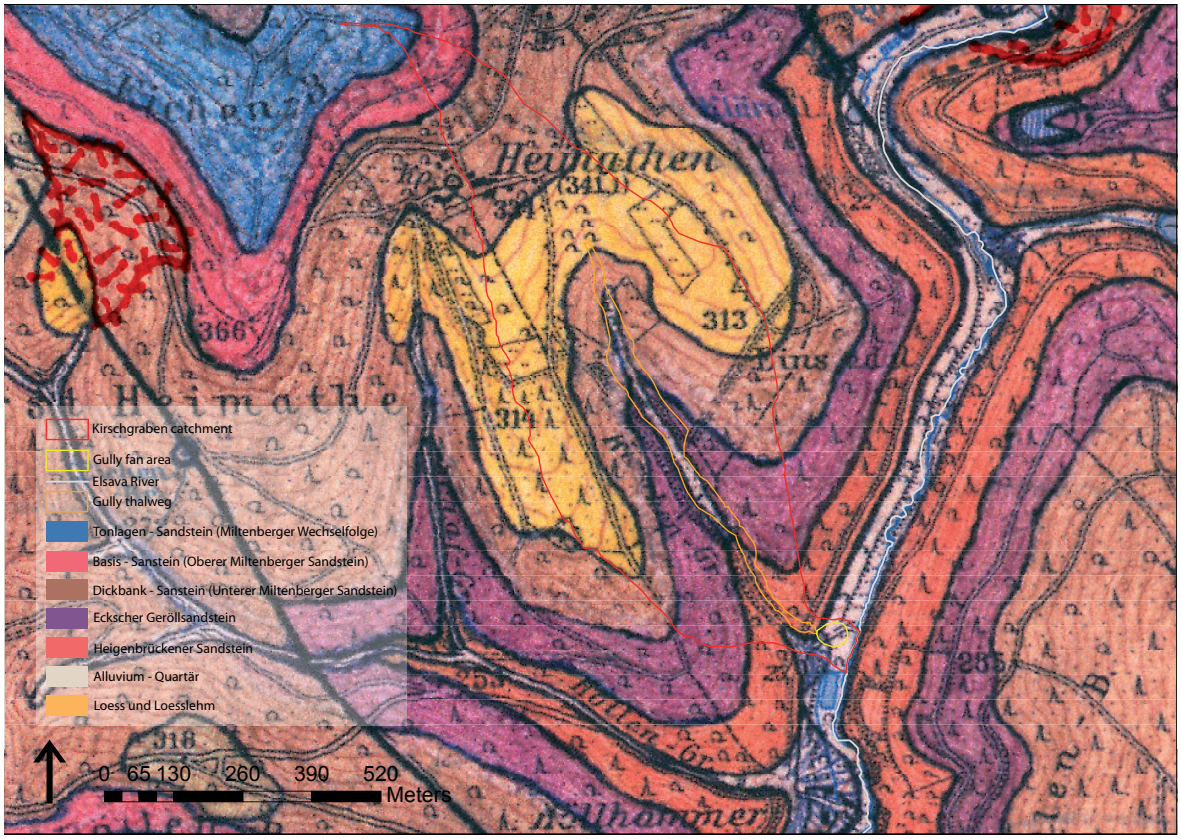

Figure 6: The Geology of the research area, redrawn from Schwarzmaier (personal communication)

Downstream (200m) of the moated site an early modern iron working site was established in 1705 AD, and intensified its production around ~ 1790 AD (Schunder, 1995) (Figure 7). These iron working sites required consistent water supplies and charcoal for energy, and worked mainly recycled iron. Prior to this, there are only scattered archaeological findings recorded from Neolithic times (Bandkeramik: 3500-2500 BC and Michelsberger Kultur: 2200 – 1800 BC) (Bachmann, 1982) and the foundation of a small iron age house, dating back to 2440 +/- 25 cal BP. Beginning in medieval times, charcoal production sites were constructed and are now found throughout the entire catchment, testifying to intensive forest exploitation (Figure 7). The development of field terraces due to agricultural practises are also a prominent landscape feature in the Kirschgraben catchment, and although presently covered by forest, they demonstrate that almost the whole area has been used for agricultural purposes for extended periods in the past.

In 1844 AD the catchment topography and land use was accurately surveyed and mapped for the first time. The results of this mapping is shown in Figure 8, and reveals a surprisingly high level of forest cover, even though the population pressure on the land in the 1850s was reported to be intensive due to high poverty levels (Virchow, 1852). During this time, the Kirschgraben catchments land use was 42 % forest, 41 % agricultural fields, 11% grassland with scattered fruit trees, 1 % pure grassland, and 2% settlement structures.

The hamlet Heimathenhof at ~ 1930 AD. In the middle-ground parts of the Kirschgaben catchment are identifiable. The forest composition looks patchy, presumably still used in more versatile ways.

The Höllhammer (early modern iron working site) painted on a bowl of a pipe ~ 1820 AD. The ruins of the moated site „Mole" is identifyable in the middle grounds, but also the Kirschgraben catchment in the background-with fields and patchy forest, partially clear-cutted.

The fan of the Kirschgraben catchment during the archaeological excavation 2009. In the foreground the foundation of the major tower is exposed, in the middle ground the moat of the castle and its terminal wall were excavated. In the background the excavations sites S1 and S3, part of this study, are located.

One of many charcoal production sites in the Kirschgraben catchment.

Figure 7: Historic photographs and illustrations of the research area

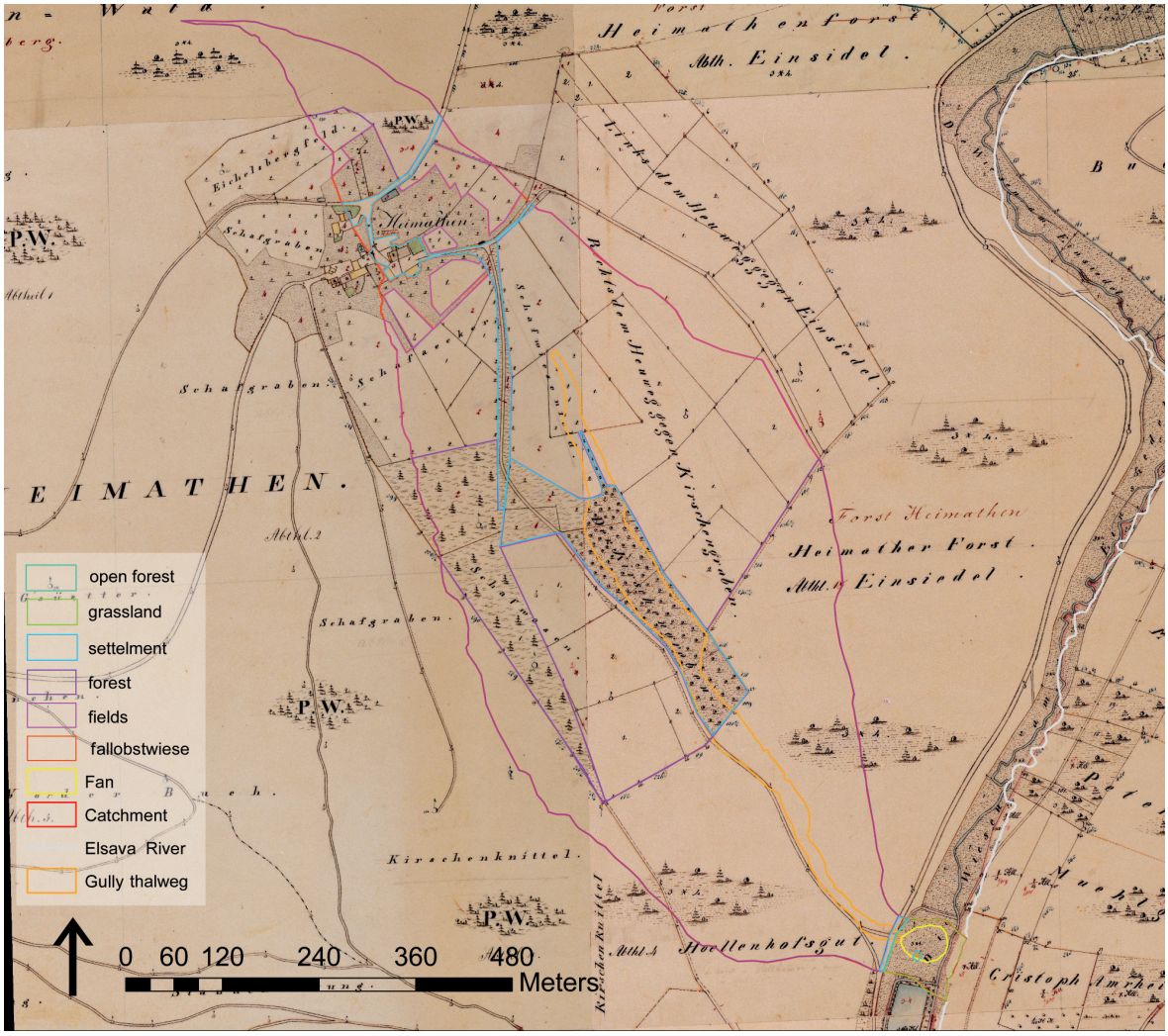

Figure 8: Land-use conditions of the research area around 1850 AD projected on the Urkatasteraufnahme (© Bayerische Vermessungsverwaltung)

Past vegetation composition through palynological analysis from a peat bog ~ 6 km east of the research area was conducted by Lagies (2005; 2006). The oldest age at the base of the peat was found to be 725 – 985 cal AD. In high – late medieval times *Quercus* is the dominant tree species, in combination with *Betula*, *Tilia* and *Corylus*. The natural forest composition would most likely have been *Fagus*, and therefore the author argues that the forest must have been structurally altered prior to the development of the peat bog. This modification is attributed to some combination of glass or charcoal production, and animal grazing, the latter of which promotes mainly *Quercus*, because the acorn is supposed to be a rich fodder for pigs. Between 1325 and 1457 cal AD the fraction of *Quercus* pollen within the peat bog archive increase. *Juniperus* together with a constantly high *Corylus* and *Tilia* percentage are interpreted to be the result of animal grazing in the forest. At the same time *Pinus* pollen also increases, which can be attributed to the effect of increasing land-opening. In the 18th / 19th century *Juniperus* pollen increases, and is interpreted to be effect of a wide

landscape opening. In the late 19th century, *Cannabis* and *Vitis* pollen indicate the onset of the cultivation of these plants in the area, and the corresponding decrease of *Pinus* pollen shows at least a partial reforestation of the area. In the beginning of the 20th century, *Picea* and *Larix* pollen give evidence for first forestry plantation (silviculture). In the uppermost peat bog layers, *Fagus* dominates over *Quercus* pollen and *Corylus* disappears because of canopy closure due to the domination of Fagus. The peat base in a small bog with the name "Birkenwasser" in the close vicinity of the Geierskopf-bog is dated back to 1275 – 1415 cal AD, in which corn and *Juniperus* pollen was detected, affirming an intensive land-use during this time (Lagies, 2004).

5. STUDY ON A LANDSCAPE SCALE

Geographers think of landscapes as a geographical unit of relatively small size, which is large enough to be a representative section of the earth surface (Fairbridge, 1968). Landscape has been described as having both constant and more variable aspects, examples of the latter apects are: fire, earthquakes, droughts and floods (Fairbridge, 1968). Because of their immediate and catastrophic influence, these factors are relatively well researched, whilst it is often the more subtly changing landscape factors upon which mankind is most dependant. These subtle and largely constant aspects are topography, plant formation, hydrography, the influence of animals, and the influence of humans. Therefore, in order to fully capture these subtle aspects we need to extend the time scales of interest, and this forms an important theme in this study. Human impact on landscapes may have fundamentally changed these aspects, and much more rapidly than the other landscape factors, with which they constantly interact. The interaction of these landscape factors and their influence on the sediment flux is the central topic of this PhD-thesis and forms the shapes the content of the following chapters.

6. ON THE PROCESSES AND TIMING OF SEDIMENT DELIVERY FROM HEADWATERS TO TRUNK STREAMS IN THE CENTRAL EUROPEAN MOUNTAINS

(accepted from *Geomorphology*)

6.1 Introduction

Previous studies of catchment slope instability as a result of human driven soil erosion and/or climatic increases in flood frequency, have been described to be the cause of silty overbank deposits in Central European rivers. The deposition of these flood loams extend from ~ 11000 years ago(Schirmer, 1991), and are very variable throughout Central Europe in the early – middle Holocene (Notebaert and Verstraeten, 2010). The rate of floodplain deposition has been found to increase from the Roman Period on (de Moor and Verstraeten, 2008; Fuchs et al., 2011; Macklin and Lewin, 2008; Notebaert and Verstraeten, 2010; Schirmer, 2007) and peaks in Medieval times (de Moor and Verstraeten, 2008; Hoffmann et al., 2008; Macklin and Lewin, 2008; Notebaert and Verstraeten, 2010; Starkel, 2002). High sediment delivery as a result of deforestation and agricultural harvesting of slopes, and the clearing of riparian vegetation have been given as possible mechanisms (Becker and Schirmer, 1977; Lang et al., 2003; Rommens et al., 2006; Szmanda et al., 2004), with the same reasoning invoked in the interpretation of sediments from lake deposits (Gale and Haworth, 2005; Zolitschka, 1998). However, studies which address the combination of timing, the source, and the cause of these deposits still remain largely speculative. One reason for this is that most studies have been carried out in the large floodplains of $> 4^{th}$ order streams and largely neglecting the slopes, gullies, and small streams which drain to them. Similarly, studies which have attempted to reconstruct human and climatic influences on the landscape have largely focused on sediment stored within colluvial layers (Kadereit et al., 2010; Lang and Hönscheidt, 1999) as a source of floodplain sediment (de Moor and Verstraeten, 2008; Fuchs et al., 2011; Hoffmann et al., 2008; Stolz, 2011). In contrast, sedimentation in contemporary reservoirs has been seen to be predominately sourced from gully erosion (Valentin et al., 2005), suggesting the development of colluvial layers is not necessarily coincident with floodplain aggradation, and that additional mechanisms are required.

Investigations into the dynamics of gully sediment supply and erosion have been undertaken almost exclusively within gully thalweg sediments (Dotterweich, 2005; Schmitt et al., 2006; Vanwalleghem et al., 2005a), or the gully fan (Smolska, 2007; Zygmunt, 2009), which means our understanding of the interactions between all potential headwater sediment sources and sinks, and their effect on sediment delivery to trunk stream floodplains remains incomplete.

In order to address this gap we investigate all available headwater sedimentary archives, including: slopes, gully thalweg, gully fan, and the floodplain sediments of the adjacent 3rd order trunk stream to which they drain. We find multiple erosion and sedimentation cycles within the gully thalweg, corresponding to changes in vegetation cover and land use, which in combination with the internal geomorphic thresholds of the system has resulted in a highly non-linear relationship between landscape change and floodplain sediment aggradation in the trunk stream. This implies that studies relying on the timing and rate of floodplain or lake aggradation being directly related to climatic or human impacts must be re-interpreted in terms of the internal thresholds and storages present within the catchments.

6.2 Research Area

We focus on a 42 ha gully catchment, which is a typical gully system within the Spessart Mountains of Central Europe (Figure 9). It receives annual rainfall of ~ 900 mm and ranges from 203 to 401 masl in relief. The catchment has a well incised gully system developed in steep slopes below a smooth plateau surface, a morphology most likely inherited from repeated glacial cycles of periglacial processes. The gully thalweg features a stepped longitudinal profile. At two locations outcrops of weathered sandstone confine the gully thalweg (Figure 9). The geology is characterised by Mesozoic red sandstone (Buntsandstein) with up to 3 m of Pleistocene loess cover on the plateau, which reduces to just a few cm of loess derived colluvial sediment on the slopes. The original loess, as with most of Central Europe, was deposited within the late Last Glacial Maximum (LGM). Both the sandstone and loess cover have undergone extensive weathering and soil development, in addition to the various periglacial and slope transport cycles, the latter of which are the focus of this study.

In terms of human influence, a hamlet is located on the plateau of the research area, first mentioned historically in 1383 AD (Bachmann, 1982), and, prior to this, some Neolithic findings have been recorded (Linear pottery: 3500-2500 BC and Michelsberger Kultur: 2200 – 1800 BC). At the mouth of the gully, where fan and floodplain of the Elsava River trunk stream intersect, a medieval moated site (~ 1200 – 1420 AD) was recently excavated. Close to the medieval site the foundation of a house was also discovered which was dated to 2529 ± 172 cal BP. In addition, charcoal production sites have been found throughout the entire catchment and testify to intense past forest exploitation. The development of field terraces due to agricultural practices are a prominent landscape feature in the Kirschgraben catchment, and although in the present day covered by forest they demonstrate that almost the whole research area has been used for agricultural purposes for as yet undefined periods in the past.

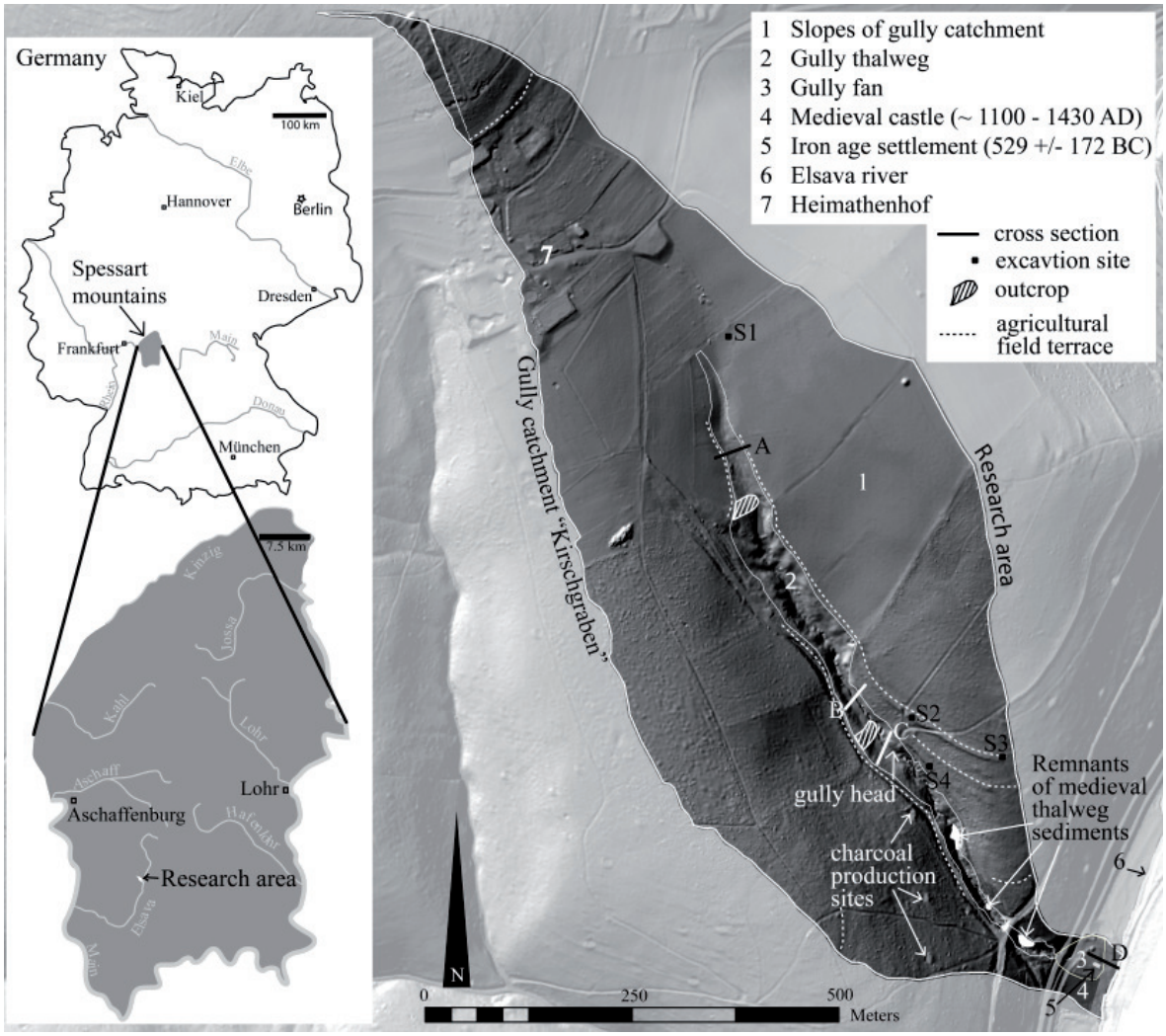

Figure 9: Map of the Kirschgraben catchment within the Spessart mountains of Central Germany (inset). The base data for this map is the digital terrain model © Bavarian Survey Office Munich, 2011.

The present day gully exhibits only intermittent runoff and minor headcut retreat, which typically occurs if the soil is water saturated during episodes of late and sudden snow melt or during high intensity precipitation events (also observed by Belyaev, 2002; Faulkner, 1985; Panin et al., 2009). Upstream of the knickpoint, pipes measuring up to one meter in diameter have developed in the gully thalweg. These pipes facilitate preferential flow during saturated conditions, when they can also collapse or connect with other pipe networks, similar to that observed by Verachtert et al. (2010). The collapse of these pipes facilitates parasitic drainage development and the formation of minor gullies which eventually results in further head-cut retreat.

6.3 Methods

6.3.1 Study sites

Five excavations through the gully thalweg and three excavations through the gully fan/floodplain were constructed 7 - 32 m in length and up to 4.20 m in depth, which in addition to natural exposures and corings from slope deposits, are the primary source of data in this study. Excavation sites were selected because of their position with respect to significant geomorphic features which we define as: aggraded and degraded thalweg deposits, the plateau surface, upper/mid/lower slopes, and the fan/floodplain deposits. In each trench the basal periglacial deposits were reached, ensuring that the complete Holocene sedimentary record was analysed. Vertical sections were carefully cleaned and each layer was sampled for grain size, bulk density, charcoal analysis, and OSL or radiocarbon dating.

6.3.2 Sediment analysis

Sediment < 2 mm was treated with H_2O_2 and subsequently analysed in a Laser Particle Size Analyser (Mastersizer 2000). The percentage of organic matter was measured by loss-on-ignition. Approximately 20 l of sediment was sieved for quantifying percentage gravel content (2 mm - 5 cm and > 5 cm), and for charcoal > 400 microns extraction.

6.3.3 Optical Stimulated Luminescence (OSL)

After cleaning the light exposed surface of the exposure, sampling was carried out directly into opaque plastic bags. Four samples were taken using opaque tubes forced into the exposure. Extracts of 90 – 200 μm sized quartz grains were obtained via standard treatments. Carbonates, feldspars, organic matter, heavy minerals and acid soluble fluorides were removed. Small multiple grain aliquots were prepared containing approximately 200 grains each. All OSL measurements were performed on a Risø TL-DA 15 reader applying a single-aliquot regenerative dose (SAR) protocol (Murray and Wintle, 2000; Wintle and Murray, 2006). The prepared quartz aliquots were stimulated with blue LED light ($\lambda = 470 \pm 30$ nm) at 125 °C for 40 s, and the resulting OSL signals were recorded through a Hoya U340 filter ($\lambda = 330 \pm 40$ nm). The preheat temperature was set to 240 °C (10 s) for the HUB-samples, and to 200 °C, 220 °C and 240 °C (20 s) for the BT-samples, the test dose cut-heat temperature to 200 °C (HUB-samples) or 160 °C (BT-samples), which were verified performing dose recovery tests on samples. The sediment dose rates were estimated by measuring the contents

Table 3: Optical stimulated luminescence (OSL) results

Sample	Lab code	Water content [%]	U [ppm]	Th [ppm]	K [%]	Dose rate [Gy/ka]	Paleodose [Gy]	OSL age [ka]
							Mean ± SD	
B1 (Fig. 2B)	HUB-0073	22 ± 3	2.94 ± 0.15	9.53 ± 0.48	1.91 ± 0.1	2.61 ± 0.14	10.83 ± 5.85	1.89 ± 0.22
B2 (Fig. 2B)	HUB-0074	22 ± 3	3.78 ± 0.19	11.99 ± 0.60	1.85 ± 0.09	2.86 ± 0.14	5.81 ± 2.39	1.18 ± 0.16
B3 (Fig. 2B)	HUB-0075	22 ± 3	3.81 ± 0.19	11.42 ± 0.57	1.81 ± 0.09	2.81 ± 0.14	1.35 ± 0.19	0.48 ± 0.03
B4 (Fig. 2B)	HUB-0076	22 ± 3	3.63 ± 0.18	11.90 ± 0.60	1.81 ± 0.09	2.81 ± 0.14	1.33 ± 0.26	0.42 ± 0.03
B5 (Fig. 2B)	HUB-0077	15 ± 3	2.51 ± 0.13	7.55 ± 0.38	2.38 ± 0.12	3.08 ± 0.16	2.17 ± 0.68	0.45 ± 0.05
C1 (Fig. 2C)	BT 565	15 ± 5	2.99 ± 0.06	10.12 ± 0.16	1.97 ± 0.05	3.07 ± 0.15	2.34 ± 0.52	0.68 ± 0.04
C2 (Fig. 2C)	BT 566	15 ± 5	2.83 ± 0.05	9.89 ± 0.15	2.08 ± 0.05	3.12 ± 0.16	5.46 ± 2.25	1.09 ± 0.11
C3 (Fig. 2C)	BT 567	15 ± 5	1.98 ± 0.04	7.17 ± 0.12	1.81 ± 0.04	2.54 ± 0.13	16.25 ± 6.37	3.71 ± 0.35
C4 (Fig. 2C)	BT 568	15 ± 5	1.44 ± 0.04	5.47 ± 0.11	1.79 ± 0.04	2.31 ± 0.11	42.17 ± 9.79	13.81 ± 1.06
D1 (Fig. 2D)	BT 643	15 ± 5	2.42 ± 0.17	7.95 ±0.13	2.24 ±0.05	3.04 ± 0.16	42.11 ± 0.78	14.65 ± 1.3
D2 (Fig. 2D)	BT 644	15 ± 5	0.95 ± 0.09	3.31 ± 0.06	1.63 ± 0.04	1.96 ± 0.10	141.72 ± 32.50	57.71 ± 7.41
D3 (Fig. 2D)	BT 645	15 ± 5	2.64 ± 0.19	9.09 ± 0.15	2.17 ± 0.05	3.11 ± 0.16	31.51 ± 6.35	8.43 ± 1.08
D4 (Fig. 2D)	BT 646	15 ± 5	2.66 ± 0.12	8.54 ± 0.10	1.99 ± 0.04	2.93 ± 0.15	8.56 ± 4.18	1.13 ± 0.15
D5 (Fig. 2D)	BT 725	15 ± 5	2.99 ± 0.08	6.89 ± 0.10	1.98 ± 0.04	2.88 ± 0.14	38.33 ± 8.64	11.69 ± 0.88
D6 (Fig. 2D)	BT 726	15 ± 5	4.31 ± 0.09	9.74 ± 0.16	2.12 ± 0.05	3.45 ± 0.17	31.85 ± 4.54	8.68 ± 0.59
D7 (Fig. 2D)	BT 727	15 ± 5	3.74 ± 0.07	10.51 ± 0.18	2.15 ± 0.05	3.40 ± 0.17	8.23 ± 1.51	1.86 ± 0.15
D8 (Fig. 2D)	HUB-0147	20 ± 3	2.89 ± 0.14	10.02 ± 0.50	2.03 ± 0.10	2.83 ± 0.14	2.92 ± 1.48	0.35 ± 0.05
D9 (Fig 2D)	HUB-0149	15 ± 3	2.72 ± 0.14	9.92 ± 0.50	2.27 ± 0.11	3.16 ± 0.16	34.02 ± 8.92	8.68 ± 0.76
D10 (Fig. 2D)	HUB-0150	15 ± 3	2.60 ± 0.13	9.66 ± 0.48	2.25 ± 0.11	3.10 ± 0.16	32.22 ± 7.57	7.97 ± 0.79
S1(1)	HUB-0026	25 ± 3	2.75 ± 0.14	13.1. ± 0.66	1.91 ± 0.10	3.05 ± 0.17	91.03 ± 6.01	29.65 ± 1.68
S1(2)	HUB-0027	25 ± 3	2.97 ± 0.15	10.90 ± 0.55	1.82 ± 0.09	2.54 ± 0.13	3.13 ± 0.67	1.11 ± 0.06
S2	HUB-0028	20 ± 3	2.51 ± 0.13	8.40 ± 0.42	2.29 ± 0.11	2.85 ± 0.15	32.8 ± 4.11	11.43 ± 0.67
S3	HUB-0071	22 ± 3	4.02 ± 0.20	12.53 ± 0.63	1.76 ± 0.09	2.88 ± 0.15	3.1 ± 0.83	0.82 ± 09
S4	HUB-0128	15 ± 3	2.37 ± 0.12	7.61 ± 0.38	2.48 ± 0.12	3.14 ± 0.16	2.21 ± 0.3	0.7 ± 0.04

of uranium, thorium and potassium applying high-resolution gamma ray spectrometry and Neutron Activation Analysis (NAA) respectively. Ceasium 137 concentrations were also obtained with this method. No radioactive disequilibrium in the ^{238}U decay chain was detected. The cosmic-ray dose rates were estimated from geographic position, elevation and burial depths (Prescott and Hutton, 1988). Equivalent dose (De) distributions were analysed with age models according Galbraith et al. (1999) taking into account dispersion parameters (standard deviation, overdispersion) and the shape of the probability density function. Narrow unimodal De distributions were analysed using the Central Age Model (CAM). If positively skewed or broad multimodal De distributions were observed, the Minimum Age

Table 4: Radiocarbon results

sample[a]	lab code	δ13C (‰)	δ14C age (years BP +/- 1σ)	calibrated age (calBP 2σ-error bounds)[b]	sample type (wood type)
2A	KIA42950	-28.66 +/- 0.31	1390 +/- 35	1351 (1311) 1271	charcoal (Fagus)
2C (1)	KIA38522	-27.04 +/- 0.29	865 +/- 30	902 (800) 698	charcoal (Fagus)
2C (2)	KIA38523	-24.48 +/- 0.25	1010 +/- 30	974 (887) 800	charcoal
2C (3)	KIA38524	-26.24 +/- 0.24	950 +/- 30	926 (860) 795	charcoal (Betula)
2D (1)	KIA42951	-25.95 +/- 0.20	6330 +/- 35	7326 (7246) 7167	charcoal (Fraxinus)
2D (2)	KIA37840	-25.31 +/- 0.22	9315 +/- 45	10661 (10481) 10302	charcoal (Betula)
2D (3)	KIA38525	-24.52 +/- 0.14	2440 +/- 25	2701 (2529) 2358	charcoal (Alnus)

[a] refers to Fig. 2
[b] calibrated ages include mean in brackets and 2σ-range

Model was applied (MAM). We also consider ages calculated by the MAM in this paper. The excellent stratigraphical control and the large number of age-estimates from multiple dating techniques (including ages calculated by the CAM model) enables us to further constrain the maximum ages calculated by the MAM. We interpret these ages comparable to those calculated by the CAM. OSL datings were rejected in case of negatively skewed or very broad De distributions without any clear peaks at low paleodoses. All palaeodose estimates, dose rates, and water contents as well as the final age calculation are provided in Table 3. OSL ages are given in years (a) before the year of measurement (± 2010).

6.3.4 Radiocarbon dating

Radiocarbon dating was carried out to cross-check with OSL dating and where exposure conditions did not allow taking OSL samples. The frequency of charcoal fragments in all layers made it possible to use charcoal for all radiocarbon datings. 20 l of charcoal samples were floated and sieved (> 400 microns), dried, and the charcoals wood species were determined. The use of short-lived woody species for radiocarbon data such as *Betula* and *Alnus* makes the date more reliable by reducing the potential "inbuilt age" (Gavin, 2001). Additionally, we tried to avoid the old-wood-effect by choosing charcoals in which the tree ring shape and size of the charcoal fragments show a young age of the charred tree. Radiocarbon dating was carried out by the Leibniz-Laboratory for Radiometric Dating

and Isotope Research at Kiel University, following standard methods (Nadeau et al., 1998; Nadeau et al., 1997) The conventional age has been calculated after Stuiver and Polach (1977). The calibration to calendar years was carried out using „CALIB rev 5.01" (Reimer, 2004). Radiocarbon ages are given in cal BP (Table 4).

6.3.5 Dating of ceramic fragments by typological sequence

Where ceramic pieces were found in the sediments, a maximum sedimentation age was established in form of the relative dating by typological sequence (Forde-Johnston, 1974). Therefore the size, proportions, material, decoration of the ceramics were analysed by experts for medieval and early modern times ceramic typology from the Institute of Archaeology of Kiel University.

6.4 Results

6.4.1 Gully thalweg sediments

Five excavations within the gully thalweg covering the whole profile were created, which can be summarised as three distinct stratigraphic relationships (Figure 10 a,b,c). Within each excavation we identified six distinct phases of deposition, some of which are separated by clear erosional boundaries, and some which appear to grade between units. These six layers provide a consistent sedimentological sequence within the different sections of the thalweg, but are not chronologically correlated between these sections. In all cases the basal Pleistocene periglacial deposits were reached (layer 1 in Figure 10 a,b,c), in which we identify a gradation between a lower sandy to upper silty matrix, all with sub-angular gravel clasts (b-axis size in average 20 cm) oriented parallel to the slope. The increase in silt composition can be attributed to an increase in the supply of loessic sediments from the slopes. In one excavation (Figure 10c) we identified clast supported imbricated gravels above the periglacial sediments. These fluvial sediments were OSL-dated to 13810 ± 1060 a (BT 568), and intercalated with sandy colluvial and/or solifluidal layers at the slope-thalweg boundary. These sediments grade into a silt-dominated solifluction layer which can be up to ~ 1 m thick. These silty solifluction deposits are easily eroded, and given that they are only found in the gully thalweg cross sections, have been stripped by subsequent Holocene slope and thalweg processes.

There is then a deep and narrow erosional unconformity between the periglacial sediments and the first Holocene deposits in all of the cross – sections (layer 2 in Figure 10 a,b,c), which are characterised by sub-angular gravel clasts (b-axis size between 20 – 30 cm) parallel to flow direction supported by a sand dominated matrix. Ages for these deposits range from

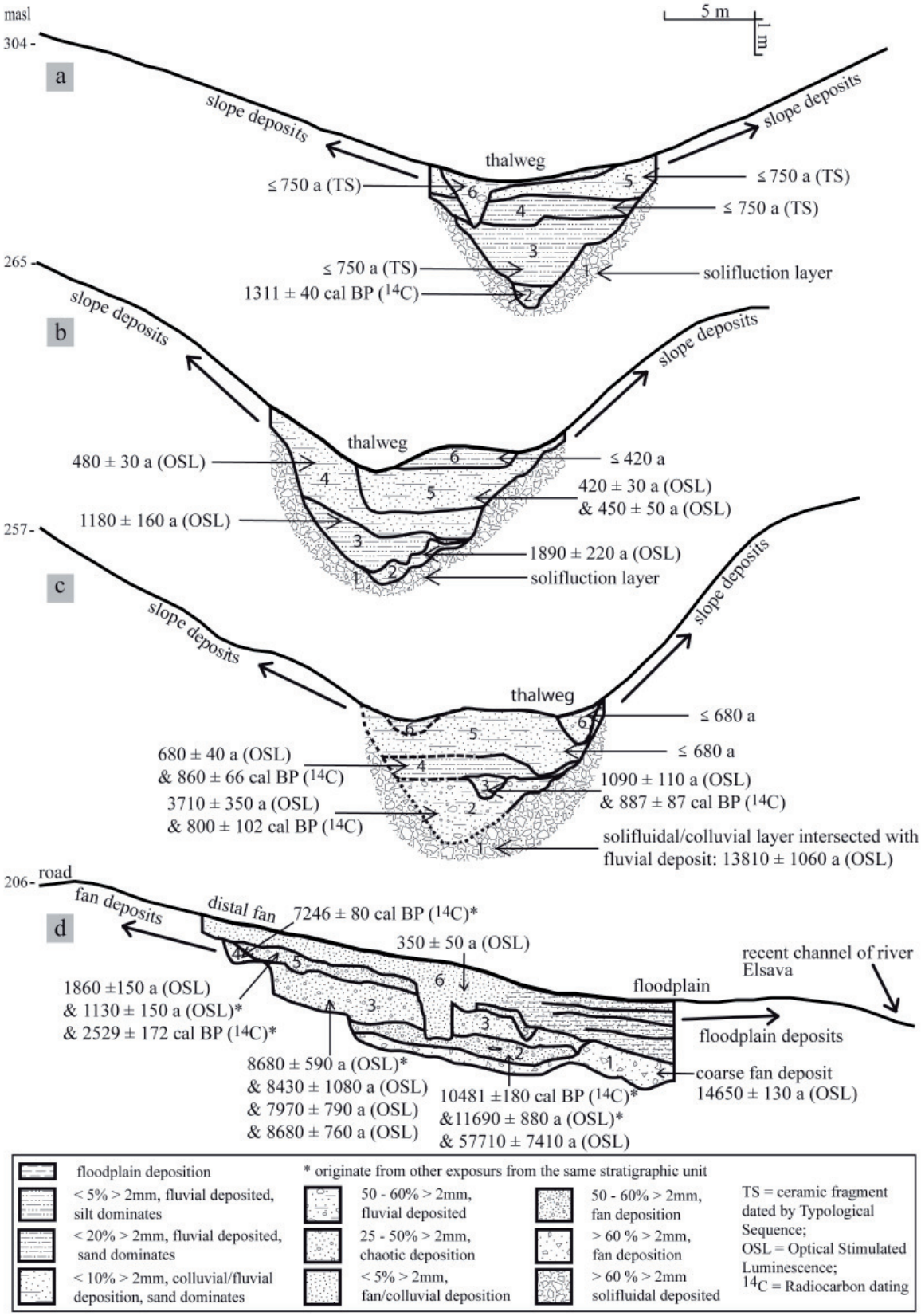

Figure 10: Cross-sections through Late Quaternary gully thalweg sediments (a, b, c). Composite cross section of three excavation sites in the gully fan sediments (d). Land surface elevations are extracted from the DEM, with the dashed lines indicating the inferred stratigraphic relationships. Locations of the cross sections are shown in Figure 9.

1311 ± 40 cal BP (KIA42950) (Figure 10a), 1890 ± 220 a (HUB-0073) (Figure 10b), 3710 ± 350 a (BT 567) (Figure 10c) and 800 ± 102 cal BP (KIA38522) (Figure 10c). The latter two ages are from the same deposit.
In the thalweg exposure c (Figure 10c) the next younger layer is a small silty channel deposit (layer 3), dated at 1090 ± 110 a (BT 566) and 887 ± 87 cal BP (KIA38523). In the mid and upper thalweg this equivalent layer is also dominated by silt, however it is much thicker, with an age of 1180 ± 160 a (HUB-0074) in the mid thalweg (Figure 10b) and a maximum age of 750 a (TS) in the upper thalweg (Figure 10a). Overlying these deposits is a laminar sandy-silt, which in the upper and mid thalweg sections grade laterally into the silty-sand slope deposits. This deposit has a maximum age of 750 a (TS) in the upper section, 480 ± 30 a (HUB-0075) (Figure 10b) in the mid thalweg, and 680 ± 40 a (BT 565) and 860 ± 66 cal BP (KIA38524) (Figure 10c) in the lower thalweg. In all sections, the next younger layer (layer 5) is dominated by sand with fine laminar bedding, and connected to the adjacent slope deposits. In the upper thalweg layer 5 has a minimum age of 750 years BP (TS) (Figure 10a), the mid thalweg has two ages 420 ± 30 a (HUB-0076) and 450 ± 50 a (HUB-0077) (Figure 10b), and in the lower thalweg is younger than ~860 BP. The most recent unit we identified (layer 6 in Figure 2) is a thin silty-sand layer, which is mostly a deposit of the modern channel beds, and can also be correlated with small channel fills of fine gravel (Figure 10 a,b,c).

6.4.2 The fan sediments

The distal fan sediments were investigated by three large exposures, all of which revealed a continuous stratigraphy that was easily cross-correlated, which is presented as a composite representative stratigraphy in Figure 10d. The proximal part of the fan is mostly obstructed by road construction and therefore could not be analysed in detail, thus the remainder of this section relates to the middle and distal fan sediments and chronology. Layer 1 in Figure 10d is a very coarse subangular gravel deposit with sandy matrix and some silt lenses embedded, with the gravels imbricated in the fan downslope direction. Corings in the bottom of the excavation site shows a gradually fining of this layer from up to down, before a discordance mark the start of a very coarse layer underneath. The deposition of layer 1 was dated by one OSL sample to 14650 ± 1300 a (BT 643). Layer 2 is also a coarse fan deposit, but with less gravel clasts and with a sandy-silty matrix. It was dated by radiocarbon to 10481 ± 180 cal BP (KIA37840) and by OSL to 11690 ± 880 a (BT 725).
In all exposures, layer 3 forms the thickest fan deposit. Unlike all other fan deposits, layer 3 is mostly poorly sorted with a lower gravel clast content and a silt dominated matrix. On top of layer 3 several boulders with a diameter of ~ 1m are accumulated and angulated parallel to the surface, partly embedded in layer 3 and layer 5. An OSL sample from the lower boundary

of layer 3 gave an age of 7970 ± 790 a (HUB-0150), two samples from the middle part of layer 3 showed an age of 8680 ± 590 a (BT 726) and 8430 ± 1080 a (BT 645). The upper part of layer 3 was dated back to 8680 ± 760 a (HUB-0149).
Layer 4 was only identified in one of the three excavation sites; this thin layer is composed of angulated gravels in a silty-sandy matrix and gave a radiocarbon age of 7246 ± 80 cal BP (KIA42951).
Layer 5 was found in all three exposures, and at one location it contains remains of an iron age house, however the building was also partly constructed into layer 3. Charcoal identified within the context of the houses fire place was dated to 2529 ± 172 cal BP (KIA38525). The gravel and boulder clasts at the top of layer 3 are partly exposed in layer 5. Due to their deposition on top of a debris-flow lobe and/or presumably minor armouring, they were exposed and later covered by fines of layer 5, which were dated to 1860 ± 150 a (BT 727) and 1130 ± 150 a (BT 646).
A clear erosional boundary between layer 5 and layer 6 at the very distal part of the fan indicates some degree of floodplain reworking by the adjacent Elsava River, this reworking took place prior to or contemporary with the construction of a water irrigation channel, most likely dug for the only 15 m distant moated medieval castle. This irrigation channel was subsequently infilled by a fine laminated, silt-dominated deposit, which also covered the whole distal fan in a thick deposit. This sediment also stratigraphically interfingers with the floodplain deposit of the Elsava River. The lower part of layer 6 was OSL dated to 350 ± 50 a (HUB-0147). The upper part of the layer had a high ^{137}Cs content, and is therefore likely to be younger than 1950 AD.

6.4.3 Slope deposits

Slope deposits of the Kirschgraben catchment show a consistant stratigraphy and composition. The lower layer is always represented by a sandy solifluction layer with a high gravel content and distinctively disrupted by periglacial frost activity. On many of the slopes, but particular well developed on the lower slope segments, a silt-dominated layer with gravel angulated parallel to the surface is deposited on top of the sandy soliflucation layer. This layer sometimes reaches in the shape of pockets into the layer underneath, demonstrating solifluctive movement downslope, and the colluvial layer exposed in pit S2 was dated back to 11430 ± 670 a (HUB-0028) (see Figure 9 for location). This grades into a fine loess cover, which was subject to fluvial and/or solifluctive erosion, except of some upper to mid slope locations. In preserved situations, it shows a Luvisol up to 2 m in thickness. The bottom of this thick Loess layer in S1 dated back to 29650 ± 1680 a (HUB-0026). With sand composing up to 20 % of this layer, intensive mixing before the last deposition must have occured. The

upper slope deposit can be found everywhere in the catchment in varying thickness, from a few centimeters up to 1.2 m. This sediment is dominated by a fine grained soil and sometimes finely laminated. In the lower parts of this layer, silt dominates, while in the top parts the sand component prevails. This sediment also facilitates the development of agricultural field terraces that are abundant in the catchment. OSL dates from several slope positions in the catchment (Figure 9) show an age from the middle part of this layer of 1110 ± 60 a (HUB-0027) (S1), 820 ± 90 a (HUB-0071) (S3) and 700 ± 40 (HUB-0128) (S4). Several ceramic fragments from this layer indicate deposition during medieval times.

6.5 Discussion: Gully erosion and sedimentation cycles

The stratigraphic evidence presented above suggests multiple phases of erosion and sedimentation, however the chronological evidence also demonstrates that these phases are not synchronous between, or within the slope, thalweg or fan sediments. Therefore, we divide the catchment record of erosion and sedimentation into five major phases of catchment activity, we then discuss the driving of these changes in the context of climate and human influences on catchment thresholds. Finally, we provide some implications for the delivery of sediment to large river floodplains and the interpretation of records derived from them.

6.5.1 Phase 1 - Connected sediment transport

During several phases of periglacial conditions in the Last Glacial Maximum (LGM) the research area was covered by up to three meters of loess, presumably stripped by sheet erosion directly following aeolian deposition. This reworked loess was also subject to solifluidal creeping, which also incorporated deeply weathered sandstone, which itself had already undergone numerous weathering and solifluction cycles. The resultant deposit is observed in broadly across all slopes, as well as below the Holocene thalweg sediments (Figure 10a and 10b). Importantly, this slope deposits are intersected stratigraphically with gravel thalweg sediments, indicating efficient transport and sediment connection from the slopes to the thalweg and finally to the gully fan, as suggested by the similar ages of these deposits throughout the thalweg and fan (Figure 10c and 10d). This suggests the deglaciation period until the Younger Dryas (YD) was partly a time of slope instability, and slope sediments were delivered to the thalweg and efficiently transported through the gully system into the fan and trunk stream (Figure 11a).

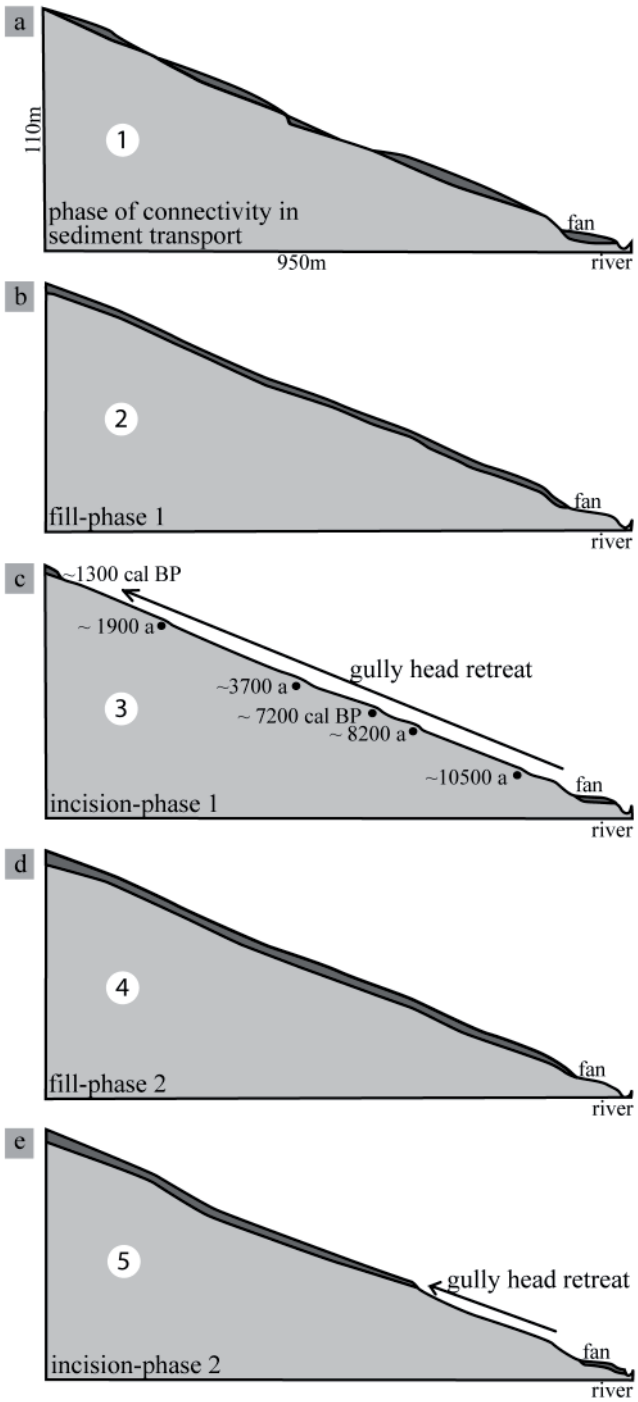

Figure 11: Conceptual longitudinal profile through the gully thalweg and fan at each of the five key time periods. These summarise the erosion- and sedimentation-cycles of the Kirschgraben catchment. Dark grey colour indicate weathered and transported sediment in the gully thalweg, black circles the approximate location of the gully head at distinct time period based on the chrono-stratigraphic evidence. Details of each phase are discussed in the text.

6.5.2 Phase 2 – Filling

The last Pleistocene evidence for regional solifluction activity was described for the Younger Dryas (Mueller, 2011; Semmel, 1976; Semmel, 2002). An important distinction within the deglacial activity however, is the lack of evidence for sediment transport in the gully thalweg during the YD. Therefore, it seems that the YD facilitated slope wash of the upper Loess layer, which in turn supports evidence for limited slope vegetation cover during this time (Behre et al., 1996). Due to later intensive soil erosion during the medieval period, the record from this time period somewhat observed, and there is clear stratigraphic evidence for deposits of this age (11430 ± 670 a) overlying older deglacial thalweg sediments. YD thalweg sediments are not well preserved due to subsequent incision phases. However we do find some loessic remnant thalweg deposits stratigraphically connected to the YD colluvial deposits. We suggest that the thalweg was heavily aggraded during this time and little sediment was transported in the gully thalweg and to the trunk stream, testified by the absence of a fan deposition during this time period (Figure 11b).

6.5.3 Phase 3 – Incision

We find no evidence for colluvial deposition between 11500 and 1100 a, which reflects increased slope stability due to rapid reforestation at the beginning of the Holocene, until the beginning of deforestation following widespread medieval settlement (Behre et al., 1996; Denzer, 1996). This reforestation and slope stability for most of the Holocene is well documented in Central Europe, particularly from areas with similar topographic settings (Behre et al., 1996). Although low erosion rates under those conditions via bioturbation most certainly occurred (Roering et al., 2002), subsequent extensive land-use (e. g. ploughing) has removed any comparatively thin deposits that my have been present.
Given stable slopes, the origin of sediment within the gully thalweg requires a different source. Basal, non-periglacial thalweg sediments become progressively younger upstream. We therefore interpret this to reflect multiple phases of gully head retreat and subsequent downstream deposition within the thalweg (Figure 11c).
In these low mountainous regions, the fan acts as a sink for the early incision phases and with time, the probability of sediment delivery to the fan decreases with increased gully head retreat. The Holocene gully head retreat began very close to the outlet of the gully with limited thalweg storage, therefore the first evidence for gully incision most sediment was delivered to the fan and the trunk stream. We find it being ~ 10500 a old, and an analogous OSL age agrees within the error range. Another OSL age measuring ~ 57700 BP of age can be rejected due to stratigraphical and chronological control of the excavation site.
Overlying this is a layer, and unique poorly sorted fan deposit, which we interpret to be the result of debris flow activity. This event happens to be in coincidence with a well documented climate cooling event (8.2 ka event) (Alley et al., 1997). The neat and last fan deposit from this incision phase dates back to 7246 ± 80 cal BP and indicate that the gully head has been retreating so far upstream, that subsequent eroded sediments will be deposited mostly within the thalweg, and only some fines reach the fan occasionally (layer 5 in Figure 10d). These thalweg deposits represent the continued advance of the gully headcut, that are now able to be stored within the gully thalweg without deposition on the fan.

Due to scarce preservation of thalweg sediments originating from head cut retreat where the modern gully has been eroding, we find the oldest thalweg sediment being of ~3710 a in age (for location see C in Figure 9). A radiocarbon dating from a medieval charcoal could be identified as erroneous, due to stratigraphical constrains: Also because 30 m upstream the next younger thalweg sediment was dated back to ~1890 a.

The youngest thalweg deposit from this incision phases is dated to ~1311 cal BP. This dating must record approximately the end of the natural thalweg incision, because the defined thalweg ends only a few meters upstream. Most likely this incision event is also reflected in layer 3 in site Figure 10b, which has the same age within the error range. Presumably this event was strong enough to erode the layer below, even though this location was not directly affected by the gully head retreat. This finding confirms the reliability of the incision model used in this paper, and the plausibility of the radiocarbon-dating in the stratigraphical context of excavation site displayed in Figure 10a.

6.5.4 Phase 4 – filling

A second gully infill is indicated by widespread colluviation in the gully thalweg and on the slopes, that is dated back at the locations S1, S3 and S4 to medieval times between ~1110 and 700 BP (Figure 11d). The largest volume of slope erosion probably found within the initial phase of deforestation during medieval times, observed similar from many researchers in Central Europe (e.g. Bork, 1983; Dreibrodt et al., 2010; Dreibrodt et al., 2009; Lang and Hönscheidt, 1999). However on some slopes, erosion following this medieval intensity can be attributed to partial reforestation after ~ 1500 AD, but may also partly reflect improved tillage effects (Houben, 2008). In all cases, we find medieval slope deposits stratigraphically interconnected with gully thalweg deposits. These thalweg deposits are in turn distinct from previous thalweg deposits in their thickness, and higher silt content, which can be attributed to their slope origin. This suggests that high sediment supply from the slopes following deforestation was able to significantly aggrade the gully thalweg. This increased sediment supply to the gully thalweg and the absence of any fan deposit from medieval times, gives evidence for reduced sediment transport capacity in the gully thalweg during this time period (Figure 11d).

6.5.5 Phase 5 - recent incision

Despite the continuity of agriculture on some slopes until the 1950s, the majority of the catchment was nonetheless covered by forest at the time of the first official mapping 1830 AD. This resulted in the almost complete cessation of colluviation in the catchment, and the onset of erosion, which restarted gully head retreat into phase 4 sediments from the base of the gully (Figure 11e). This has led to a resumption of sedimentation on the gully fan, covering a medieval irrigation trench and dated to ~350 a. With gully head retreat continuing to its present position half way up the gully thalweg, the process of gully erosion runs until

present times. Fan sediments from phase 5 are also the first Holocene fan sediments found to be intersected with floodplain deposits from the Elsava River. This phase marks also an apparent dramatic increase in floodplain sedimentation rate. We suggest that this increase of sediment supply may in turn have lead to a major change in flow regime from multi-thread to meandering (Montgomery, 2008).

6.5.6 Climate, human or threshold driven erosion?

In order to determine the mechanisms of catchment erosion and stability we first consider the way in which sediment supply from slopes to the gully, and the transport capacity of the gully, are modified. It is well established that the ratio of sediment supply and sediment transport capacity determines erosion and deposition within the channel bed, however the threshold at which one or the other occurs is dynamic. In our catchment, this is manifest in the cessation of gully head retreat at the end of phase 3, and abrupt transition to thalweg aggradation, which we interpret to be the result of a large increase in sediment supply, which has not been able to be matched thalweg sediment transport. This increase of sediment supply from the slopes coincides with medieval conversion of the forested landscape to agricultural fields, this suggesting human impact is the primary driven of this abrupt shift in gully thalweg supply and transport ratio in a system that would have otherwise maintained punctuated gully head retreat.

That this is the case is also evident in the most recent phase of gully activity, in which there has been a resurgence of thalweg incision. This can be attributed to a decline in sediment supply from slope erosion, due to partial reforestation of the catchment, as well as improved tillage practices in the remaining agricultural fields. The impact of humans on slope erosion is well documented, however we note that this does not necessarily result in sediment delivery to the fan and trunk stream, which is a crucial and neglected process in studies which attempt to link the timing of floodplain sediment deposition with human impact.

On the other hand, the degree to which sediment can be transported within the gully channel is a function of the sediment load and stream power. As noted above for most of the Holocene period, prior to human activity, the sediment load was comparatively low, however discharge within the stream is highly episodic, and is strongly dependant on antecedent conditions.

It is also apparent that during this period of lower sediment supply, gully head retreat was not a continuous process and was instead the result of punctuated or discrete incision events. This leads us to conclude that the key driver of these incision events was low frequency, high magnitude climatic events that were able to overcome the necessary hydrological thresholds for sustained overland flow. Comparing our record of incision events with regional records of hydrological change (Figure 12), high and low lake levels which are indicative for sustained

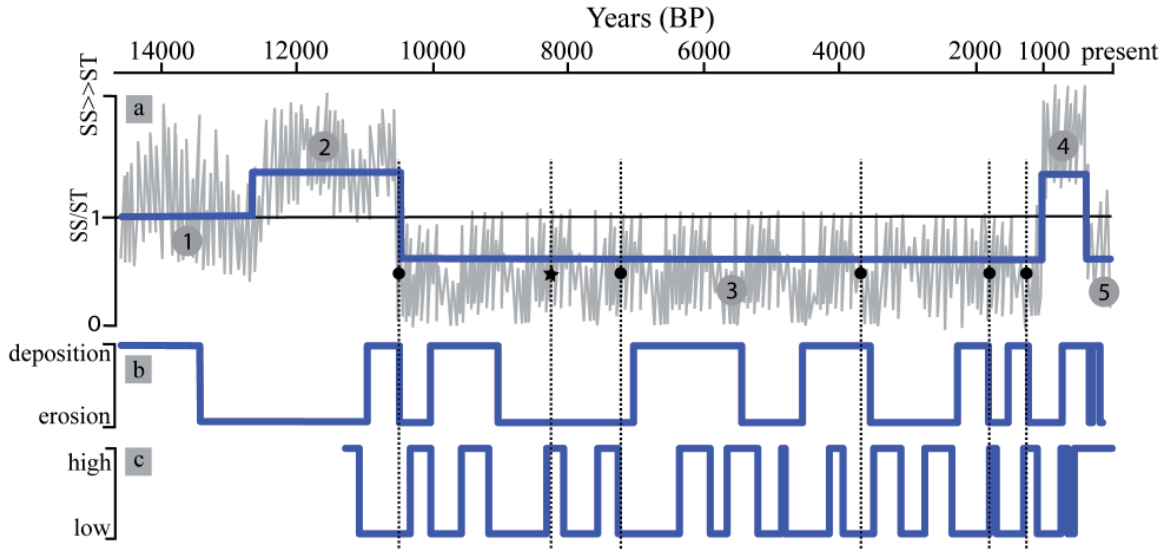

Figure 12: (a) Assumed ratio between sediment supply (SS) and sediment transport capacity (ST) in the gully thalweg during the Late Quaternary. The light grey line shows an idealised stochastic variation of this ratio about the mean (blue line). Black circles indicate gully head retreat events, and the star marks the timing of the only recorded Holocene debris flow event. Numbers indicate five phases in which the ratio shows a particular pattern: 1 = effective sediment transport connectivity; 2 = 1st fill-phase; 3 = 1st incision-phase; 4 = 2nd fill-phase; 5 = 2nd incision-phase, and correspond with phases to those in Figure 11.
(b) River erosion and deposition phases in Central Europe after Schirmer (1991) and Schirmer (2007). Phases dominated by deposition are interpreted by Schirmer (1991) as periods of relative morphological stability, whereas those dominated by erosion, also described as "breaks", are interpreted as active phases.
(c): Lake levels from Southern central Europe (French and Swiss Jura mountains) after Magny (2004). High lake levels are interpreted as wet climatic phases, and low lake levels as dry climatic phases.

changes in the water table (Magny, 2004), are not matched by gully incision. In contrast, we find that in 4/6 recorded events gully head retreat occurs directly at the point of transition between depositional (stable) and erosive (active) phases in the large rivers of Central Europe (Schirmer, 1991; Schirmer, 1997). This suggests there can be a correlation between the large climatic events responsible for gully incision and the broader climatic conditions necessary for initial transitions in the behaviour of large rivers. However, it is important to note that there are at least two incision events in our gully that do not match this interpretation, and importantly that there are also transitions in large river behaviour, for which we find no matching gully incision. In the case of the latter this can be explained by the fact that although large events are required for gully incision, not all large events may produce noticeable reaction. In the case of the former, gully incision has occurred within regional phase of large river erosion, a period in which large event may occur in our catchment, but not easily recorded in a large river. One such extreme runoff event also resulted in a unique debris

flow deposit. This occurred at the same time as a well established climatic deterioration phase ~ 8200 years ago, which indicates, that the catchments response is sensitive to climate change. Nonetheless it appears that the majority of the incision record throughout most of the Holocene has been generated by climatic events nested within large scale changes in rainfall magnitude. However these were not the same hydrological conditions that have raised water tables and sustained high lake levels.

6.5.7. Implications for sediment delivery from headwaters to floodplains and streams in small to medium scale catchments

An important finding is the contrasting role of vegetation. The first, and temporally most significant, effect is to maintain slope stability and thereby reduce sediment supply and increase sediment transport capacity within the thalweg itself, resulting in incision. The second is that its absence results in large scale slope erosion, excess sediment supply and reduced thalweg transport capacity. However, its overall effect is controversial (Temmerman et al., 2007). This comes from too simplistic models how vegetation acts on the landscape, which are only rarely considering the complex interaction of vegetation and land-surface-processes (Dietrich and Perron, 2006). From intensive in loess covered, soft undulating hills from the European Loess Belt, it is evident that gully incision is caused by linear concentration of sheet wash during high precipitation events on bare field surfaces (Valentin et al., 2005). Therefore the existence of old gullies was often attributed to human land use and high precipitation events (Vanwalleghem et al., 2003). We find that this result is not transferable to mountainous regions, where slopes are steeper and gullies develop in pre-shaped surface forms, in which surface runoff is canalised. Here, slopes vegetation cover is a pre-condition for gully incision.

Consequently we find, that sediment erosion of the gully thalweg and therefore sediment delivery to fans and floodplains (or lakes) occurs under forested conditions, happen in time periods, in which minor or no human impact on surface processes occur. In many studies all over the world has been observed, that sediment delivery to floodplains, lakes, fans, or gully thalweg sediments was enhanced during periods of low population density or when even no settlements are recorded (Anselmetti et al., 2007; Belyaev et al., 2004; Klimek and Latocha, 2007; Panin et al., 2009; Smolska, 2007). Most of these studies focused on sediment sinks such as lakes, fans and floodplains, and conclude that there is a delayed response in the sediment delivery from the slopes to sediment sinks or alternatively suggest a climatic rather than a human dominance on catchment erosion processes. If we consider headwater catchments in terms of a cascading sediment system (Lang et al., 2003), sediment sinks on the slopes or the gully thalweg must be filled up, until some tipping point, triggered

perhaps by a change to wetter conditions and exceeding of an internal threshold, after which sediment can be eroded and transported to a fan, floodplain and lake. Major difficulty arises in many studies when this sediment delivery and/or transport of sediment through the gully system and to the next sink is entirely attributed to human impact, since this process is more complex. But additionally, most of the studies attribute the time, when sediments are actually transported through the gully to the next sink also to high human impact. From our observations, we conclude that without considering slopes and gully thalweg sediments, the reconstruction of human impact only from fan, floodplain or lake sediments alone might lead to an erroneous interpretation of the sedimentary archive.

6.6 Conclusion

We find that the Late Quaternary surface processes of a steep gully system in Central Europe occur in multiple gully erosion and sedimentation cycles. These cycles depend largely on the relation between sediment supply and sediment transport capacity. After a phase of efficient sediment transport connectivity between the slopes, thalweg and fan during the deglacial period, the thalweg was aggraded during the Younger Dryas as a result of high sediment supply from the slopes and lower transport capacity in the thalweg, instigated by a reduction in vegetation during this time. The majority of the Holocene record (11500 – 1200 a) is then dominated by a series of gully incision events, which occur as a result of internal hydrological thresholds, and are most likely triggered by extreme climate events under well vegetated conditions. The onset of intense human agricultural activity during medieval times led to large scale slope erosion due to vegetation removal and subsequent thalweg – re-aggradation. The recovery of most of the catchment vegetation in the last ~ 500 years, has re-stabilised the slopes and modified the internal threshold of sediment supply/ sediment transport capacity, such that the gully has begun a new incision phase. This has implications for our understanding of sediment delivery from small headwater catchments to trunk streams, since the gully system itself has a large storage capacity and sediment delivery to the gully fan and trunk streams and their floodplains does not occur until vegetation has re-stabilised the slopes, and allow sediment transport capacity to increase.

7. QUANTIFICATION AND COMPARISON OF HUMAN AND NATURAL HOLOCENE SEDIMENT FLUX OF THE SLOPES AND GULLIES FROM CENTRAL EUROPE

(submitted to: *Geomorphology*)

7.1 Introduction

The Holocene sediment budgets of catchments of many sizes have become a topic of increasing geomorphic and archaeological interest in Central Europe (Fuchs et al., 2011; Houben et al., 2006; Stolz, 2011), especially with recent advances in absolute dating of sediment layers in catchments (Brown et al., 2009). Sediment budgets are also proved useful for analysing and quantifying human impact on catchments erosion and deposition (Reid and Dunne, 2003). For this purpose, the Coon Creek catchment in North America remains the benchmark for sediment budgets (Trimble, 2008), since this study was able to make extensive use of direct observations, and historic photographs for both quantification of sediment transfer and chronological control. Unfortunately such detailed sedimentary datasets are not available for the majority of catchments, especially when longer timescales, such as the Holocene, are of interest. In such cases modelling approaches have been used to tackle the complex erosion and accumulation story of river basins (de Moor and Verstraeten, 2008), however there is not enough known about the principles of sediment delivery process to model catchment evolution reliably in different landscapes (Trimble and Crosson, 2000). This is primarily due to a lack of knowledge about the vegetation cover further back in time, and also its changing influence upon land surface processes (Temmerman et al., 2007). Where humans have influenced the landscapes, they altered or removed the existing vegetation cover which subsequently changed the balance of geomorphological processes. Although a robust Holocene sediment budget suffers from these drawbacks, and a detailed knowledge of all the transport processes and storage dynamics of a catchment is difficult to construct over time (Dietrich et al., 1982), recent advances in chronological age control, and digital elevation models complemented with simple geostatistics, allow basic field data to be transformed into whole catchment sediment budgets. Applying these tools to a headwater catchment in the Spessart mountains of Central Europe, we are able to reliably reconstruct the Holocene sediment flux and in doing so aim to determine the mechanisms responsible for any variations, and the relationship between the source (inputs), sediment sinks, and the fate of sediment exported from the gully system.

7.2 Research area

We approach the problem of constructing a sediment budget by confining the catchment size to 0.42 km^2 and selected a region in Central Europe where pre-medieval agriculture is not expected to be likely and historical land use and settlement structure has been well researched (Denzer, 1996), such that any hillslope instability from agriculture is likely to have happened in only one phase.

Figure 13 shows the location and a map of the Kirschgraben research area, a gully catchment typical for the region, which ranges from 203 to 401 m in elevation and receives a mean annual rainfall of ~ 900 mm. The catchment exhibits a well incised gully system developed in steep slopes below a smooth plateau surface, a morphology most likely inherited from repeated glacial cycles of periglacial processes. The gully thalweg has a stepped longitudinal profile. At two locations outcrops of weathered sandstone restricts the gully thalweg. The geology is distinguished by Mesozoic red sandstone (Buntsandstein) forming a plateau which is loess-covered with a thickness of up to 3 m, and slopes where just a few cm of loess derived colluvial sediment is present. The loess mantle mostly originates in the late Last Glacial Maximum (LGM) (chapter 6). Both the sandstone and loess cover have undergone extensive weathering and soil development, in addition to the various periglacial and fluvial slope transport cycles, the latter of which is quantified in this study.

In terms of human influence, all modern existing settlements in the area had been established at ~ 1300 AD, which is known from written sources. However, the analysis of settlement types of the area suggests early medieval settlement activity from ~ 800 AD onwards (Denzer, 1996). A hamlet is located on the plateau of the research area, first mentioned historically in 1383 AD. At the end of the gully, where the gully fan and floodplain of the Elsava River intersect, a medieval moated site (~ 1200 – 1420 AD) was also recently found and excavated. Prior to this, there are scattered findings Neolithic findings (Bandkeramik: 3500-2500 BC and Michelsberg culture: 2200 – 1800 BC) (Bachmann, 1982) and the foundation of a small iron age house, however there is no evidence of any significant land-use during these periods. Throughout the entire catchment charcoal production sites (medieval – present) are found, testifying to the intensivity of past forest exploitation. Field terraces due to agricultural land-use are a further prominent landscape feature in the Kirschgraben catchment, although now covered by forest, they demonstrate that almost the whole catchment has been convicted for agricultural purposes for the last for several hundred years.

This paper builds on work described in chapter 6, and a brief summary of the major stratigraphy interpretation from this study is given here and in Table 5. After a phase of connectivity and sediment transport during the deglacial period (phase 1) and a phase of high sediment supply from the slopes to the gully thalweg during the Younger Dryas (YD, phase

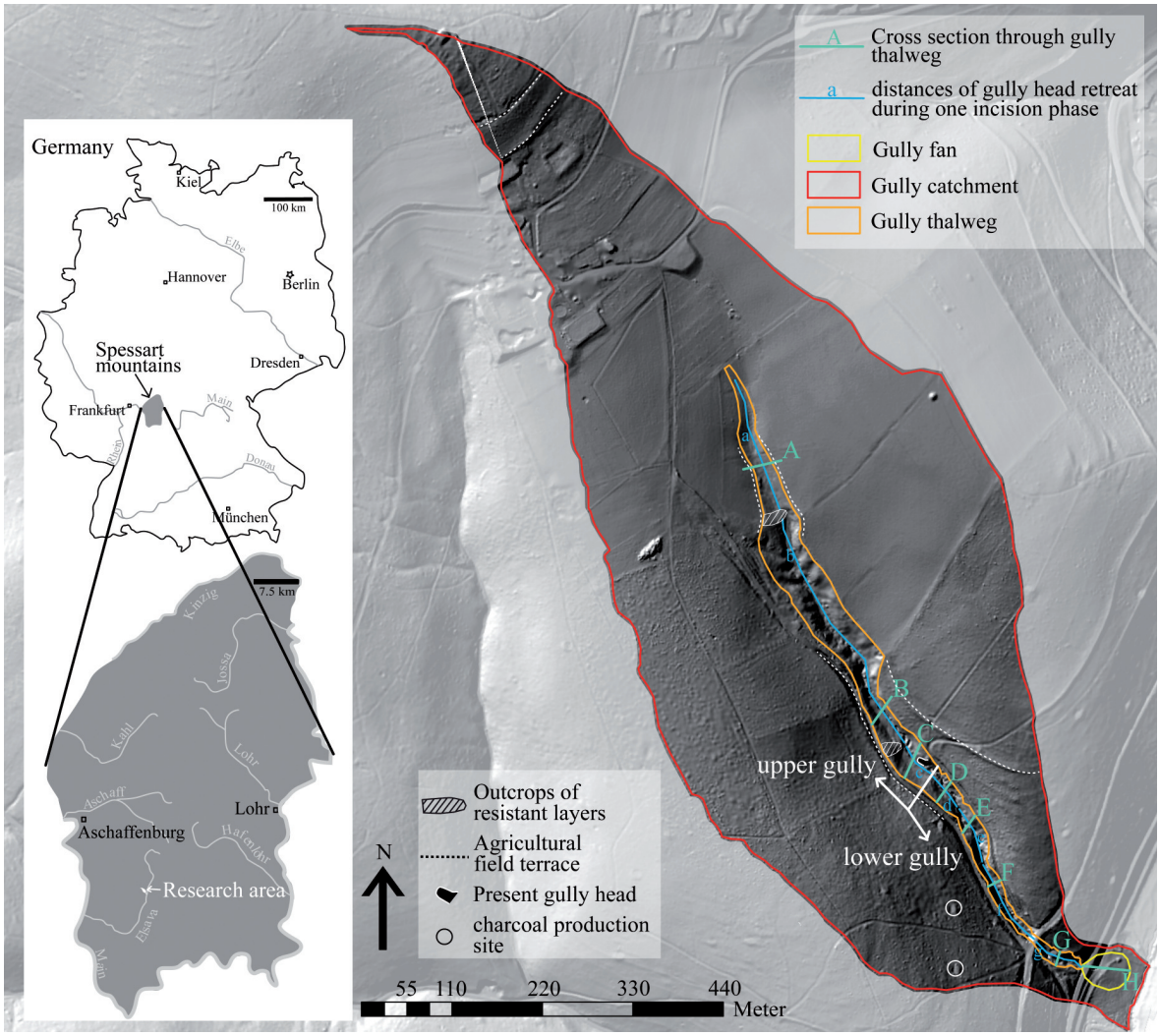

Figure 13: Location and map of the research area projected on the 1 m digital elevation model (DEM) (© by Bavarian Survey office Munich, 2011)

2), gully headcut retreat in the thalweg sediments was the dominant process for most of the Holocene (phase 3). Sediment supply form the slopes abruptly increased as a result of human deforestation in the medieval period, which also diminished the transport capacity of the channel and resulted in thalweg aggradation. The thalweg was then increasingly re-incised as catchment reforestation increased from 500 ys BP to present and sediment supply from the sloped decreased. Chapter 6 demonstrate a clear differentiation between human induced and natural sediment flux from stratigraphic evidence. This study suggests that the surface processes in this catchment strongly depend on the relation between sediment supply and sediment transport capacity.

Table 5: Phases of erosion and deposition in the Kirschgraben catchment

Phase [2]	Slope process [2]	Thalweg process [2]	Vegetation cover [2]	~ start [a]	~ end [a]
1	Sheet erosion solifluction	Aggradation and erosion	patchy	?	14700[1]
2	Sheet erosion solifluction	Aggradation	patchy	11500[1]	12800[1]
3	---	Gully head retreat	complete	12800[2]	1200[2]
4	Sheet erosion	Aggradation	patchy	1200[2]	500[2]
5	no	Gully head retreat	complete	500[2]	0

[1] From (Alley et al., 1993)
[2] From Larsen et al (submitted)

7.3 Methods

7.3.1 Separation in catchment areas

Because we base our quantification of past sediment flux on the major erosional processes that dominate the catchments sediment flux history (sheet erosion on the slopes and gully head retreat in the thalweg), we separated the quantification process in slope area and gully thalweg area. Due to different preservations states of the thalweg sediments, we separated it into lower and upper gully for practical reasons. Also, we divided the thalweg longitudinally into seven segments based on significant geomorphic changes in the gully profile, such as: the outcropping of resistant layers, sudden reduction in thalweg width and increase in gully gradient. For each segment a representative gully cross section containing estimates of both gully and sediment deposit geometries was used to estimate the total sediment volume. This approach does not claim to reconstruct all erosional phases, it targets the estimation of the overall amount of thalweg sediments as exact as possible.

7.3.2 Field and laboratory methods

Within the Kirschgraben catchment, we excavated 3 trenches in the fan area, 4 trenches through the gully thalweg sediments and 4 pits in the slope sediments, their size ranging between 15 to 35 m in length and 1 to 4 m in depth. Sediment thickness measurements from the trenches were complemented with 183 1m-corings covering the entire catchment, as

well as measurements from road exposures. Sediment sampled from each excavation were collected and analysed for granulometry and organic matter contents, and 40 OSL (Optical Stimulated Luminescence) and 11 ^{14}C (Radiocarbon)-age controls were established. To calculate the mass of the sediments, bulk density of each layer was calculated by estimating the percentage of fine grained soil (< 2mm) and coarse grained soil (> 2mm) in the exposures using the method of KA5 (AGBoden, 2005). In order to determine bulk density of the fine grained soil and including an error estimation, three to five constant volume samples per layer were taken in the field, dried at 105°C, and the average bulk density per layer was calculated from their weight. However, due to high gravel content and/or unstable conditions of the excavation sites this approach was not possible in all exposures. In this case we estimated bulk density from layers of the same age with similar sediment properties. For the coarse grained sediment, an average bulk density of 2.22 gcm^{-3} was assumed (Carmichael, 1984) which is the same as the local sandstone bedrock, the only lithology of which the gravel clasts are composed. Volume calculations were provided with a general 10 % error and divided into fine and coarse sediment on base of estimation from the field, and multiplied by the specific bulk density to calculate the mass.

7.3.3 LIDAR dataset, GIS database and statistical analysis

The sediment thickness and chronological data were integrated into an ArcGIS database. A 1m raster digital elevation model (airborne LiDAR data, (c) by Bavarian topographical survey) was used to establish the elevation of the coring sites, and to delineate flow directions, flow paths and the catchment boundary. Because we base our calculations on the major erosional processes that dominate the catchments sediment flux history, we separated the catchment into contributing slope area and gully thalweg area. For practicality we also divided the gully thalweg area into the lower and the upper gully areas. The longitudinal gully profile exhibits major breaks in slope, which corresponds to the outcrops of more resistant layers, or significant reduction of channel width. For each of these seven segments we use a representative gully thalweg stratigraphic cross section, which estimates the channel and sediment geometries, to calculate the total sediment volume along the entire thalweg. This approach does not claim to reconstruct all erosional phases, it targets the estimation of the overall amount of thalweg sediments as exact as possible. Providing an independent calculation of thalweg sediment volume and an additional estimation of the volume of colluvial deposits on the hillslopes, the thickness of colluvial layers was spatially modelled. In more detail,the thickness of the colluvial layer that developed under human influence, as measured in corings and excavations (n=183 points, thickness 0-1.44 m, mean thickness 0.37 m) was mapped by Universal Kriging (c). This approach combines a regression model that predicts the target variable (thickness) by a linear combination of covariates with a

stochastic model for the auto-correlated errors.

Assuming a dominant role of topography for the spatial distribution of the colluvial layer, the covariates for the deterministic model were derived from the digital elevation model using the appropriate functions in SAGA GIS (Conrad, 2007); in order to decrease the influence of small scale surface variation, especially with respect to the modern age road network, the DEM was first resampled to 10 m resolution using a mean filter. After analysing the dependence of the thickness of the colluvial layer on several such covariates, a linear combination of the following terrain attributes was used for the model:

- Curvature class after Dikau (1988). Curvatures were derived from the DEM using the algorithm by Zevenbergen and Thorne (1987), curvature classes were filtered with a 5x5 cell moving window majority filter in order to decrease small-scale variability. Some curvature classes (e.g. concave hillslope elements) are assumed to reflect topographic situations where colluvia are likely to be deposited. The variable 'curvature class' was used in the analysis as a factor.
- Flow accumulation (local catchment area of each raster cell), assuming that large catchment sizes provide more runoff for erosion of soils and colluvial layers. This covariate was $\log_{10}$-transformed.
- Mean catchment slope, i.e. slope gradient averaged over the local catchment area of each raster cell). It is hypothesised that steep catchments produce more colluvium.
- Stream power index, calculated by multiplying local specific catchment area with the tangent of local slope (Moore et al., 1993). It is assumed that high stream power is indicative of local erosion while low stream power may promote deposition. This attribute was also $\log_{10}$-transformed.

With the function variofit of geoR (Ribeiro and Diggle, 2001), a 'pure nugget' model with a nugget of 0.065 was fitted, using a weighted least squares method, to the empirical variogram of the trend residuals of the 183 data points. Using the krige.conv function in geoR, the colluvial layer thickness was then estimated for each node of a regular grid covering the study area. As the variogram exhibits no spatial autocorrelation of the trend residuals, the UK result is equivalent to a linear prediction model.

The model was validated using leave-one-out cross-validation (function xvalid in geoR), which means that the value of the target variable at each data point is compared to the value predicted by a model which does not include the respective data point. From the raster map of modelled colluvial layer thickness, the total volume of the colluvial layer was estimated by multiplying the thickness on each raster cell [m] with 100 m² (corresponding to the planimetric area of a cell) and summing up these values for the gully and hillslope subareas, respectively.

7.3.4 Calculation of sediment mass

To quantify the sediment mass of the different catchment areas, we calculated the total mass (*M*, in kilograms (kg)) of the catchment slope, thalweg and fan as separate sections. We calculated *M* using:

$$M = \sum f_i(AD)\rho_i \quad (1)$$

where the sediment volume is estimated as the product of area (A m^2) and distance or length (D m), and ρ is the bulk density of the sediment (g/cm^3). This volume is then separated into the estimated coarse and fine sediment fractions (f_i) and their respective bulk densities (ρ_i), with the resulting total mass equal to the sum of the mass of both these fractions. *v1* and *v2* being the volume (m^3) estimates of the coarse and fine fractions (f_i) respectively from equation 1.

7.4 Results

All results are reported in Table 7, with *v1* and *v2* being the volume (m^3) estimates of the coarse and fine fractions (f_i) respectively from equation 1.

7.4.1 Quantification of slope erosion

The Holocene colluvial layer can be identified by an almost homogenous colour (on the 10YR sheet of the Munsell soil colour chart) and nearly constant bulk density (on average 1.3827 g/cm³ ± 0.02; n = 9) measurements. In order to determine the spatial distribution of the layer using as much field data as possible, we excavated 8 trenches, and collected 183 1m-core samples throughout the entire catchment. As described in the methods section, the thickness of the colluvial layers as determined in the 183 core samples was predicted on a 10m raster using Universal Kriging. Generally, the predicted map reflects our field data. The resulting map (Figure 14) indicates thick colluvial deposits along the gully thalweg, on the adjacent footslopes, and in the uppermost quarter of the catchment. Generally, the map reproduces the fact that the total thickness of the Holocene colluvial sediments increases downslope, this increase being more pronounced for slopes with a higher inclination (Figure 14a). In the NW of the catchment slopes are less steep and therefore the layer thickness is relatively high. Agricultural field terraces, clearly visible in Figure 14 as areas of artificially increased sediment thickness are mostly located at the lower slope and therefore do not alter

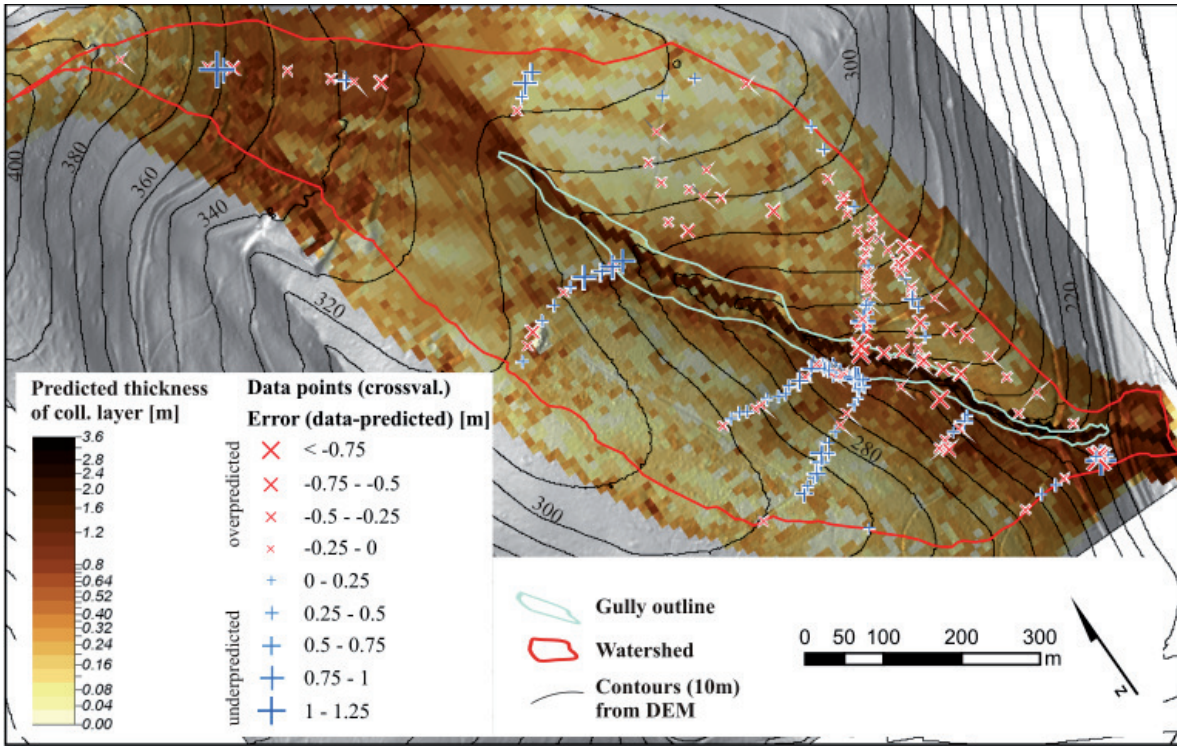

Figure 14: Predicted thickness of the Holocene colluvial layer in the Kirschgraben catchment area. The points at the locations of corings and excavations (n=183) indicate under- and overprediction by the UK model as calculated using leave-one-out cross-validation.

the general trend of increasing sediment thickness downslope. Point signatures in Figure 14 show the location of the 183 corings and indicate whether (and to which degree) colluvial thickness was over- or underestimated by the UK model (result of leave-one-out cross-validation). It appears that there is a tendency of overpredicting colluvial thickness on the left side of the gully, with considerable overestimation towards the gully margins, and a tendency of underprediction on the right side.

The distribution of measured and predicted colluvial thickness (Figure 15a) shows that the median of measured and predicted values is similar, both distributions are positively skewed, but that the distributions strongly differ in their spread. Due to the use of a statistical relationship of the target variable and the covariates used in the interpolation, some of the predicted values exceed the highest one measured in the field (n=90, 1.4% of raster cells), or even fall below zero (n=309, 4.9%). Hence, for the subsequent calculation of volume, negative values were set to zero. Figure 15b shows a cross-validation comparison of measured and predicted colluvial thickness for the 183 sites where thickness of the colluvial layers was mapped. The graph shows that low thickness tends to be overestimated while higher thickness tends to be underestimated by the model; the coefficient of determination of a linear regression (dotted line in Figure 15b) is R^2=0.35.

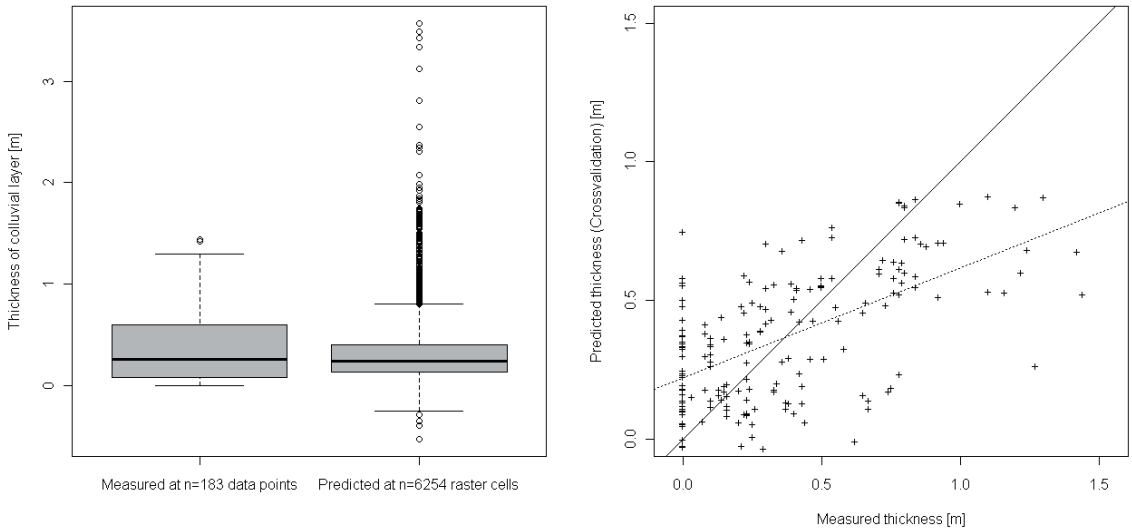

Figure 15
(a) boxplots of the distributions of measured (n=183 data points) and predicted (n=6254 raster cells) thickness of the Holocene colluvial layer. (b) The box forms the interquartile range (q75-q25), with the thick lines indicateing the median value. The whiskers extend 1.5 times the interquartile range, and data exceeding this range (outliers) are plotted as single points. (b) Measured vs. predicted thickness at 183 data points (corings, excavation sites) produced by leave-one-out cross-validation. The continuous line represents a 1:1 fit of predicted and measured data, the dotted shows the simple linear regression.

By adding up the predicted colluvial thickness within the mapped gully outline and within the remaining catchment, respectively, the volume of the colluvial layers was estimated for the 'gully' and 'hillslope' subunits (Table 6 shows descriptive statistics of the predicted colluvial thickness and the volume calculation). Based on these calculations, the colluvial deposits within the gully subunit amount to 20941 m³, and to 118480 m³ in the remaining hillslope

	Gully	**Hillslope**
Area [m²]	25600	397000
Range of colluvium thickness [m]	0.08-3.49	-0.25-3.34
Mean thickness [m]	0.82	0.30
Median thickness [m]	0.58	0.25
Std. deviation [m]	0.58	0.24
Volume estimation [m³]	20941	118480
	+/- 2048	+/- 31760
	139421	
	+/- 33808	
	(whole catchment)	

Table 6: Descriptive statistics of predicted colluvium thickness in two subunits of the Kirschgraben catchment and resulting estimation of colluvium volume

Table 7: Results of quantification

location[a]	phase of deposition[b]	phases of erosion[b]	area in cross section [m²]	distance of gully head retreat [m]	coarse sediment [%]	v1 [m³]	fine sediment [%]	v2 [m³]	ρ1 [g cm^{-3}]	ρ2 [g cm^{-3}]	m1 [t]	m2 [t]	m (total) [t]
Slopes													
	3	3			5	6236.97 ± 623.7	95	118502.43 ± 11850.24	2.22 ± 0.02	1.3827 ± 0.0002	13846.07 ± 1391.51	163853.31 ± 16385.35	177699.38 ± 16444.33
Thalweg[a]													
upper gully - A	2	2	8.04	110	25	221.1 ± 22.11	75	663.3 ± 66.33	2.22 ± 0.02	1.6466 ± 0.0193	490.84 ± 49.33	1092.19 ± 109.97	1583.03 ± 120.53
	3		25.3	110	5	139.04 ± 13.9	95	2641.76 ± 264.18	2.22 ± 0.02	1.4815 ± 0.02	308.67 ± 31.02	3913.77 ± 395.09	4222.44 ± 396.31
upper gully - B[c]	2	2	10.2	300	40	1224 ± 122.4	60	1836 ± 183.6	2.22 ± 0.02	1.6466 ± 0.0193	2717.28 ± 273.08	3023.16 ± 304.39	5740.44 ± 408.93
	3		18.9	300	5	283.2 ± 28.32	95	5380.8 ± 538.08	2.22 ± 0.02	1.3827 ± 0.02	628.70 ± 63.18	7440.03 ± 751.75	8068.74 ± 754.4
upper gully - C	2	2	10.2	60	40	244.8 ± 24.48	60	367.2 ± 36.72	2.22 ± 0.02	1.6466 ± 0.0193	543.46 ± 54.62	604.63 ± 60.88	1148.09 ± 81.89
	3		18.9	60	5	56.64 ± 5.66	95	1076.16 ± 107.62	2.22 ± 0.02	1.3827 ± 0.02	125.74 ± 12.64	1488.01 ± 150.35	1613.75 ± 150.88
lower gully - D	2	2	27.5	80	40	880 ± 88	60	1320 ± 132	2.22 ± 0.02	1.6466 ± 0.0193	1953.6 ± 196.33	1321.65 ± 133.07	3275.25 ± 237.18
	3	4	14.5	80	5	58 ± 5.8	95	1102 ± 110.2	2.22 ± 0.02	1.3827 ± 0.02	128.76 ± 12.94	1103.38 ± 111.49	1232.14 ± 112.24
lower gully - E	2	2	6.4	95	40	243.2 ± 24.32	60	364.8 ± 36.48	2.22 ± 0.02	1.6466 ± 0.0193	539.90 ± 54.26	366.45 ± 36.9	906.35 ± 65.62
	3	4	6.4	95	5	30.4 ± 3.04	95	577.6 ± 57.76	2.22 ± 0.02	1.3827 ± 0.02	67.49 ± 6.79	578.98 ± 58.5	646.47 ± 58.89
lower gully - F[d]	2	2	20	80	40	640 ± 64	60	960 ± 96	2.22 ± 0.02	1.6466 ± 0.0193	1420.8 ± 142.79	961.65 ± 96.82	2382.45 ± 172.52
	3	4	34	80	5	136 ± 13.6	95	2584 ± 258.4	2.22 ± 0.02	1.3827 ± 0.02	301.92 ± 30.34	2585.38 ± 261.23	2887.3 ± 262.99
lower gully - G	2	2	31	80	40	992 ± 99.2	60	1488 ± 148.8	2.22 ± 0.02	1.6466 ± 0.0193	2202.24 ± 221.32	1489.65 ± 149.99	3691.89 ± 267.36

Table 7 (continued)

	3		4	7.7		80		5	30.8 ± 3.08	95	585.2 ± 58.52	2.22 ± 0.02	1.3827 ± 0.02	68.38 ± 6.87		586.58 ± 59.27	654.96 ± 59.67	
		thickness 1[m][f]		thickness 2 [m][f]		thickness 3 [m][f]												
Fan - H[a]									39.32 ±			2.22 ±	1.42 ±			1058.47 ±	1145.77 ±	
Layer 5[e]	4	0.61		0.16		0		5	3.93	95	747.14 ± 74.71	0.02	0.0142	87.3 ± 8.77		106.38	106.74	
									728.27 ±			2.22 ±				728.27 ±	2345.02 ±	
Layer 4[e]	3	0.38		0.73		1.08		60	72.83	40	485.51 ± 48.55	0.02	1.5 ± 0.015	1616.76 ± 162.48		73.19	178.21	
									807.36 ±		3229.45 ±	2.22 ±				5491.04 ±	7283.38 ±	
Layer 3[e]	3	1.22		2.69		4.16		20	80.74	80	322.95	0.02	1.7 ± 0.017	1792.35 ± 180.13		551.84	580.5	
									207.31 ±			2.22 ±	1.56 ±			484.3 ±	944.63 ±	
Layer 2[e]	3	0.42		0.07		0		40	20.73	60	310.97 ± 31.1	0.02	0.016	460.23 ± 46.26		48.68	67.15	

[a] refers to Figure 13
[b] refers to Table 5
[c] refers to Figure 16
[d] refers to Figure 17
[e] refers to Figure 18 a
[f] refers to Figure 18 b

area. For the whole catchment, colluvial volume is estimated to be 139421m³. The results must be seen as a coarse estimation: The mean standard error of the UK model for colluvial thickness (+/- 0.27 m, resulting in a volume error of +/- 27 m³ for each 10x10m raster cell) is often in the range of predicted colluvial thickness, and hence the volume could be 60% lower or up to 90% higher than the prediction given here. Based on the spatial distribution of errors (Figure 14) we tend to consider the volume of the colluvial layers within the gully thalweg as overestimated. For this reason, and because we had more data available for the alternative thalweg sediment quantification described under x and x, we used the thalweg volume calculation from x for further calculations, and will be discusses there. After substracting the thalweg volume, the volume of colluvial deposits were incorporated into equation 1 and the total mass of the Holocene colluvial deposits within the catchment is estimated as 177.70 +/- 16.44 kt (Table 7).

7.4.2 Quantification of the gully thalweg erosion and deposition

7.4.2.1 The upper gully thalweg

The stratigraphic reconstruction and resulting area calculations for the upper gully area are shown in Figure 16, with the sedimentary sequence following cyclical erosion and deposition (phases 2 – 4 in Table 5).

In order to calculate the volume of sediment eroded in phase 3, we must first reconstruct

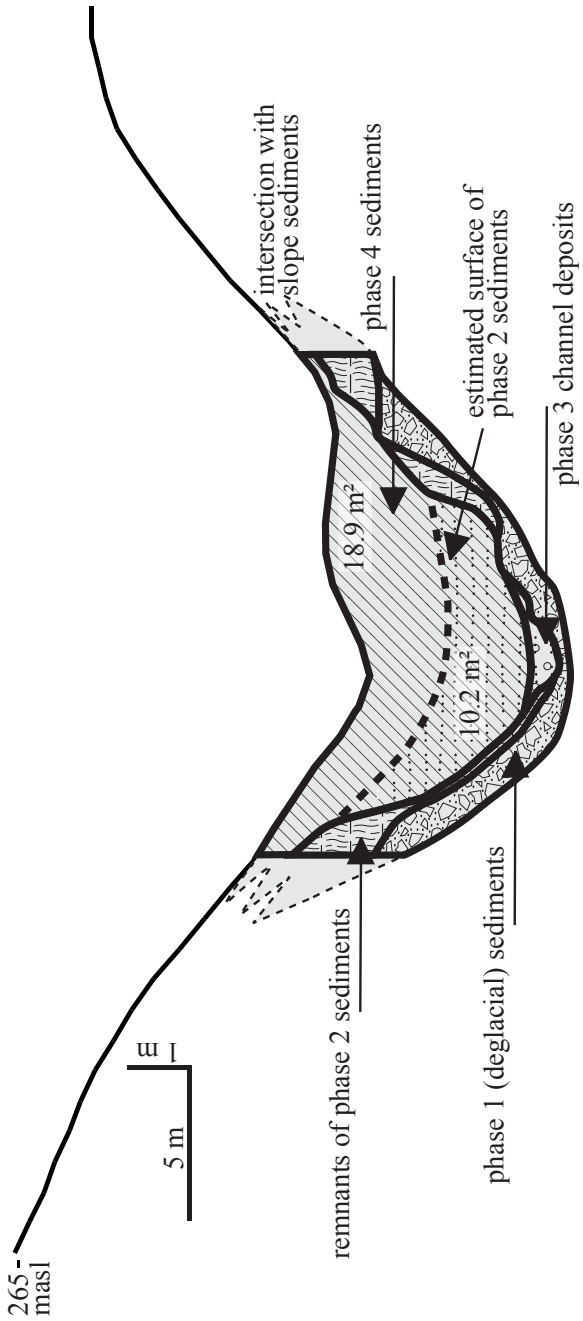

Figure 16
Cross-section through the gully thalweg sediments (modified from chapter 6)

the previous (phase 2) thalweg surface. This is done using the inclination of the phase 2 remnant deposit within the banks on both sides of the modern channel to create the probable phase 2 channel bed surface (Figure 14). The net volume of sediment eroded from the thalweg during phase 3 is therefore calculated using equation (1) with the channel area equal to the surface extending down to the periglacial base, and was found to be 8.47 ± 0.43 kt eroded in phase 3 (Table 7).

Sediments deposited during phase 4 are abundant in the upper thalweg section. Their area can be calculated directly without estimating the past profile (Table 6) with the resulting mass equal to 13.9 ± 0.87 kt (Table 7).

7.4.2.2 The lower gully thalweg

In the lower, narrower section of the gully thalweg, sediments from previous depositional phases are only rarely preserved, however we found four locations where residuals of phase 2 and/or phase 4 were present, allowing the late Pleistocene and late Holocene thalweg surface to be estimated for these locations (Figure 17).

Using equation (1) we estimate the lower gully to have eroded 10.26 ± 0.4 kt during phase 3 and 5.42 ± 0.3 kt during phase 5.

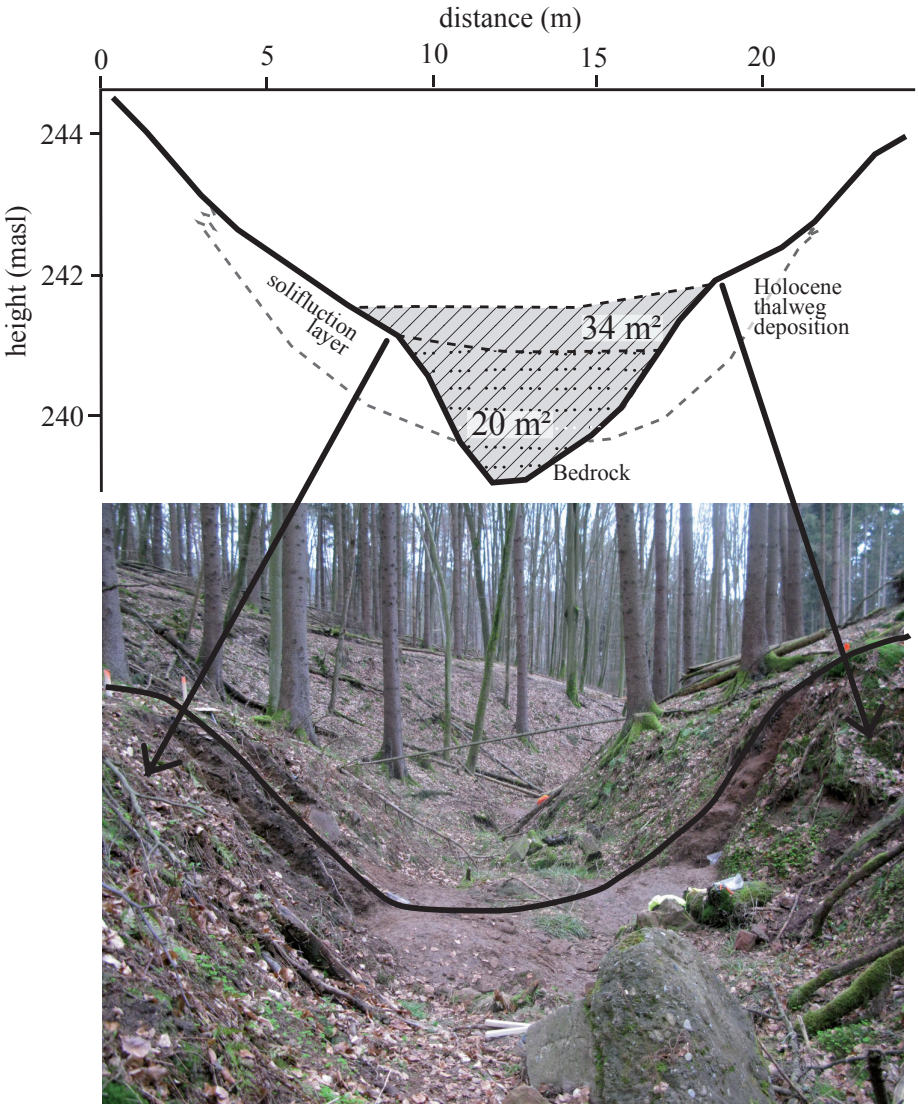

Figure 17: DEM extracted cross-sections through gully thalweg showing remnant deposits (upper graph). Field investigations (lower picture) showing those sediments on the left side of the photo to have been influenced by Late Pleistocene solifluction, and typical Holocene colluvial type deposits on the right. The boulder in the foreground indicates the erosional base of this part of the gully.

7.4.3 Quantification of the gully fan deposition

A composite stratigraphy comprised of the major sedimentary layers was constructed with these being deposited in phase 2 and phase 5 (Table 5) Fan apex sediments were generally not accessible, and this gap in data was overcome by estimating the height of the apex from a regression based on the modern surface topography, and field measurements of the change of sediment thickness of each separate layer, which were taken every meter in the exposures in the distal fan sediments (n = 7-16). The slopes of the regression equations for the layers 3 and 4, which constitutes the bulk of the fan apex were positive, while for layers 2 and 5 was negative (Figure 18a). The total height of the sum of there reconstructed apex layers (layer 3 and 4) was then estimated to be 6.09 m above the floodplain, which matches the actual topographic difference (6.1 m) and suggests that this basic reconstruction is realistic.

In order to calculate the volume of the Holocene fan deposits we extracted the approximate surface area of the fan from the DEM (A_{total} = 1996 m²). Assuming an idealised wedge shape of the fan, a circle segment was constructed with the same area, with a radius equal to the maximum edge length for the fan (50 m), we divided this wedge into three segments, which have equal edge lengths (16.6 m) and their areas were then calculated separately (219m², 656m², 1121m²) (Figure 18b). The thickness of each layer in the middle of each distance of each segment along the wedge radius then simply was multiplied by the area the results then used in equation (1) (Figure 18b).

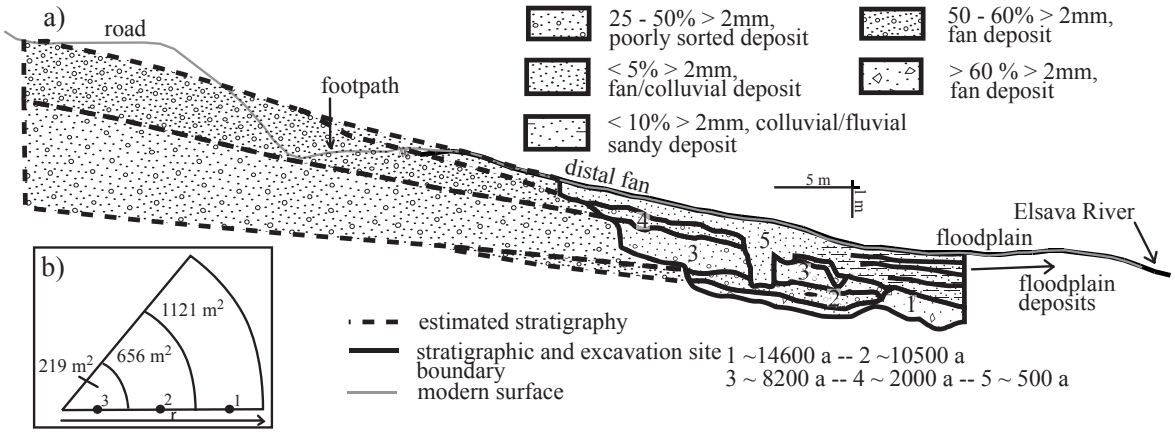

Figure 18: (a) Cross-section through the gully fan (modified from Larsen et al, submitted). Dashed lines indicate the estimated prediction of the sedimentary layers based on a regression of the existing topographic surface. (b) Schematic illustration of the quantification procedure of the fan based on an idealised geometry

7.5. Discussion

7.5.1 A Holocene sediment budget for the Kirschgraben catchment

Our quantification of the erosion and deposition processes from the deglacial period to the present is summarised in Figure 19 and Table 8, and a brief discussion of the assumptions and importance of these results are described here. Beginning in the YD, we cannot determine the original volume of sediment stored on the slopes, however the estimation of cross sectional geometry from the configuration of the preserved sediments allows us to estimate that ~ 18.73 ± 0.59 kt of sediment was transported to the gully thalweg within this 1400 year period (phase 2) of climatic cooling (- 5.6 °C relative to present) (Alley et al., 1993). The onset of the Holocene and the return of warmer climatic conditions also favoured the re-growth of catchment vegetation, and the initiation of gully head retreat due to reduced sediment supply from the slopes. This initiation ~ 10500 years ago began close to the gully mouth and therefore these initial sediments were deposited in the fan area. Our results indicate that

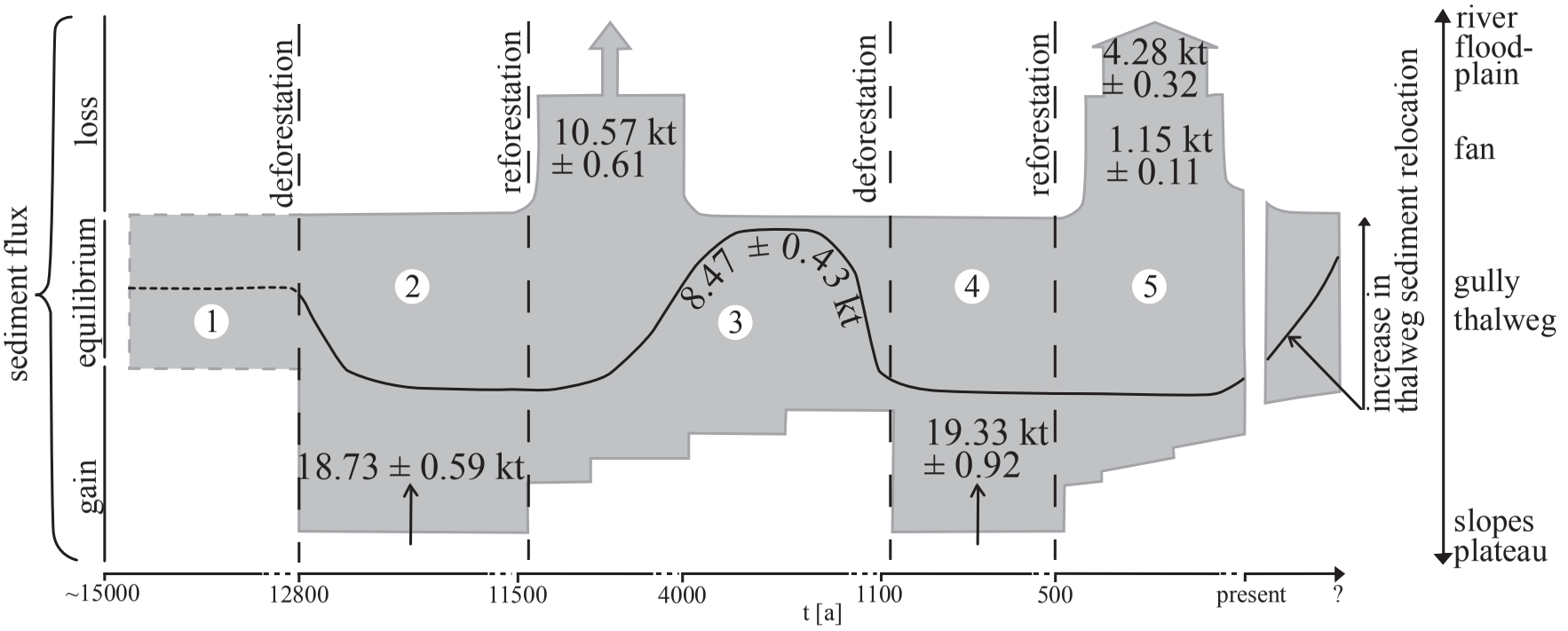

Figure 19: Schematic Holocene sediment budget for the Kirchgraben catchment in Central Europe. Numbers represent the phases detailed in Table 5. The solid line indicates approximate changes in the talweg sediment storage.

Table 8: Sediment flux of the Kirschgraben catchment

location[a]	phase[b]	sum m [kt]
slopes	4	177.7 ± 16.44
thalweg		
upper gully	3	8.47 ± 0.43
upper gully	4	13.90 ± 0.87
lower gully	3	10.26 ± 0.4
lower gully	5	5.42 ± 0.3
thalweg deposition	4	19.33 ± 0.92
thalweg deposition	2	18.73 ± 0.59
fan	5	1.15 ± 0.11
fan total	3	10.57 ± 0.61
layer 3 + 4	3	9.63 ± 0.61
layer 2	3	0.95 ± 0.07
floodplain		
transport to floodplain and stream	3	-0.32
transport to floodplain and stream	5	4.28 ± 0.32

[a] refers to Figure 13
[b] refers to Table 5

most of the deposition in these initial stages (phase 3) occurred in the distal part of the fan, and is calculated at only 0.9 ± 0.067 kt of sediment.

The continuation of gully head retreat was punctuated, which is well illustrated by the deposition of a debris flow (8200 a), which comprises the bulk of the fan apex. Poorly sorted (boulders to fines) sediment deposited during the YD as a result of solifluction processes was excavated from the lower gully most likely during a single event, which we estimate to be ~ 9.63 ± 0.61 kt and dominates the sediment budget of the fan. The accuracy of these masses can be checked by comparing the sum of the Early Holocene fan deposits (10.57 ± 0.61 kt) with the geometric estimate of the lower gully channel incised into the YD deposits from which the fan sediments are derived. The resulting estimate (10.26 ± 0.4 kt) is almost identical to the volume of Early Holocene fan sediments and suggests that the sediment budget is balanced entirely within the headwater catchment alone, and that fan development derived from the initial stages of thalweg incision does not supply significant sediment to the trunk streams. From 8200 – 1200a gully thalweg incision continued upstream, and we estimate that this process lead to the mobilisation of 8.47 t ± 0.43 kt of sediment which was reworked down the gully thalweg, but never exported to the fan or trunk stream. This period (phase 3) of relative stability marks the bulk of the timescale for the sediment budget presented here and therefore as a function of time, suggests a very low level of erosion from a headwater catchment under 'natural' conditions.

At the beginning of the medieval period intensive agriculture upon the slopes resulted in catchment wide deforestation and slope instability. This instability resulted in the most significant mobilisation of sediment in the entire sediment budget (phase 4), with an estimated 177.7 ± 16.44 kt eroded or reworked down-slope throughout the whole catchment. A further important result is that only ~ 19.33 ± 33 kt, or 11 % of this sediment was able to actually

enter the gully thalweg, with the rest of the sediment (89 %) remaining on the mid to lower slope segments, which in turn represent the most significant sediment store in the catchment. This small percentage of sediment delivery to the thalweg was however sufficient to lower the transport efficiency of the channel and therefore aggrade the channel bed to its highest level within the timescales investigated here.

The return of vegetation to most of the catchment following the end of the medieval period and continuing until early modern times stabilised the slopes and effectively stopped the delivery of sediments from the slopes to the thalweg, allowing the transport efficiency of the channel to increase. This has resulted in the lower gully incising down to resistant weathered layers or bedrock, and can be interpreted as the beginnings of a second phase of gully head retreat (phase 5), with the modern knickpoint midway up the channel long profile. The erosion of these medieval thalweg sediments has resulted in a second phase of fan deposition, however we estimate only 1.15 ± 0.11 kt of sediment has been deposited here, which is much lower than the mass excavated from the lower gully thalweg (5.42 ± 0.30 kt) as estimated from channel geometry. We can resolve this discrepancy if the remaining sediment (4.2 ± 0.32 kt), or ~ 79 % of the eroded thalweg, has been exported beyond the fan and incorporated into the alluvium and sediment load of the trunk stream (Elsava River).

7.5.2 Climatic versus human drivers in the sediment budget

Our results indicate that the two phases of slope erosion (YD and medieval period) delivered a similar mass of material to the thalweg, and although this may represent an upper limit to the ability of the slopes to supply sediment to the channel, it does suggest that both these phases of slope instability were able to erode similar amounts of material. This similarity is all the more remarkable given the very different mechanisms responsible for their occurrence, with the YD (phase 2) vegetation reduction being the result of climate deterioration, and widespread catchment deforestation at the beginning of the medieval period being the work of human activity. These different forcings appear to have the same net effect, which is the reduction of soil vegetation cover to levels that allow rill erosion of the soil surface and the delivery of sediment from the slopes to the gully channel without obstruction.

An important contrast is however the timescales over which these phases of instability occurred, with the YD climatic deterioration affecting slope erosion for 1400 years, while the medieval period produced the same result in only 600 years. The mechanisms for slope instability during the YD would have included extensive solifluction and other periglacial transport processes, and therefore complete deforestation is neither required nor likely (Mueller, 2011; Semmel, 2002). On the other hand, the absence of these relatively slow transport processes during the medieval period would require almost complete catchment

deforestation to allow soil cohesion from roots and flow obstruction from woody material to be removed. Thus we can estimate that the human control of slope erosion is a factor of ~2.3 more efficient than that occurring under the most favourable of natural conditions in headwater catchments.

7.5.3 The balance of sediment available from headwater catchments

Comparing the large phases of sediment input to the gully thalweg and those of sediment output, it is clear that more sediment is delivered to the thalweg during slope erosion than is exported during phases of slope stability. More specifically, the net export of sediment from the thalweg throughout the Holocene and up to the medieval period is ~ 56 % of the sediment supplied from the slopes during the YD, and the sediment exported during the last ~ 500 years is only ~ 28 % of the sediment supplied during the medieval period. A fundamental implication is that that the output of sediment from the gully thalweg does not necessarily contain the signal of catchment erosion that was imposed upon it, with the multitude of channel sediment transport and storage feedbacks and processes effectively filtering out any environmental response of headwater catchments to human and climatic perturbations that might be contained within the sediments.

Another important contrast in our results is the difference between the cycles of erosion and deposition from the YD and throughout most of the Holocene, and that which occurred from the medieval times to the present. In the first case, the sediment balance between slope erosion and thalweg and fan deposition can be completely accounted for, while in the second case almost 80 % of the sediment cannot be balanced and must therefore have been exported to the Elsava River alluvium and beyond. We explain this difference, despite a much longer and more extensive phase of gully head retreat up to the medieval period, as being due to the calibre of sediment supplied to the thalweg. As already discussed, the periglacial transport processes in the YD would enable a greater range of sediment size material (boulders to fine sediment) to be delivered directly to the thalweg, and in contrast the dominance of rill erosion processes following catchment deforestation in the medieval period limited the sediment size to mostly fine grained material. The aggradation of the thalweg with fine grained sediment in turn facilitated more rapid gully incision, and a much higher proportion of sediment able to be transported in suspension, than during any other time in the Holocene. This last phase of thalweg incision thus represents the first time that significant amounts of sediment, relative to the overall budget, have been exported beyond the gully fan and able to be incorporated into the alluvium of the trunk stream, and therefore this most recent and continuing phase of sediment export is also the most geomorphicly significant for the larger catchment network in the last 15 000 years. A final implication from these results is that the

dynamics of catchment processes inferred from deposits within large river basins cannot be determined unless variations in the sediment budgets of the headwater catchments from which they drain are known.

7.6 Conclusion

We find that the broad trends in sediment fluxes reveal that erosion and deposition processes in the catchment are largely controlled by the abundance of vegetation over this time. More specifically, increased slope erosion and thalweg sedimentation coincides with the removal of vegetation cover during the Younger Dryas or early medieval times, and subsequent reforestation during the early Holocene and again in early modern times stabilised the slopes leading to a dramatic reduction in the thalweg sediment supply. Adjusting to the new thresholds, in each case the gully then began to erode the thalweg sediment store through headward knickpoint retreat for much of the Holocene, and again reactivated in early modern times. Therefore, phases of deforestation are followed by sediment input to the thalweg from the slopes, and phases of reforestation are followed by a sediment output from the thalweg into the floodplain and trunk stream. Importantly, the quantified sediment fluxes reveal that these inputs and outputs are not always in balance, and that in general more sediment is delivered to the thalweg during slope erosion phases than is exported during phases of slope stability. In addition, we find that human driven slope instability is a factor of 2.3 more efficient than under the most favourable natural conditions in the Younger Dryas. The most recent, and continuing phase of sediment export is also the most geomorphically significant, and is the only time in the last ~15 000 years that a large percentage of the thalweg erosion budget (79 %) is able to be incorporated into the alluvium of trunk streams.

8. HOLOCENE SEDIMENT FLUX ORIGINATING IN DIFFERENT CULTIVATION TECHNIQUES IN A CENTRAL EUROPEAN CATCHMENT

(Manuscript, to be submitted to: *The Holocene)*

8.1 Introduction

The past soil erosion dynamics of many European landscapes remain difficult to constrain, as different catchments will have different responses to the same impacts, which might include deforestation or changes in land use practices. Despite this, it has been possible in some cases to assess broad changes in floodplain sedimentation and the river regime and link these to various changes in land use (Dotterweich, 2008; Trimble, 2009). Nonetheless, large uncertainties remain, especially in calculating actual rates of soil loss and sedimentation, and then linking these rates with quantitative estimates of other catchment conditions such as vegetation cover. In addition, it is also unclear if all impacts have a similar impact on soil erosion, or whether there are measurable differences depending on the type of land use that can be constrained. For example, it has been suggested that Neolithic hillslope sediment fluxes were less intensive than in Medieval times, despite exactly the same landscape being occupied in both cases (Bork and Lang, 2003). Surprisingly, medieval soil erosion is often still found to dominate the colluvial sediment record, even though hundreds of years of more recent agriculture have worked the same soil. This is even more intriguing given that by 1850 AD, an equal or higher amount of catchment deforestation and population levels were present (Schlueter, 1952). Since most of the Medieval soil erosion can be attributed to hillslope processes, it is difficult to disentangle any potential climatic contribution, however, some authors have suggested that this is only likely to be minor (Dotterweich and Dreibrodt, 2011; Lang, 2003). Therefore, the relative impact of different land-use techniques appears to be a crucial factor, and forms the basis of this investigation.

Whilst soil erosion and the resulting sediment flux can be estimated through the analysis of colluvial layers, the effect of different cultivation techniques can only be investigated if the changes in local vegetation cover can also be accounted for. This study aims to combine this information for the Holocene period by analysing charcoal fragments from the same sediments in which we quantify the sediment flux. It is found that cultivation techniques appear to be very different in the past and therefore must be considered in studies addressing past soil erosion rates. Furthermore, unsustainable medieval land-use yielded very high soil erosion rates and in this case led to an abandonment of agriculture and has an on-going influence upon the sediment dynamics of the present landscape.

8.2 Research area

The location and map of the Kirschgraben catchment is shown in Figure 20, which is a typical steep catchment in the Spessart Mountains (203 – 401m), 42 ha in size, and receives a mean annual rainfall of ~ 900 mm. The catchment exhibits a well incised gully system developed in steep slopes below a smooth plateau surface, a morphology most likely inherited from repeated glacial cycles of periglacial processes. The geology is distinguished by Mesozoic red sandstone (Buntsandstein) and forms a plateau which is loess-covered with a thickness of up to 3 m, and slopes where just a few cm of loess derived colluvial sediment is present. The loess mantle mostly originates in the late Last Glacial Maximum (LGM) (chapter 6). Both the sandstone and loess cover have undergone extensive weathering and soil development, in addition to the various periglacial and fluvial slope transport cycles.

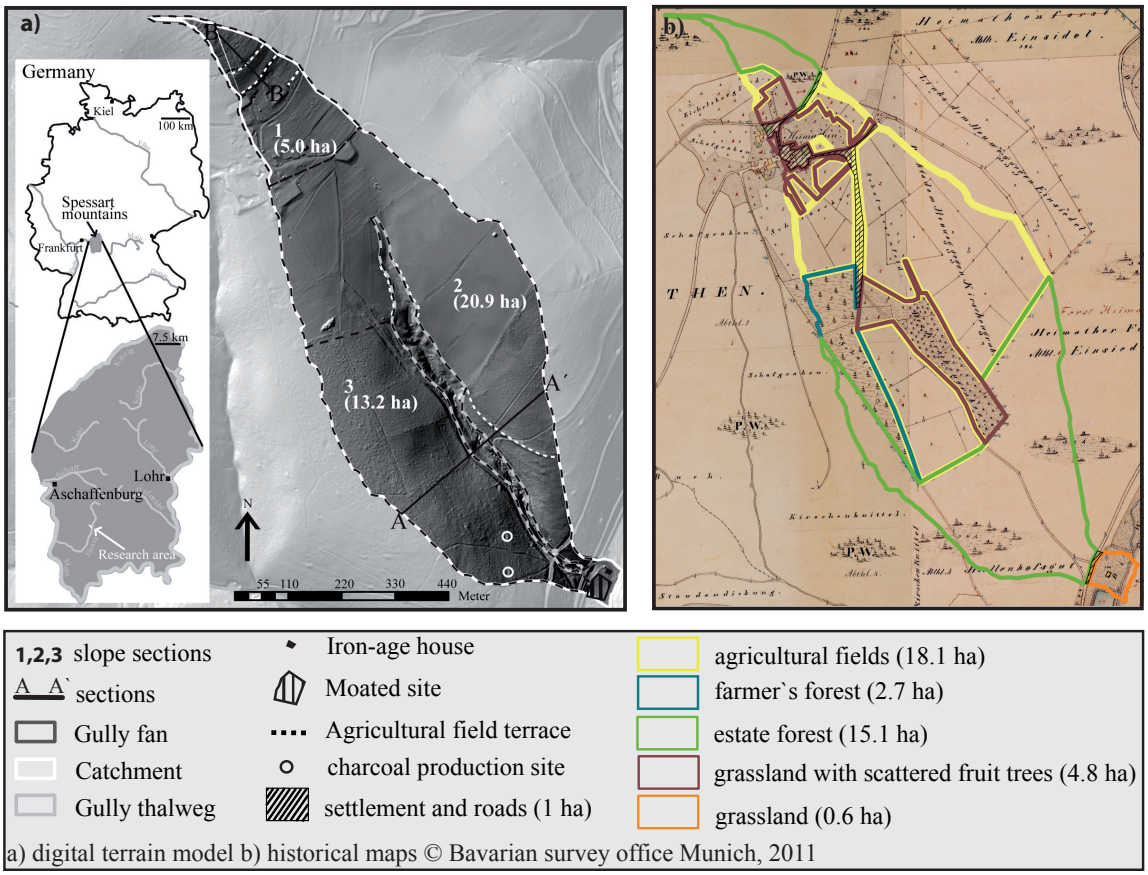

Figure 20: (a) Map of the Kirschgraben catchment within the Spessart mountains of Central Germany (inset). (b) Historical map of the research area from 1850 AD.

In terms of human influence, all modern existing settlements in the area had been established by ~ 1300 AD, according to written sources. However, analysis of settlement types of the area suggests early medieval settlement activity began from ~ 800 AD onwards (Denzer,

1996), and therefore it is likely that landscape cultivation has been fairly continuous since this time. A hamlet is located on the plateau of the research area, first mentioned historically in 1383 AD. At the end of the gully, where the gully fan and floodplain of the Elsava River intersect, a medieval moated site (~ 1200 – 1420 AD) was also recently found and excavated. Prior to this, there are also scattered Neolithic findings (Linear Pottery: 3500-2500 BC and Michelsberg culture: 2200 – 1800 BC) (Bachmann, 1982) and the foundation of a small iron age house (2800 – 1970 a), however, there is no evidence of any significant land-use during these earlier periods. Charcoal production sites (medieval – present) are also found throughout the entire catchment, testifying to the intensity of past forest exploitation. The development of field terraces due to agricultural practises are also a prominent landscape feature in the Kirschgraben catchment, although now covered by forest, they demonstrate that almost the whole catchment has been converted for agricultural purposes for at last several hundred years.

8.3 Methods

8.3.1 Field and laboratory analysis

Sediment thickness measurements from the trenches were complemented with 183 1m-corings covering the entire hillslopes of the catchment, as well as measurements from road exposures. In each trench the basal periglacial deposits were reached, ensuring that the complete Holocene sedimentary record was analysed. Vertical sections were carefully cleaned and each layer was sampled for grain size, bulk density, charcoal analysis, and OSL or radiocarbon dating, avoiding areas with enhanced bioturbation. To calculate the mass of the sediments as exact as possible, the percentage of fine (< 2 mm) and coarse grained sediment (> 2 mm) was estimated in each layer in the vertical sections of the excavation sites using the method of KA5 (AGBoden, 2005). Sediment < 2 mm was treated with H_2O_2 and subsequently analysed in a Laser Particle Size Analyser (Mastersizer 2000). The percentage of organic matter was measured by loss-on-ignition. Bulk density of the fine grained soil and their error estimation were determined by taking three to five constant volume samples per layer, drying them at 105°C, and calculating the average bulk density per layer from their weight. For the coarse grained sediment, an average bulk density of 2.22 gcm^{-3} was assumed (Carmichael, 1984), with a standard error of 1% , which is the same standard error as fine grained measurements. Sandstone is the local bedrock, the only lithology of which the gravel clasts are composed.

8.3.2 Charcoal analysis

Taxonomical determination of charcoal fragments from palaeo-archives can be used to give information about local past vegetation cover (Dreibrodt et al., 2009; Touflan et al., 2010). In this study charcoal fragments from kilns and from terrestrial sediments are analysed. Kiln sites were sampled along trenches in which their full lateral extension was exposed. Because the kilns did not present any observable stratification, ~ 500 g of material was randomly taken from the whole kiln section. For the analysis of charcoal record from sediments, ~ 20 l of sediment were sampled per layer based on the sediment sequence stratigraphy, and treated following a protocol adapted from (Carcaillet and Thinon, 1996). Samples were first watered and floating charcoal fragments were removed, then it was gently sieved through 5 mm, 2 mm and 400 µ mesh size, and charcoal fragments were extracted by hand from the sediments accumulated per class of size. Charcoal and sediments were dried and weighed to calculate their anthracomass (mg of charcoal / kg of sediment) which allows comparison of charcoal concentration (Carcaillet and Thinon, 1996). At least 30 charcoal pieces per sample were identified, from four size classes (< 2mm, 2 mm – 1cm, 1cm – 3 cm, > 3 cm in diameter), to minimize a biased analysis towards charcoal that is more or less likely to break into fragments. The taxonomical analysis was using a reference collection of modern charred wood species and wood anatomy atlases (Schweingruber, 1990). If all size classes were not abundant, the next smallest size class was identified instead. Usually, determination to the genus level is possible, but due to a good knowledge of plant distribution in Central Europe, determination to species is in most of the cases reliable (Nelle, 2003).

8.3.3 Optical Stimulated Luminescence (OSL)

After cleaning the surface of the exposure in pits, night time samples for OSL were collected directly into opaque plastic bags. Four samples were taken using opaque tubes forced into the exposure. Extracts of 90 – 200 µm sized quartz grains were obtained via standard treatments. Carbonates, feldspars, organic matter, heavy minerals and acid soluble fluorides were removed. Small multiple grain aliquots were prepared containing approximately 200 grains each. All OSL measurements were performed on a Risø TL-DA 15 reader applying a single-aliquot regenerative dose (SAR) protocol (Murray and Wintle, 2000; Wintle and Murray, 2006). The prepared quartz aliquots were stimulated with blue LED light ($\lambda = 470 \pm 30$ nm) at 125 °C for 40 s, and the resulting OSL signals were recorded through a Hoya U340 filter ($\lambda = 330 \pm 40$ nm). The preheat temperature was set to 240 °C (10 s) and the test dose cut-heat temperature to 200 °C, which were verified by performing preheat and dose recovery tests on samples HUB-0028, HUB-0030 and HUB-0031. The sediment dose rates

were estimated by measuring the contents of uranium, thorium and potassium applying high-resolution gamma ray spectrometry and Neutron Activation Analysis (NAA) respectively. No radioactive disequilibrium in the ^{238}U decay chain was detected. The cosmic-ray dose rates were estimated from geographic position, elevation and burial depths (Prescott and Hutton, 1988). Equivalent dose (De) distributions were analysed with the Central Age Model (CAM) and the Minimum Age Model (MAM, sigma b = 0.1) according Galbraith et al. (1999), taking into account dispersion parameters (standard deviation, overdispersion) and the shape of the paleodose distribution. Narrow unimodal De distributions were analysed using the Central Age Model (CAM). If positively skewed or broad multimodal De distributions were observed (overdispersion > 14%), the Minimum Age Model was applied (MAM). All palaeodose estimates, dose rates, and water contents as well as the final age calculation are provided in Table 9. OSL ages are given in thousands of years (ka) before the year of measurement (2010).

8.3.4 Radiocarbon dating

Radiocarbon dating was carried out to cross-check with OSL dating and where exposure conditions did not allow taking OSL samples. The high frequency of charcoal fragments in all layers made it possible to use charcoal for all radiocarbon datings. The use of short-lived woody species for radiocarbon data such as *Betula* and *Alnus* and the selection of charcoal that has a small number of year rings makes the date eventually more reliable by reducing the potential "inbuilt age" (Gavin, 2001; Gavin et al., 2003). Radiocarbon dating was conducted at the Leibniz-Laboratory for Radiometric Dating and Isotope Research at Kiel University, following standard methods (Nadeau et al., 1998; Nadeau et al., 1997). The conventional age has been calculated after Stuiver and Polach (1977). The calibration to calendar years was carried out using CALIB v5.01 (Reimer, 2004). Radiocarbon ages are given in cal BP (Table 10).

8.3.5 Dating of ceramic fragments by typological sequence

Where ceramic pieces were found in the sediments, a maximum sedimentation age was established in form of the relative dating by typological sequence (Forde-Johnston, 1974). Therefore the size, proportions, material, decoration of the ceramics were analysed for medieval and early modern times ceramic typology from the Institute of Archaeology of Kiel University.

Table 9: Optical stimulated luminescence (OSL) results

Sample[a]	Lab code	Water content [%]	U [ppm]	Th [ppm]	K [%]	Dose rate [Gy/ka]	Paleodose [Gy]	OSL age [ka]
A OSL 1	HUB-0104	20 ± 3	3.66 ± 0.18	14.14 ± 0.71	2.09 ± 0.1	3.24 ± 0.16	79.77 ± 1.63 (CAM)	24.6 ± 1.32
A OSL 2	HUB-0103	20 ± 3	3.29 ± 0.16	11.0 ± 0.55	2.04 ± 0.1	2.96 ± 0.15	3.21 ± 0.26 (MAM)	1.08 ± 0.1
A OSL 3	HUB-0101	21 ± 3	3.19 ± 0.16	11.56 ± 0.58	1.97 ± 0.1	2.88 ± 0.15	1.72 ± 0.18 (MAM)	0.60 ± 0.07
B OSL 1	HUB-0028	20 ± 3	2.51 ± 0.13	8.4 ± 0.42	2.29 ± 0.11	2.85 ± 0.15	32.53 ± 0.79 (CAM)	11.43 ± 0.67
B OSL 3	HUB-0030	20 ± 3	2.53 ± 0.13	9.6 ± 0.48	2.25 ± 0.11	2.88 ± 0.15	2.91 ± 0.19 (MAM)	1.01 ± 0.08
B OSL 4	HUB-0031	15 ± 3	1.77 ± 0.09	6.8 ± 0.34	2.99 ± 0.15	3.10 ± 0.16	1.01 ± 0.01 (CAM)	0.33 ± 0.02
C OSL 1	HUB-0146	10 ± 2	1.13 ± 0.06	4.61 ± 0.23	2.0 ± 0.1	2.48 ± 0.11	2.59 ± 0.07 (CAM)	1.05 ± 0.06
C OSL 2	HUB-0145	10 ± 2	1.22 ± 0.06	4.68 ± 0.23	2.15 ± 0.11	2.64 ± 0.12	1.34 ± 0.05 (CAM)	0.51 ± 0.03

Table 10: Radiocarbon dating (^{14}C) results

Sample[a]	Lab code	δ13C (‰)	δ14C age (years BP ±1σ)	Calibrated age (calBP 2σ-error bounds)[b]	Sample/wood type
B ^{14}C 1	KIA43249	-22.62 +/- 0.19	1140 +/-25	1168 (1070) 972	charcoal (Betula)
B ^{14}C 2	KIA41464	-26.40 +/- 0.19	925 +/- 25	921 (851) 781	charcoal (Betula)

[a] refers to labels in Figure 21
[b] calibrated ages include mean in brackets and 2σ-range

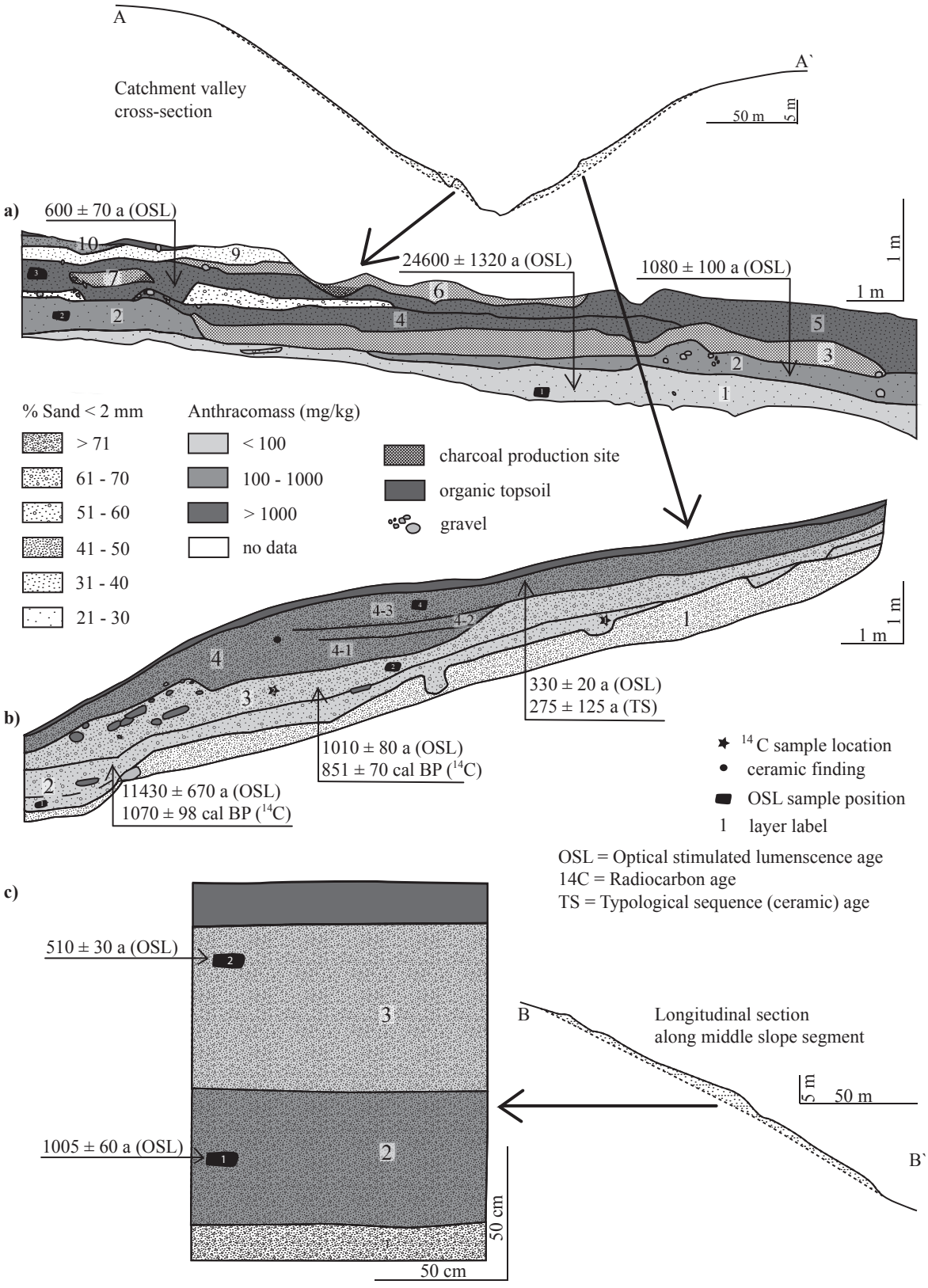

Figure 21 Exposures of hillslope sediments (a,b,c). Longitudinal and valley cross-sections extracted from the DEM. Locations are shown in Figure 20a.

8.4 Results

8.4.1 Stratigraphy

Three excavation sites were chosen to incorporate a range of slope positions, and their interpreted stratigraphic layers are shown in Figure 21, with sites 21a, 21b and 21c located where the colluvial layer reaches its largest thickness on the slope. Excavation site 2a also incorporates charcoal production sites, or kilns, which can be easily recognised as round topographic features partially dug into the sediments throughout many of the slopes within the catchment.

Table 11: Summary of results

excavation site[a]	layer[a]	age	sand content [%]	anthracomass [mg/kg]	kiln sites
2a	1	24600 ± 1320 a	24	96	
	2	1080 ± 100 a	28	344	
	3				kiln site
	4		32	9375	
	5			4428	
	6	600 ± 70 a	35	4974	
	7				kiln site
	8				kiln site
	9		37		
	10		64	950	
2b	1				
	2	11430 ± 470 a		48	
		1070 ± 98 cal BP			
	3	1010 ± 80 a	67	94	
		851 ± 70 cal BP			
	4-1		70	44	
	4-2		73	82	
	4-3	330 ± 20 a	82	102	
		275 ± 125 a			
2c	1		84.5		
	2	1050 ± 60 a	88	614	
	3	510 ± 30 a	88.1	45	

[a] refers to Figure 21

The age, sand content, and anthracomass (charcoal content) of all stratigraphic sections are given in Table 11. The basal hillslope sediments are a sandy weathering layer (layer 1 in 2b and c of unknown age. In Figure 21a and 21b a cryo-turbated and twisted silty sediment was deposited on top or remobilised between 24600 ± 1320 a (HUB-0104, exposure 2a), and

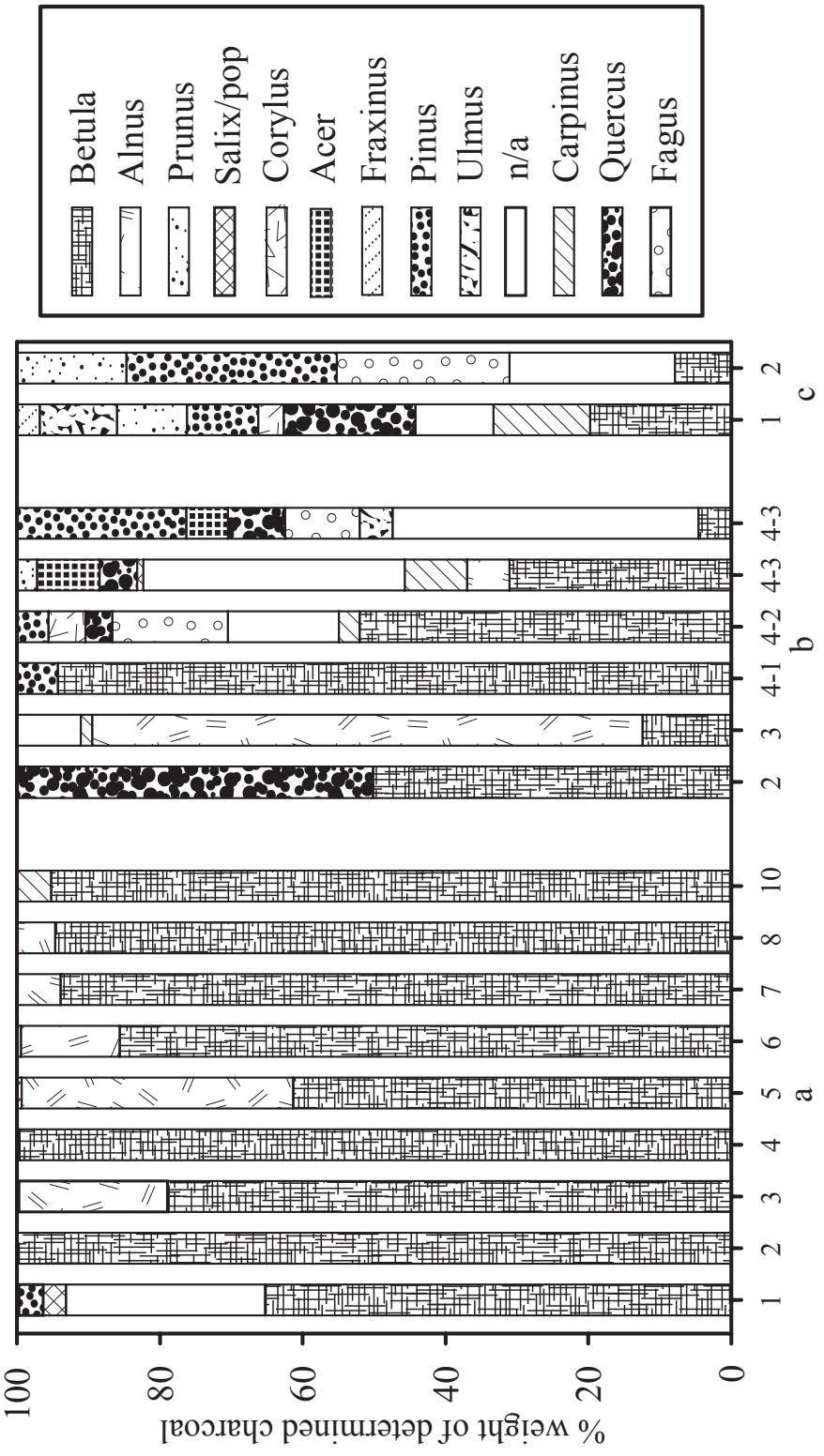

Figure 22: Percentage (wt %) of wood species from the charcoals fragments in each layer. The labels refer to the segments in Figure 21.

11430 ± 670 a (HUB-0028) and 1070 ± 98 cal BP (KIA43249) in exposure 2b, The charcoal content of these deposits are dominated by *Betula* and *Quercus*. The clear cryoturbation of this layer makes it obvious that the medieval age must be erroneous. Immediately above this deposit, the onset of medieval hillslope deposits is found at around 1050 a (layer 2 in 2a

and 2c and layer 3 in 2b). These are characterised by an increase in anthracomass and sand content, however, the peak in both these measurements is not reached until the next layers, which are approximately between 1050 and 300 years in age. In 2a and 2c the anthracomass decreases in the top layer, while the sand content increases. In 2b however, sand content and anthracomass generally increase towards the surface. The kiln sites in Figure 21a were dug into of the existing hillslope deposits during the entire period of colluviation, and are comprised entirely of charcoal (up to 5cm diameter) and ash. Other kiln deposits are also found in the sourrounding area, with similar charcoal contents.

8.4.2 Wood species analysis from charcoal fragments

In Figure 22a a clear dominance of the pioneer forest tree species *Betula* can be observed in all layers, accompagnied mostly by other pioneer species. Layer 1 shows besides *Betula* (65 %) a component of *Salix/Populus* (3 %) and *Pinus* (4 %). Layer 2 – 8 show a clear dominance of *Betula*, with changing components of mainly the pioneer wood species *Alnus*. In layer 10 a 5 % content of Carpinus can be detected, the only late successional forest tress species in the charcoal record of this excavation site

The wood species analysis of Figure 22b displays a more divers forest composition. Layer 2 shows a composition of half *Betula* and half *Quercus*. This composition changes dramatically in layer 3: While the late successional forest tree species *Quercus* and *Carpinus* hold only a minor percentage, the pioneer wood species *Betula* but especially *Alnus* dominate. In layer 4 the wood species composition from charcoal fragments shows an increasing diversity with decreasing depth and with it an increase in late successional wood species: Betula decreases from 94 % to only 6 %, and late successional forest tree species, like Carpinus, Fagus and Quercus increase as well as the diversity of pioneer species. Layer 4 – 3 was sampled and analysed 2 times for charcoal to investigate if major differences appear in the composition appear. Even though differences in wood species composition appear, the trend towards a reduction of Betula and an increase of other pioneer tree species as well as late succesional tree species is clearly visible.
Wood species analysis from Figure 22c displays a high diversity of species and in comparison with 3a and 3b also a relative high content of late successional forest species. Notable is the high component of Prunus in both layers.

8.5 Discussion

8.5.1 Pre- medieval forest composition

Anthracomass in the pre-Holocene layers is very low (< 100 mg/kg) (Figure 21a layer 1 and 21b layer 2). This is because natural fire events from lightning and/or extreme droughts (for Central European conditions) are rare and presumably not very wide spread. Therefore, the charcoal that is preserved is less likely to reflect the complete forest composition. Charcoal from these layers is dominated by *Betula*, a pioneer forest tree species, as well as *Pinus* and *Salix/populous*, with minor occurrences of *Quercus* and *Carpinus*. The total absence of *Fagus* in the charcoals of these layers could be due to human impact through the introduction of animal grazing in the forest, a widespread land-use in Central Europe (Williams, 2000). This hypothesis is supported by the presence of *Quercus* and *Betula,* which are favoured by animal grazed forests (Walentowski, 2001). In any case, the vegetation cover must have been sufficient to promote widespread slope stability such that no colluvial layers from pre-medieval Holocene times were developed. This is not to say that hillslopes were inactive, since it has been shown that soil can also be transported downhill by bioturbation and creeping under vegetated conditions (Hughes et al., 2009; Roering et al., 2002). However, the one order of magnitude increase in agricultural soil erosion rates in the late Holocene (Montgomery, 2007) is likely to obscure any record of soil erosion due to these processes, and therefore cannot be determined in this study.

8.5.2 Medieval and early modern times cultivation

The first medieval age for slope sediments coincides with the development of laminated Holocene colluvial layers. Given the evidence for relatively stable and vegetated hillslopes throughout most of the Holocene, these layers must originate from the clearing of catchment vegetation for agricultural use. This landscape conversion in turn led to greatly enhanced erosion rates, with subsequent deposition of colluvial hillslope sediments on the agricultural fields themselves. The build-up of these deposits at tenure borders over time were then transformed in places through parallel tilling, which turns over the soil and creates an effective sediment trap at the lowest topographical property border. The potential to trap eroded hillslope sediments was likely intensified by the presence of gravel piles, which developed through manual removal from the fields and their replacement at the field borders. This would have been common practice since large gravels are known to have hindered agricultural practises of the time (Keller, 1856).
The influence of medieval and early modern agriculture is also evident in the transition of

Table 12: Hillslope sediment flux

Land-use area[a]	V (coarse sediment) [m³]	V (fine sediment) [m³]	ρ1 [g/cm³]	ρ2 [g/cm³]	m (coarse sediment) [kt]	m (fine sediment) [kt]	m (total) [kt]	lowering rate [mm/yr]	erosion rate [t/yr]
			2.22 ±	1.38 ±					58.98 ±
1	1117.8 ± 111.78	21238.2 ± 2123.82	0.02	0.02	2481.52 ± 249.16	29366.06 ± 2967.17	31847.56 ± 2977.61	0.83 ± 0.09	6.31
			2.22 ±	1.38 ±					303.03 ±
2	11528 ± 1152.8	219032 ± 21903.2	0.02	0.02	25592.16 ± 2569.58	302855.55 ± 30600.73	328447.71 ± 30708.43	1.62 ± 0.17	32.41
			2.22 ±	1.38 ±					483.01 ±
3	7232.5 ± 723.25	137417.5 ± 13741.75	0.02	0.02	16056.15 ± 1612.12	190007.12 ± 19198.46	206063.33 ± 19266.02	1.62 ± 0.17	51.66

[a] for location see Figure 20a

wood species recorded in the charcoal (Figure 22). In each excavation the basal Holocene sediments show a distinct percentage of late successional wood species such as *Quercus* and *Carpinus*. They also have a lower sand content. The onset of medieval hillslope erosion, however, shows the divergence of wood species between sites, with 3a being clearly dominated by the pioneer species *Betula* and *Alnus*. The small percentage of the late successional wood species *Carpinus* in layer 10 indicates most likely the onset of the present forest, which is now dominated by late successional forest species. Figure 22b shows a clear dominance in pioneer wood species in the first Holocene layers, indicating a high degradation of the forest in the vicinity of the site. This is followed by an increase in diversity and late successional wood types in the younger layers, showing a less high intensity for forest exploitation since ~ early modern times. Figure 22c shows a high diversity and the abundance of late successional tree species throughout the layers, with species that are not detectable in the sediments of the sites 2a and b. The presence of *Prunus* is also a clear indicator of human impact. These differences in charcoal species composition suggest different land-use practices at the three different excavation sites (2a-c).

8.5.3 Holocene sediment flux

We use a classification of the different land use types to quantify hillslope soil erosion due to each of these land-uses. The areas in which the three different land-use types were cultivated was defined by the divergence of the charcoal record (see above) and the main topographic and stratigraphic features, from which the past land-use techniques are visible in the present landscape. Land-use area 1 (Figure 20a) can

be defined by the high density of agricultural field terraces, land-use area 2 by the abundance of one big agricultural field terrace mostly located at the lower slope segment. Land-use area 3 is indicated by the alternating deposition of pure charcoal layers eroded from charcoal production sites and sedimentary layers. The time period for the duration of specific land-uses were estimated from the ceramic, radiocarbon, and OSL derived ages. This can only by a rough estimation because of the error-range of the ages, and also because we were not able to date the very top and the very bottom of the sedimentary sequence (see location of samples in Figure 21a-c).
Chapter 7 quantified the Holocene sediment for this catchment and found that 90% of hillslope soil eroded during medieval times remains on the lower hillslopes, with the remainder delivered to the gully channel. Therefore, in order to provide accurate conditions prior to the onset of medieval soil erodion, the hillslope sediment volume calculated above is increased by 10% for land-use areas that are adjacent to the gully thalweg. The volume data was then converted to lowering rates (mm/yr) and erosion rates (t/yr) for each land use type according to the method of chapter 7, with the results given in Table 12.

8.5.4 Medieval and early modern times cultivation in land-use area 2

The amount of colluviation caused in this land-use area is enormous (303.03 ± 32.41 t/yr) and the lowering rate of 1.62 ± 0.17 mm/yr is comparable with the lowering rates from other intensively cultivated fields throughout the world (Montgomery, 2007). Additionally, wood species determined from the charcoal record indicate a highly degraded forest in medieval times, then an increase in charcoal production in early modern times, and finally a gradual reforestation to a high diversity forest until the present. This is also displayed in an increase of anthracomass with decreasing depth.

8.5.5 Medieval cultivation in land-use area 1

The medieval cultivation techniques in land-use area 1 show a comparatively low erosion rate of 58.98 ± 6.31 t/yr and a lowering rate of 0.83 ± 0.09 mm/yr. This low erosion rate also fits to those published by Montgomery (2007) for agriculture upon small field sizes, and the high abundance of agricultural field terraces within this land-use type suggest a slightly more sustainable agricultural technique. The close vicinity of the settlement are also the driver of wood species composition with a high *Prunus* content, and suggests a more garden-like agricultural cultivation with small fields and presumably stripes in between on which all tree-species find optimal conditions to grow and are cut down and burnt locally when they

produce to much shade for the crops cultivated nearby. This approach can be still observed in present times.

8.5.6 Shifting cultivation (field – grazing land – forest) on land-use area 3

In land-use area 3 there is no evidence for the occurrence of agricultural field terraces, and colluvial sediments are deposited mainly on the lower slope segment. To enable this colluviation, the fields above must have been temporarily deforested and used for agricultural purposes. Dating evidence suggests that this was the case between 1080 and 600 a. In turn, large charcoal production sites were dug partially into these colluvial layers, and subsequently buried by renewed colluviation. Charcoal production practices did not usually select distinct wood species (Ludemann, 2010; Nelle, 2003), and so it is likely that the forest of land-use area 3 was dominated by *Betula* and *Alnus* throughout the entire period of cultivation. It can therefore be argued that the development of alternate layering within charcoal production sites is the product of shifting cultivation of agriculture and forestry. This is similar to the modern birch-mountains technique from the ~ 300 km distant mountainous region in Central Europe (Oberdorfer and Reich, 1990; Walentowski, 2001),. These authors show that after an initial clearing of the forest in which timber was used for construction work, the surface was burnt to enrich the soil with nutrients and to clear the surface for a simple cultivation of field crops like wheat and oat. These fields are reported to have been highly productive for a few years of crop cultivation, but then productivity decreased quickly after a few years and these areas were subsequently used for grass and/ or hay production. Birche trees (*Betula*), which are the major pioneer wood species, were then encouraged to grow by limiting the grazing of animals and/ or even by spreading of birch seeds. After ~ 20 years, the birches were harvested and a new cultivation cycle began. To our knowledge, this study finds for the first time evidence that this cultivation technique must have been already common in medieval times, and therefore should be considered as a common cultivation technique, at least for the mountainous regions of Central Europe (Figure 23). This land-use technique has fundamentally altered the forest composition for hundreds of years and still influences the tree composition of modern forests (Oberdorfer and Reich, 1990). The quantified hillslope erosion for this cultivation technique is surprisingly high and even higher than the erosion rate of land-use area 2, especially considering that the period of intensive agriculture in this area was shorter since it was interrupted by phases of forestry and grassland. It can therefore be argued that such high erosion rates (483.01 ± 51.66 t/yr) and lowering rates (1.62 ± 0.17 mm/yr) are due to the absence of agricultural field terraces, which would have otherwise caused the erosion rates to decrease through time by a gradual decrease in slope

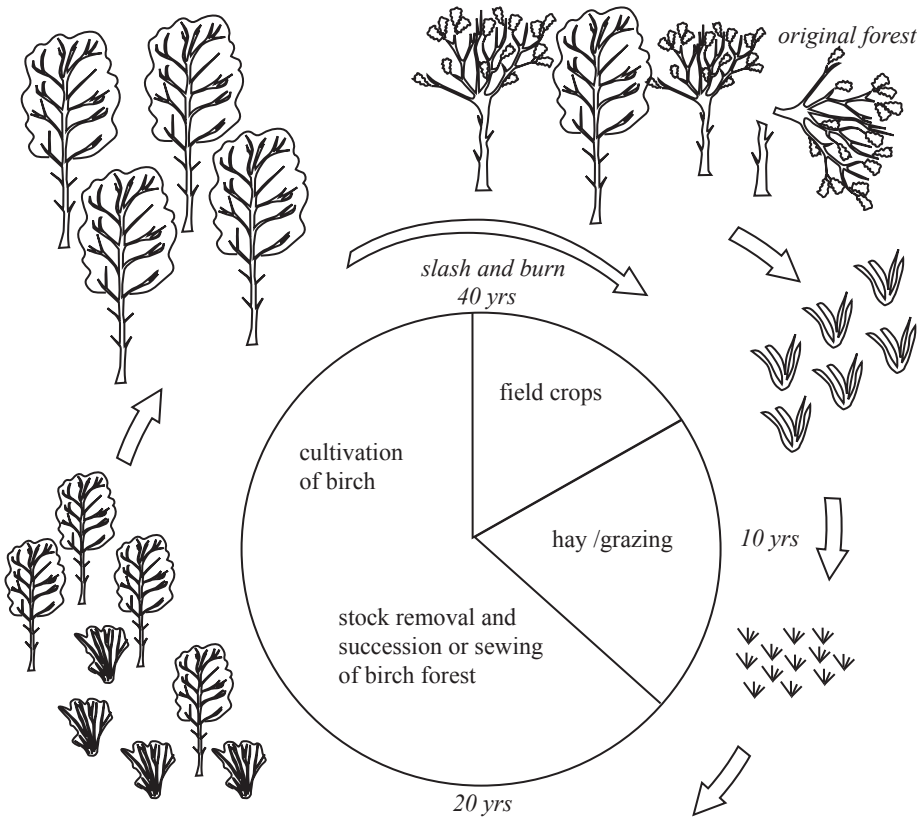

Figure 23: The birch-forest cultivation technique. Modified from Walentowski (2001)

8.6 Implications

8.6.1 Implications for studies dealing with past sediment flux

Cultivation techniques can be very variable throughout a catchment and control hillslope sediment flux. Therefore, it is absolutely necessary to take them into consideration in studies dealing with past soil erosion. This study provides evidence that smaller field sizes and the development of agricultural field terraces lead to a reduction in past sediment flux, and is a promising variable with which to explain variations in past soil erosion.

8.6.2 Medieval landscape degradation

This study has reconstructed soil erosion rates that are greater than the natural soil erosion rates through bioturbation and soil creep by at least two orders of magnitude (Montgomery, 2007). Lowering rates > 1 mm/yr equal the natural soil erosion in active alpine environments, but are also common upon cultivated fields with a moderate gradient, and means that soil production rates can no longer match these high erosion rates. Consequently, this implies that the medieval erosion rates presented here were likely to lead to a complete degradation of the land, and render agriculture impossible. Slope sediments in the research area were

eroded and re-deposited several times until they reached a long-term sediment sink in a field terrace or lower slope segment. This process is revealed in the grain size composition of the Holocene colluvial layers. During hundreds of years of cultivation slope sections susceptible to erosion lost their silty upper layers and greater amounts of sand from the underlying sandy weathering layer was gradually mixed into the colluvial deposits. We can therefore use the percentage of sand in the colluvial layer over depth as a measurement of degradation (Figure 24a).

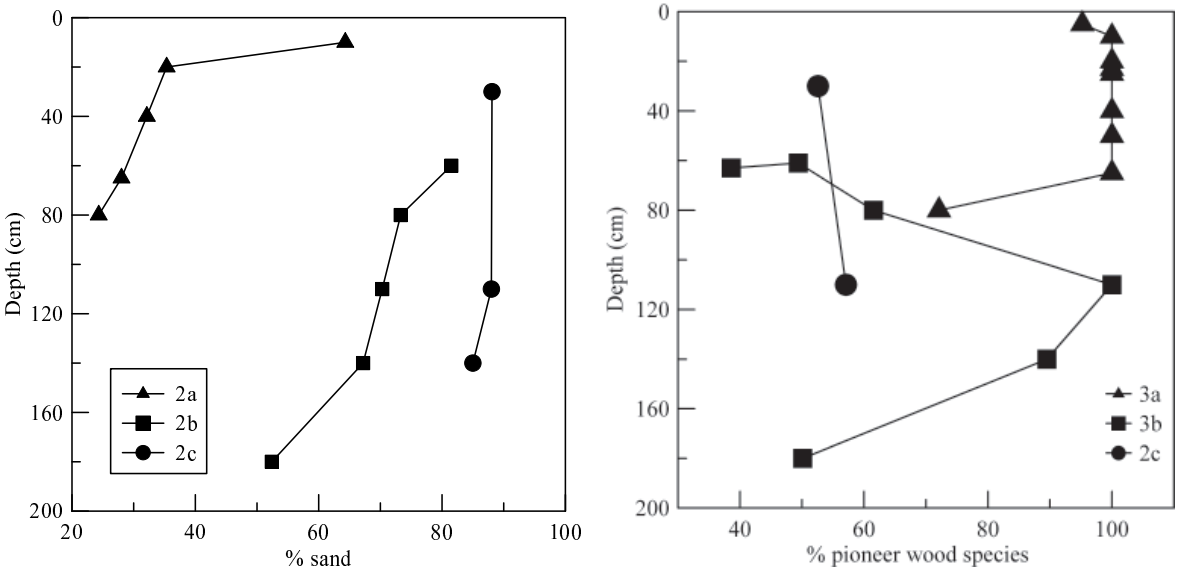

Figure 24: (a) Percentage of sand in sediment < 2mm. Labels refer to Figure 2. (b) percentage by weight of all pioneer wood species from the analysed charcoal fragments

This process irretrievably erodes the fertile Loess cover, however, despite this it is important to note that the natural vegetation in this area has widely been able to recover from medieval degradation (Figure 24b). It has been speculated that the intense drop in human population in late medieval times was due to the wide degradation of whole landscapes (Bork, 1998). It is similarly likely that the regional famine of the 1850s (Virchow, 1852) was also caused by an increase in population density upon a landscape which was recovering from medieval degradation, and had lost its very productive capacity.. The land use pattern revealed in the map from this period (Figure 20b) shows that despite high population pressures and the urgent need for more agricultural products, 42 % of the landscape was still covered with forest (and has increased to 70 % at the present). It is likely that only a few hundred years of intense agriculture and soil loss significantly reduced the productivity of the Kirschgraben catchment to such an extent that the land was no longer suitable for the cultivation techniques available at the time. Humans have not fundamentally changed their cultivation techniques on a global scale since medieval times and erosion rates from fields are still commonly >

1 mm (Montgomery, 2007), and therefore the area of permanently degraded landscapes are still increasing with time.

8.7 Conclusion

This study finds that the reconstruction of past land-use techniques is possible by using a combination of wood analysis from soil charcoal and the geomorphological context of the deposits in which they are contained. Furthermore, land-use techniques control differences in hillslope erosion rates within the same catchment. Conventional medieval and early modern agriculture caused a lowering rate of 1.62 ± 0.17 mm/yr on one catchment slope. The reconstructed land-use of the birch – mountains, a popular medieval land-use technique, surprisingly led to the same lowering rate as the common medieval agricultural practices, presumably due to the absence of field terrace construction using this technique. A much smaller erosion rate was found for the land-use area on where field sizes were small, presumably this was cultivated as gardening-like agriculture. The lowering rate for this land-use technique is approximately one order of magnitude lower: 0.83 ± 0.09 mm/yr. This means that different land-use techniques strongly influence the resulting hillslope soil erosion rates which in turn may be highly variable, and it is therefore important to address this issue when reconstructing past soil erosion rates.

9. THE LEGACY OF HISTORIC DAMMING IN CENTRAL EUROPEAN FLOODPLAINS

Chapter 6, 7 and 8 focus on the process, timing and quantity of sediment delivered from hillslopes and gullies to the adjacent trunk stream and its floodplain. On basis of these results, chapter 9 provides the outline for a study that focuses on the development of these floodplains in the Spessart mountains. It also evaluates the geomorphic significance of increased sediment load in the rivers originating from hillslope and/or gully erosion, as well as the often neglected effect of valley bottom damming on sediment trapping due to backwater effects.

9.1 State of the art and preliminary work

9.1.1 Introduction – The problem

Historically distinctive river forms among many rivers around the world are often masked by centuries, and in some cases millennia, of human influence. In a study of North American rivers, Walter and Merritts (2008) found evidence that human modification of riverscapes has been so intensive that even some fundamental notions of how rivers work (Leopold and Langbein, 1964; Leopold et al., 1964) may carry the bias of human influence (Montgomery, 2008). This study demonstrated that fundamental changes to the flow regimes of these rivers occurred in only ca. 200 years of European occupation due to damming of the valley bottoms, which in concert with increased soil erosion from changed land use, resulted in widespread aggradation of floodplain sediment, termed “legacy sediments”. Higher sediment delivery from the slopes alone cannot provide the necessary conditions for floodplain aggradation in these rivers, since the sediment storage capacity on slopes, gullies and colluvial fans is very high (Bork, 1983; Bork, 1988; Bork, 2006; Dotterweich, 2008; Dreibrodt et al., 2009) and only rarely coincides with adjacent alluvial valley sedimentation (Fuchs et al., 2011; Stolz, 2011). Therefore, we consider the valley bottom damming, and subsequent retardation of the flow regime, to be a fundamental requirement for this large scale morphological change.

9.1.2 Theoretical Framework

Meandering rivers of varying capacity are a common landscape feature in the valley bottoms of Central Europe. Traditionally considered of Holocene age, their floodplains were most likely deposited as overbank silts and clays by migrating single thread channels (Schirmer,

1995a). These systems are to our knowledge only sparsly described in low order streams, however larger capacity rivers and their deposits, such as the Main and Rhine river valleys in Germany, have received comparably greater attention (Becker and Schirmer, 1977; Hoffmann et al., 2008; Schirmer, 1995b). The overbank deposits of such large river systems are however more complex since they have already occurred in fluvial cycles over the Holocene (Schirmer, 1995a), although the largest and most recent deposits, beginning in the Medieval Age and continuing until the present, have been interpreted as more intense phases of aggradation due to human impact on the surrounding catchments (Hoffmann et al., 2008). This scenario entails high sediment delivery following deforestation from unstable and harvested slopes, and the clearing of riparian vegetation as mechanisms of sediment release, although the exact timing and source of these sediments remains largely speculative (Becker and Schirmer, 1977; Hoffmann et al., 2008; Lang et al., 2003; Rommens et al., 2006; Schirmer, 1995b; Szmanda et al., 2004). River systems as large as the Main and Rhine are however proportionately less sensitive to changes in flow regime and sediment delivery than the smaller order streams which feed them, since in this case valley bottom damming can influence the entire width of a river and its floodplain. We therefore expect the largest changes due to valley bottom damming to have occurred in these smaller order systems, where catchment processes remain poorly understood, and where the new EU legislation will have the greatest impact.

9.1.3 Historical dams

Intensive historic damming in the flood plains of the 1st to 3rd order streams in Germany is a well documented landscape feature (Gräf, 2006; Hahn, 2001; Klápště, 2005; Mager et al., 1989; Mück, 2010; Switalski, 2005). The ages of these dams are largely unknown, however this damming technique is believed to have been initiated during Roman occupation, from where it spread until high medieval times over Central and Northern Europe, and was subsequently abandoned from ~ 1900 AD onwards with the introduction of modern drive techniques (Downward and Skinner, 2005). Given their potential importance in determining morphological change, this study will determine and quantify the onset and magnitude of the impact of humans on the riverscapes of the Central European mountain belt. We differentiate between three types of historic dams: 1. Flow routing for irrigation to increase hay production (*Wässerwiesen*), 2. Control of instantaneous water release for the transport of logged wood to the trunk stream (rafting of timber), 3. Flow regulation for gravity driven power supply of mill drive systems (mills, mining, glas factories, hammer mills). It is unclear if the development of different technologies occurred simultanously, or occurred within distinct cultural phases. Furthermore, each dam type would have had different sediment trapping and flow regulation

efficiencies, with type 1 possibly trapping little sediment, while type 2 and 3 would have been much more efficient flow regulators. Therefore by examining the timing and magnitude of human impact, we will also answer specific questions concerning the different dam types and their effect on sediment transport, the timing of historical technology development, and the relative impact of these different technologies on riverscape transformations.

9.1.4 Implications for erosion

As hydrological agents dams reduce the magnitude and timing of flood peaks, increase the duration of low flow conditions, and ultimately may lead to lower geomorphological and ecological complexity (Graf, 2006). Schenk and Hupp (2009) demonstrated that historically dammed rivers in the US exhibit gaining sediment budgets upstream of these structures, while downstream they tend to be highly erosional, which in turn may lead to the development of armoured layers downstream of dams (Graf, 2006). In addition, hydraulic modelling suggests that historic mill dams can reduce flood velocities by up to 80% via backwater ponding (Pizzuto and O'Neal, 2009). The combination of these processes inevitably leads to the deposition of sediments upstream, and a higher potential for the erosion of sediments downstream of the dam, however only to the point at which the bed can be armoured and graded to the average flow conditions. Therefore, the destruction of historic dams through time, or the removal of dams as a consequence of the Water Framework Directive of the EU, has the potential to increase the bank erosion of dam derived legacy sediments as the channels gain greater stream power, become more unstable, and attempt to adjust to pre-damming conditions (Downward and Skinner, 2005; Walter and Merritts, 2008).

9.1.6 Importance and Impact

This future research will test if historical dams a typical Central European low mountain range, the Spessart Mountains, developed legacy sediments, and are therefore also vulnerable to erosion, through the processes described above. This research will directly inform and contribute to river management decisions by providing a reasonable estimate of the volume of legacy sediments and to evaluate a base for further research on erosional and accumulative processes after removal of dams. Futhermore, the restauration of altered systems are unlikely to be successful without an understanding of the dam-related alterations that created the present situation (Graf, 2006). If our hypotheses are proven to be right, we developed the

basic knowledge and methodology for a successful handeling of future dam removals all over the European Union in the next decade.

9.1.7 Study Area

This project will focus on 1st to 3rd order rivers in the Spessart Mountains (Figure 25), located in the heart of the Central German mountain belt and part of the upper Main River catchment (Figure 25). This area was chosen exemplarily for Central Europe since it is ideal because

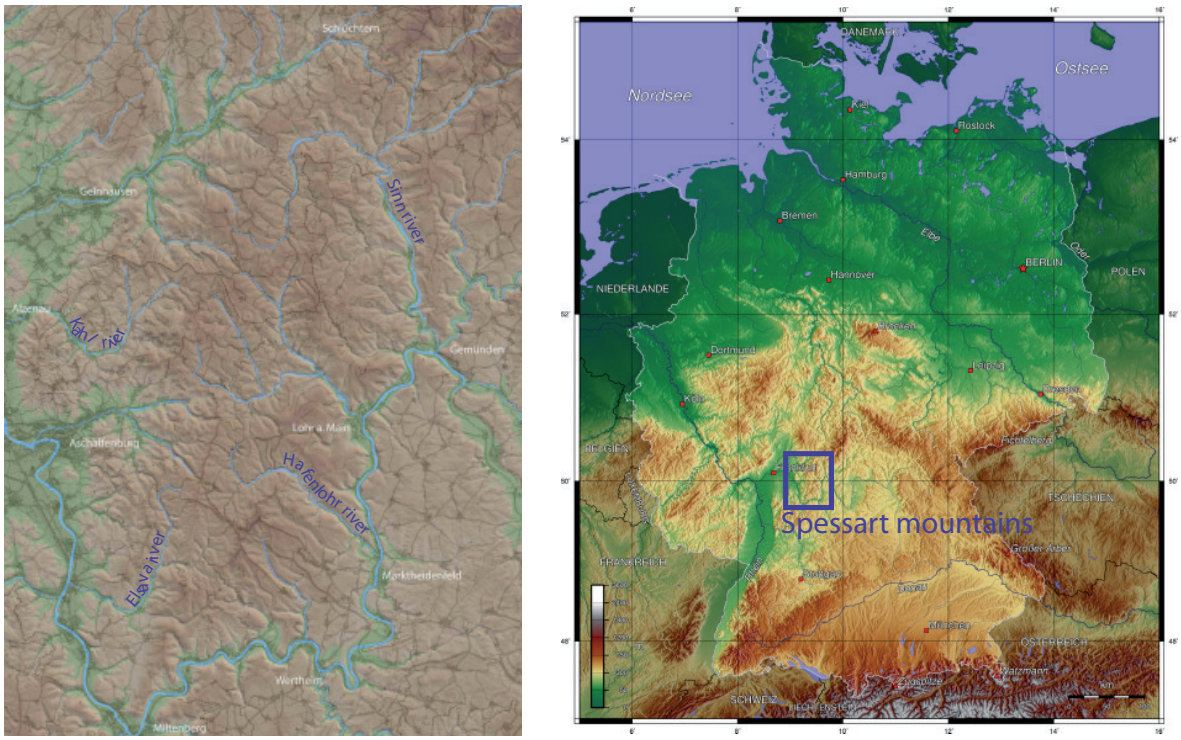

Figure 25: Left: Map of Spessart Mountains; right: Map of Central Europe (with rough location of the research area)

of the variety of historical damming features present in these valleys (Table 13), and also because of the imminent removal of these features under the Water Framework Directive[1] of the EU.

We will analyse four catchments of similar topography and geology but of different stream order, so as to control for increases in discharge and sediment load on the quantity of legacy sediments preserved behind dams. Specifically, the catchments are: The Hafenlohr (1st order

1 http://www.wasserrahmenrichtlinie.bayern.de/massnahmenprogramme/doc/rhein_mp_2009.pdf; "Maßnahmen zur Verbesserung der biologischen Durchgängigkeit der Fließgewässer", S.46.

Table 13: Type of dams

River	Type of dams
Kahl	mining, mills, glas factories
Elsava	mills, hammer mills
Hafenlohr	Mills, hammer mills), glas factories, rafting of timber, *Wässerwiesen*
Sinn	mills, *Wässerwiesen*

catchment), the Elsava and Kahl Rivers (2nd order catchments), and the Sinn (3rd order catchment) (Figure 25).

9.1.8 Existing data and previous work

We have evidence from two historical maps for the existence of dams and data bases in the proposed study area:

1. The "Pfinzing"-map (Figure 26) which provides the location of mill sites around 1600

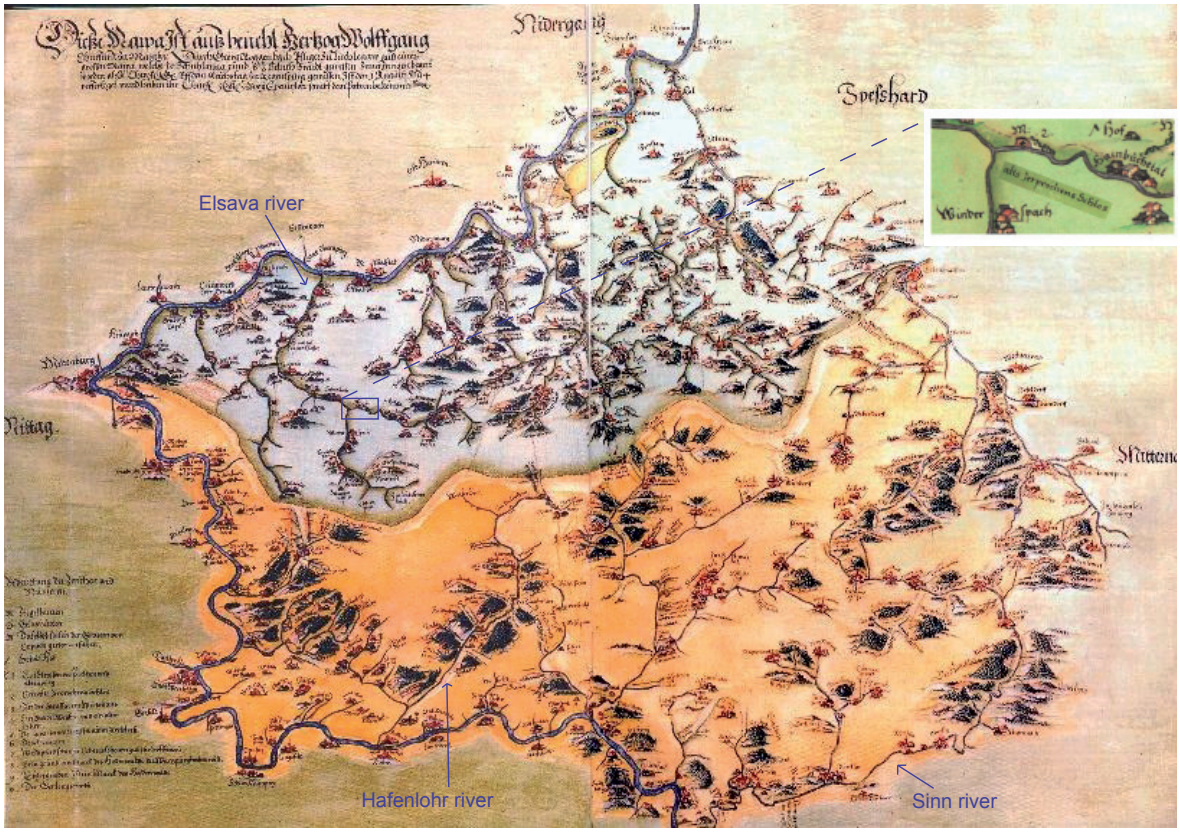

Figure 26: "Pfinzing" Spessart-map from 1594 (map is orientated with west to the top). The enlarged window shows the details of the mapped riverscapes: M2 describes a mill site (and subsequent valley bottom damming in that area).

AD. Its detail concerning rivers and infrastructure is unique for Germany at this time, and 2. The "Urkataster"-map (Figure 27) which reliably provides the location of all existent dams at around 1840 AD. This spatial data can be further supplemented by two important written sources: 1. "Sechserbuch" which provides accounts of Early Modern water utilisation techniques and possible the position of dams around the town Frammersbach (Leng, in prep), and 2. The "Wasserwirtschaftsamt" dataset which details the locations and properties of all existing dams in the research area.

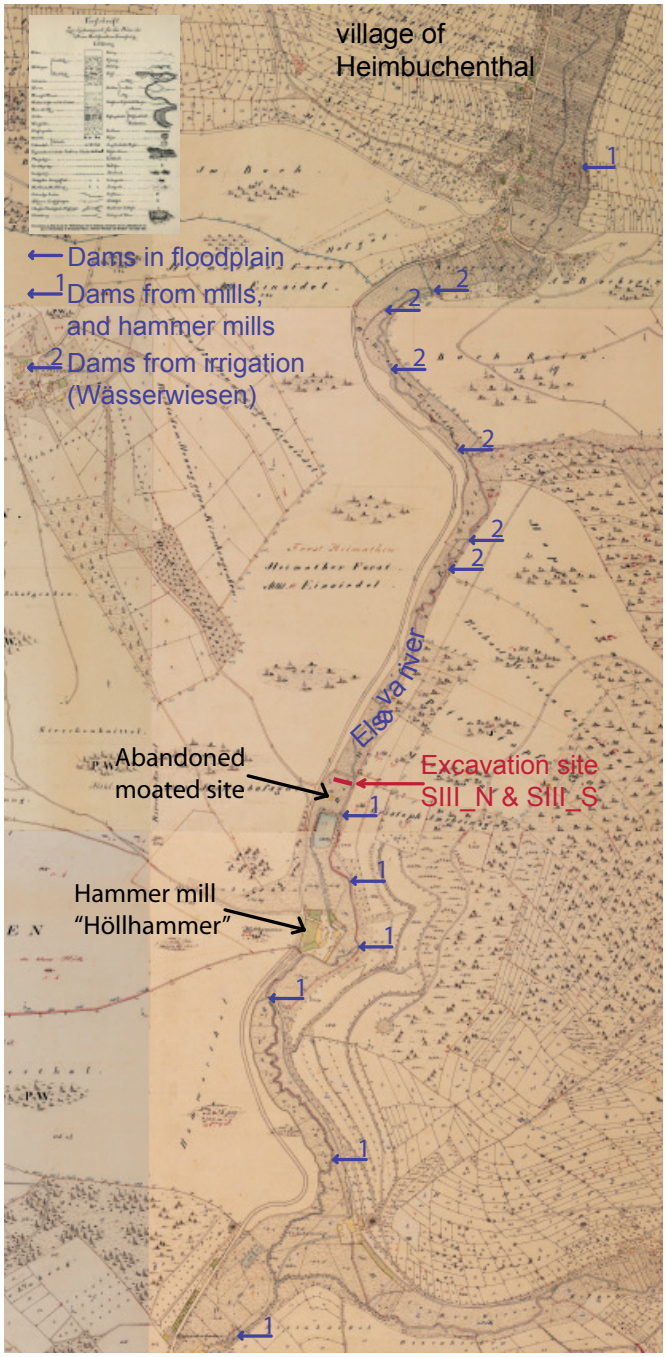

Preliminary analysis of high resolution digital elevation models has revealed that the floodplain sediments deposited behind dam structures can be accurately delineated and quantified remotely (Figure 28). This complements detailed stratigraphic investigations, of which the initial results reveal a clear sedimentary distinction between older Holocene channel sediments, and the well laminated floodplain loams which are the focus of this study (Figure 29). Our preliminary results indicate these valley bottoms have basal river gravels and sands which indicate high fluvial activity around 8150 ka, followed by a phase of stability marked by the development of extensive wetland soils. A mixed load multi-thread, presumably braided channel system, has subsequently incised into this

Figure 27: Extract from the Bavarian "Urkatasteraufnahme" referring to a part of the Elsava River floodplain. It shows a detailed mapping of dams (indicated by blue arrows). These maps are available for the whole research area and provide the location of all dams existent around 1840 AD (depending on the year of mapping of the individual map). Scale: 1:25000.

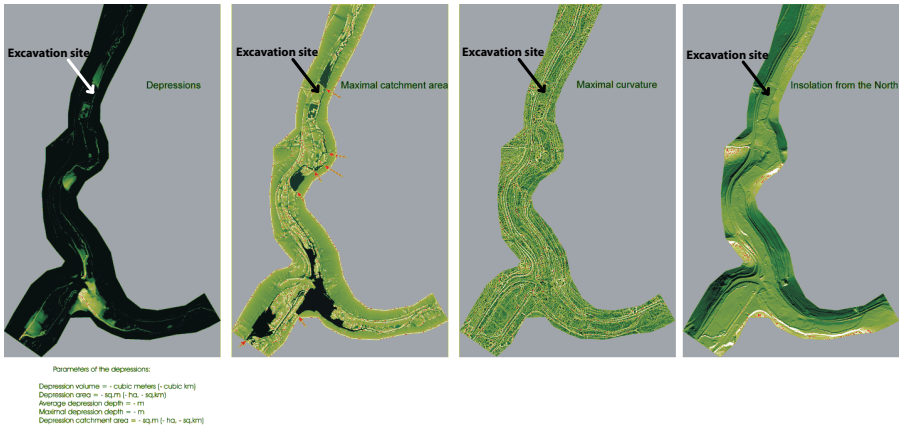

Figure 28 Geomorphometric analysis based on a DEM of the Elsava River (catchment area and curvature analysis).

wetland soil, presumably in the Late Holocene, indicating a return to higher energy fluvial conditions. The final phase is a switch to the modern meandering system, and is marked by the onset of overbank flood loams. We hypothesise that this depositional change is a direct result of backwater effects induced by valley bottom damming. The development

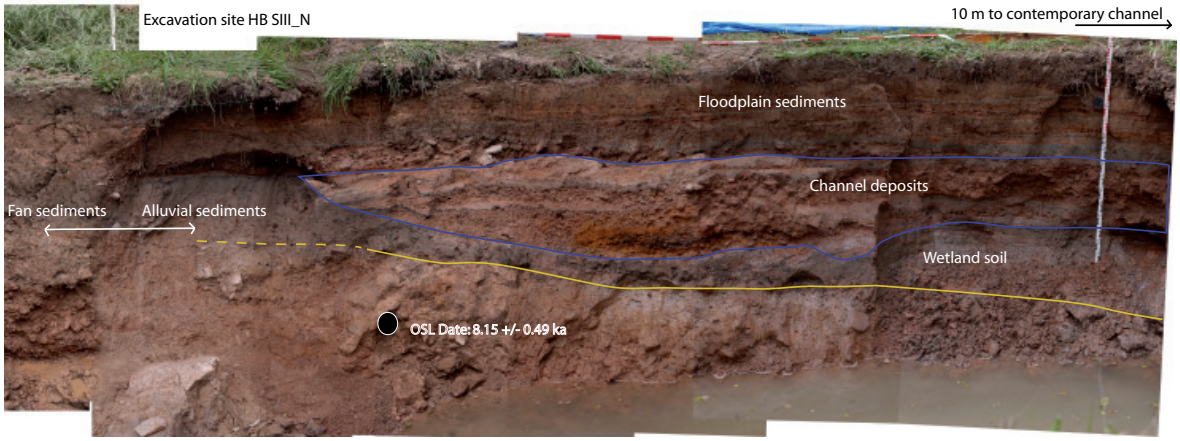

Figure 29: Excavation site HB SIII_N. The blue line indicates the channel deposits. The yellow line shows the lower border of the wetland soil. The OSL sample was taken from a sand lens in the angular gravel fan deposit that intersects with rounded gravel channel deposits. We have evidence from stratigraphic analysis that legacy sediments are common in this region and that the flow regime of the Elsava River has changed substantially. Approximatly 30 m upstream of a medieval mill site we excavated a 35 m long and 4 m deep trench in the gully fan and floodplain sediments. We chose an area where the riverbed is confined by the fan sediments on one side and a valley with steep slopes on the other side. The site has been stratigraphically logged and analysed in detail. In the alluvial sediments, enlarged in the figure above, we find a partially stripped black wetland soil unconformably overlying sandy-gravely river bed sediments. The next phase of deposition was river channel sands and gravels and associated silty overbank deposits. The hydromorphic superimposition (orange/ black colours) is due to rsing ground water levels, most probably as a result of subsequent damming. This sequence is topped by an accumulation of gravel (presumably from the gully fan), and was closely followed by a fine layered flood loam deposit that intersects with the fan sediments, and forms the focus of this study.

of a detailed chronology as a part of this study will allow this hypothesis to be tested, and the timing of landscape responses to human modification of rivers to be compared across catchments.

9.2 Scientific approach and methods

This future research will adjust established approaches for the assessment of legacy sediments, as described in detail by Walter and Merritts (2008) and Pizutto and O`Neil (2009) for North American rivers. We also aim to test our hypotheses by gathering and analysing data in the following steps: i) Collating data from all relevant historical written sources and archaeological studies, ii) geo-referencing of historical maps, iii) mapping the position and elevation of dams from governmental institutional data, aerial photographs, and LIDAR derived DEMs iv) geomorphometric utilisation of high resolution topographic data (LIDAR) to identify and quantify slackwater deposits behind in-stream dams, v) detailed field investigation of the sedimentary architecture and environmental archive preserved within the legacy sediments, vi) establish and compare detailed chronologies of the deposits using radiocarbon and luminescence dating techniques, and vii) model the hydraulic impact of dams on stream flow, and predict the potential landscape changes following their removal.

9.3 Objectives

This study will provide the basic research necessary to determine the potentially adverse effects of dam removal in specific management situations. In order to achieve this, our study has four specific aims:

1. To quantify the extent and rate of legacy sediment accumulation as a result of different damming techniques in valley bottom floodplains within the Central European mountain belt.
2. Compare the onset and extent of legacy sediments between catchments of differing stream orders in order to determine the regional propagation of the impact of damming.
3. Evaluate the potential risks arising from dam removal, such as: changes in erosive capacity of the streams, increased channel instability and its impact on the riparian zone, and increased sediment mobilisation and transport.
4. Develop a clear template for further research that can be used within other European streams that have accumulated floodplain legacy sediments, and are also likely to have in-stream dam structures removed

10. SUMMARY OF CONCLUSIONS

The research presented in this thesis broadly addresses aspects of the timing, cause, effect, and quantity of sediment fluxes in a small first order gully catchment from Central Europe. The main conclusions of this work, given as three separate chapters (chapters 6 – 9), are presented below. Possible avenues for further research are given also given sequentially.

Chapter 6 finds that the Late Quaternary surface processes of a steep gully system in Central Europe occur in multiple gully erosion and sedimentation cycles. These cycles depend largely on the relation between sediment supply and sediment transport capacity. After a phase of efficient sediment transport connectivity between the slopes, thalweg and fan during the deglacial period, the thalweg was aggraded during the Younger Dryas as a result of high sediment supply from the slopes and lower transport capacity in the thalweg, instigated by a reduction in vegetation during this time. The majority of the Holocene record (11500 – 1200 a) is then dominated by a series of gully incision events, which occur as a result of internal hydrological thresholds, and are most likely triggered by extreme climate events under well vegetated conditions. The onset of intense human agricultural activity during medieval times led to large scale slope erosion due to vegetation removal and subsequent thalweg re-aggradation. The recovery of most of the catchment vegetation within the last ~ 500 years has re-stabilised the slopes and modified the internal threshold of sediment supply/ sediment transport capacity, such that the gully has begun a new incision phase. This has implications for our understanding of sediment delivery from small headwater catchments to trunk streams, since the gully system itself has a large storage capacity and sediment delivery to the gully fan and trunk streams and their floodplains does not occur until vegetation has re-stabilised the slopes, and allows the sediment transport capacity to increase.

These broad trends in sediment fluxes over the Holocene are then quantified in chapter 7, and this reveals that erosion and deposition processes in the catchment are largely controlled by the abundance of vegetation over time. More specifically, increased slope erosion and thalweg sedimentation coincides with the removal of vegetation cover during the Younger Dryas or early medieval times. Subsequent reforestation during the early Holocene and again in early modern times stabilised the slopes leading to a dramatic reduction in the thalweg sediment supply. Adjusting to the new thresholds, in each case the gully began to erode the thalweg sediment store through headward knickpoint retreat throughout most of the Holocene, a process which reactivated again in early modern times. Therefore, it is concluded that phases of deforestation are followed by sediment input to the thalweg from the slopes, and phases of reforestation are followed by sediment output from the thalweg into

the fan and floodplain of the trunk stream. Importantly, this quantification of sediment fluxes reveals that inputs and outputs are not always in balance and that in general more sediment is delivered to the thalweg during slope erosion phases than is exported from the thalweg during phases of slope stability. In addition, we find that erosion due to human driven slope instability is ~ 2.3 time more efficient than under the most favourable natural conditions for slope instability (the Younger Dryas). The most recent and continuing phase of sediment export is also the most geomorphically significant, and is the only time in the last ~15 000 years that a large percentage of the thalweg erosion budget (79 %) is able to be incorporated into the alluvium of trunk streams.

The reconstruction of past land-use techniques is investigated in chapter 9, and is found to be possible using a combination of wood analysis from soil charcoal and the geomorphological context of the deposits in which they are contained. Furthermore, land-use techniques are found to control differences in hillslope erosion rates within the same catchment. Conventional medieval and early modern agriculture caused a lowering rate of 1.62 ± 0.17 mm/yr on one catchment slope. The reconstructed land-use of the beech – mountains, a popular medieval land-use technique, surprisingly led to the same lowering rate as the common medieval agricultural practices, presumably due to the absence of field terrace construction using this technique. A much smaller erosion rate was found for the land-use area on where field sizes were small, presumably this was cultivated as gardening-like agriculture. The lowering rate for this land-use technique is approximately one order of magnitude lower: 0.83 ± 0.09 mm/yr. This means that different land-use techniques strongly influence the resulting hillslope soil erosion rates which in turn may be highly variable, and it is therefore important to address this issue when reconstructing past soil erosion rates.

In chapter 9 an outline for future research problems is given, and is based on the findings presented in the research chapters of the thesis. This work, as well as studies other than that presented here, have proposed that accelerated slope erosion due to deforestation and agricultural land use is a possible reason for the aggradation of some Central European floodplains, however, this process only explains the delivery of sediment to these rivers. It is proposed in this chapter that valley bottom damming caused by dams of largely unknown age, (widespread within German 1st to 4th order streams), were also a critical mechanism for the effective trapping of this increased sediment load. This study proposes to determine the onset and magnitude of this first impact of humans on riverscapes as a result of valley bottom damming, and examine the possible management implications. The extensive sedimentation of loam rich floodplains was probably encouraged by dam induced changes to the flow regime,

and in turn caused the channels to change from multithread to meandering. This floodplain loam now overlies palaeo-wetland soils, which would have formed an efficient carbon sink at the time of their formation. The urgency of such information is paramount given that these dams are due to be removed according to the Water Framework Directive throughout the EU. Potentially, this may lead to large and sustained sediment pulses as legacy sediments and carbon rich wetland soils are remobilised via increased bank erosion. The quantification of sediments that may potentially be remobilised is therefore critical knowledge that can be used to support the management of rivers that will be affected by dam-removal.

11. BIBLIOGRAPHY

AG Boden, 2005. Bodenkundliche Kartieranleitung, 5. Schweizerbart`sche Verlagsbuchhandlung, Stuttgart.

Alley, R.B., Mayewski, P.A., Sowers, T., Stuiver, M., Taylor, K.C., Clark, P.U., 1997. Holocene climatic instability: A prominent, widespread event 8200 yr ago. Geology, 483-486.

Alley, R.B., Meese, D.A., Shuman, C.A., Gow, A.J., Taylor, K.C., Grootes, P.M., White, J.W.C., Ram, M., Waddington, E.D., Mayewski, P.A., Zielinski, G.A., 1993. Abrupt increase in Greenland snow accumulation at the end of the Younger Dryas event. Nature, 362.

Anselmetti, F.S., Hodell, D.A., Ariztegui, D., Brenner, M., Rosenmeier, M.F., 2007. Quantification of soil erosion rates related to ancient Maya deforestation. Geology, 35(10), 915-918.

Bachmann, K., 1982. Heimbuchenthaler Geschichtsbuch. 1282-1982., 1. Heimat-und Geschichtsverein Heimbuchenthal, Heimbuchenthal.

Becker, B., Schirmer, W., 1977. Palaeoecological study on the Holocene valley development of the River Main, southern Germany. Boreas, 6(4), 303-321.

Behre, K.-E., Brande, A., Küster, H., Rösch, M., 1996. Germany. In: B.E.B. Berglund, H.J.B.; Ralska-Jasiewiczowa, M.; Wright, H.E. (Ed.), Palaeoecological Events During the Last 15000 Years: Regional Syntheses of Palaeoecological studies of Lakes and Mires in Europe. Wiley & Sons Ltd, pp. 509 - 550.

Belyaev, V.R., 2002. Characteristics of gully formation at the different natural settings. Geomorfologia, 2, 105-110.

Belyaev, V.R., Wallbrink, P.J., Golosov, V.N., Murray, A.S., Sidorchuk, A.Y., 2004. Reconstructing the development of a gully in the Upper Kalaus basin, Stavropol region (southern Russia). Earth Surface Processes and Landforms, 29(3), 323-341.

Bork, H.-R., 1983. Soil erosion, holocene and pleistocene soil development In: H.-R. Bork, W. Ricken (Eds.), Catena : Supplement. Catena Verlag, Cremlingen.

Bork, H.-R., 1988. Bodenerosion und Umwelt : Verlauf, Ursachen und Folgen der mittelalterlichen und neuzeitlichen Bodenerosion; Bodenerosionsprozesse, Modelle und Simulationen, Landschaftsgenese und Landschaftsökologie. Selbstverl. Abteilungen f. Physische Geographie u. Landschaftsökologie u. f. Physische Geographie u. Hydrologie d. TU, Braunschweig.

Bork, H.-R., 1998. Landschaftsentwicklung in Mitteleuropa : Wirkungen des Menschen auf Landschaften. Perthes Geographiekolleg. Klett-Perthes, Gotha.

Bork, H.-R., 2006. Landschaften der Erde unter dem Einfluss des Menschen. WBG, Darmstadt.

Bork, H.-R., Lang, A., 2003. Quantification of past soil erosion and land use / land cover changes in Germany

Long Term Hillslope and Fluvial System Modelling. In: A. Lang, R. Dikau, K. Hennrich (Eds.). Lecture Notes in Earth Sciences. Springer Berlin / Heidelberg, pp. 231-239.

Brown, A.G., Carey, C., Erkens, G., Fuchs, M., Hoffmann, T., Macaire, J.-J., Moldenhauer, K.-M., Walling, D.E., 2009. From sedimentary records to sediment budgets: Multiple approaches to catchment sediment flux. Geomorphology, 108(1-2), 35-47.

Carcaillet, C., Thinon, M., 1996. Pedoanthracological contribution to the study of the evolution of the upper treeline in the Maurienne valley (North French Alps): methodology and preliminary data. Review of Palaeobotany and Palynology, 91(1-4), 399-416.

Carmichael, R.S., 1984. CRC handbook of physical properties of rocks. , Volume III. CRC Press Inc., Boca Raton FL.

Conrad, O., 2007. SAGA-Entwurf, Funktionsumfang und Anwendung eines Systems für Automatisierte Geowissenschaftliche Analysen. PhD, University of Goettingen, Goettingen.

Darwin, C., 1899. Die Bildung der Ackererde durch die Thätigkeit der Würmer mit Beobachtung über deren Lebensweise, Charles Darwin's gesammelte Werke; aus dem Englischen übersetzt von J. Victor Carus Schweizerbart, Stuttgart, pp. 184.

de Moor, J.J.W., Verstraeten, G., 2008. Alluvial and colluvial sediment storage in the Geul River catchment (The Netherlands) -- Combining field and modelling data to construct a Late Holocene sediment budget. Geomorphology, 95(3-4), 487-503.

de Vente, J., Poesen, J., Arabkhedri, M., Verstraeten, G., 2007. The sediment delivery problem revisited. Progress in Physical Geography, 31(2), 155-178.

Denzer, V., 1996. Relikte und persistente Elemente einer laendlich gepraegten Kulturlandschaft mit Vorschlaegen zur Erhaltung und methodisch-didaktischen Aufbereitung am Beispiel Waldhufensiedlungen im Suedwest-Spessart. In: M. Domroes, E. Gormsen, W. Klaer (Eds.), Mainzer Geographischen Studien. Geographisches Institut der Johannes-Gutenberg-Universität, Main, pp. 287.

Dietrich, W.E., Dunne, T., Humphrey, N.F., Reid, L.M., 1982. Construction of sediment budgets for drainage basins. In: F.J. Swanson, R.J. Janda, T. Dunne, D.N. Swanston (Eds.), Sediment Budgets and Routing in Forested Drainage Basins. Pacific Northwest Forest and Range Experiment Station, Oregon, pp. 5-23.

Dietrich, W.E., Perron, J.T., 2006. The search for a topographic signature of life. Nature, 439(7075), 411-418.

Dikau, R., 1988. Entwurf einer geomorphographisch-analytischen Systematik von Reliefeinheiten. Heidelberger Geographische Bausteine, 5. Institute of Geography, Heidelberg.

Dotterweich, M., 2005. High-resolution reconstruction of a 1300 year old gully system in northern Bavaria, Germany: a basis for modelling long-term human-induced landscape evolution. The Holocene, 15(7), 994-1005.

Dotterweich, M., 2008. The history of soil erosion and fluvial deposits in small catchments of central Europe: Deciphering the long-term interaction between humans and the environment -- A review. Geomorphology, 101(1-2), 192-208.

Dotterweich, M., Dreibrodt, S., 2011. Past land-use and soil erosion processes in Europe. Pages news, 19(2), 49-51.

Downward, S., Skinner, K., 2005. Working rivers: the geomorphological legacy of English freshwater mills. Area, 37(2), 138-147.

Dreibrodt, S., 2005. Detecting heavy precipitation events during the Holocene from soils, gully fills, colluvia and lake sediments examples from the Belauer See catchment (northern Germany). Zeitschrift der Deutschen Gesellschaft für Geowissenschaften, 156, 573-588.

Dreibrodt, S., Lubos, C., Terhorst, B., Damm, B., Bork, H.R., 2010. Historical soil erosion by water in Germany: Scales and archives, chronology, research perspectives. Quaternary International, 222(1-2), 80-95.

Dreibrodt, S., Nelle, O., Lütjens, I., Mitusov, A., Clausen, I., Bork, H.-R., 2009. Investigations on buried soils and colluvial layers around Bronze Age burial mounds at Bornhöved (northern Germany): an approach to test the hypothesis of `landscape openness‘ by the incidence of colluviation. The Holocene, 19(3), 487-497.

Enters, D., Dörfler, W., Zolitschka, B., 2008. Historical soil erosion and land-use change during the last two millennia recorded in lake sediments of Frickenhauser See, northern Bavaria, central Germany. The Holocene, 18(2), 243-254.

Fairbridge, R.W., 1968. The Encyclopedia of Geomorphology. In: R.W. Fairbridge (Ed.), The encyclopedia of geomorphology. Reinhold Book Corp, New York, pp. 1295.

Faulkner, H., 1985. Gully evolution in response to both snowmelt and flash flood erosion, Wn Colarado. In: V. Gardiner (Ed.), International Geomorphology. John Wiley, Manchester.

Foley, J.A., Ramankutty, N., Brauman, K.A., Cassidy, E.S., Gerber, J.S., Johnston, M., Mueller, N.D., O/‘Connell, C., Ray, D.K., West, P.C., Balzer, C., Bennett, E.M., Carpenter, S.R., Hill, J., Monfreda, C., Polasky, S., Rockstrom, J., Sheehan, J., Siebert, S., Tilman, D., Zaks, D.P.M., 2011. Solutions for a cultivated planet. Nature, 478(7369), 337-342.

Forde-Johnston, J., 1974. History from the Earth. Phaidon Press Limited, London.

Fuchs, M., Will, M., Kunert, E., Kreutzer, S., Fischer, M., Reverman, R., 2011. The temporal and spatial quantification of Holocene sediment dynamics in a meso-scale catchment in northern Bavaria, Germany. The Holocene.

Galbraith, R.F., Roberts, R.G., Laslett, G.M., Yoshida, H., Olley, J.M., 1999. Optical dating of single and multiple grains of quartz from Jinmium Rock Shelter, Northern Australia: Part I, experimental design and statistical models. Archaeometry, 41(2), 339-364.

Gale, S.J., Haworth, R.J., 2005. Catchment-wide soil loss from pre-agricultural times to the present: transport- and supply-limitation of erosion. Geomorphology, 68(3-4), 314-333.

Gavin, D.G., 2001. Estimation of inbuilt age in radiocarbon ages of soil charcoal for fire history studies. Radiocarbon, 43(1), 27-44.

Gavin, D.G., Brubaker, L.B., Lertzman, K.P., 2003. An 1800-year record of the spatial and temporal distribution of fire from the west coast of Vancouver Island, Canada. Canadian Journal of Forest Research, 33(4), 573-586.

Gräf, D., 2006. Boat mills in Europe from early medieval to modern times, 51. Veröffentlichungen des Landesamtes für Archäologie mit Landesmuseum für Vorgeschichte, Dresden.

Graf, W.L., 2006. Downstream hydrologic and geomorphic effects of large dams on American rivers. Geomorphology, 79(3-4), 336-360.

Hahn, M., 2001. Wässerwiesen im Spessart. Traditionelle Kulturlandschaftselemente und ihre traditionelle Bedeutung. Diplom/Masters, Universität Würzburg, Würzburg, 140 pp.

Hoffmann, T., Lang, A., Dikau, R., 2008. Holocene river activity: analysing 14C-dated fluvial and colluvial sediments from Germany. Quaternary Science Reviews, 27(21-22), 2031-2040.

Houben, P., 2008. Scale linkage and contingency effects of field-scale and hillslope-scale controls of long-term soil erosion: Anthropogeomorphic sediment flux in agricultural loess watersheds of Southern Germany. Geomorphology, 101(1-2), 172-191.

Houben, P., Hoffmann, T., Zimmermann, A., Dikau, R., 2006. Land use and climatic impacts on the Rhine system (RheinLUCIFS): Quantifying sediment fluxes and human impact with available data. CATENA, 66(1-2), 42-52.

Hughes, M.W., Almond, P.C., Roering, J.J., 2009. Increased sediment transport via bioturbation at the last glacial-interglacial transition. Geology, 37(10), 919-922.

Kadereit, A., Kühn, P., Wagner, G.A., 2010. Holocene relief and soil changes in loess-covered areas of south-western Germany: The pedosedimentary archives of Bretten-Bauerbach (Kraichgau). Quaternary International, 222(1-2), 96-119.

Keller, G., 1856. Romeo und Julia auf dem Dorfe, Die Leute von Seldwyla. Vieweg Verlag, Braunschweig.

Klápště, J., 2005. Water management in medieval rural economy : les usages de l'eau en milieu rural au Moyen Âge. In: J. Klápště (Ed.), Ruralia Inst. of Archaeology, Acad. of Sciences of the Czech Republic, Lyon, Villard-Sallet, pp. 269.

Klimek, K., Latocha, A., 2007. Response of small mid-mountain rivers to human impact with particular reference to the last 200 years; Eastern Sudetes, Central Europe. Geomorphology, 92(3-4), 147-165.

Lagies, M., 2004. Palynologische Untersuchungen zur Vegetations- und Siedlungsgeschichte von Spessart und Odenwald während des jüngeren Holozäns. PhD, TU Berlin, Berlin, 137 pp.

Lagies, M., 2005. Palynologische Untersuchungen zur Vegetations- und Siedlungsgeschichte von Spessart und Odenwald während des jüngeren Holozäns. Materialhefte zur Archäologie in Baden-Württemberg, 73, 163-271.

Lagies, M., 2006. Neue pollenanalytische Forschungen in Spessart und Odenwald - eine Zusammenfassung. Carolinea, 63, 113-134.

Lang, A., 2003. Phases of soil erosion-derived colluviation in the loess hills of South Germany. Catena, 51(3-4), 209-221.

Lang, A., Bork, H.-R., Mäckel, R., Preston, N., Wunderlich, J., Dikau, R., 2003. Changes in sediment flux and storage within a fluvial system: some examples from the Rhine catchment. Hydrological Processes, 17(16), 3321-3334.

Lang, A., Hönscheidt, S., 1999. Age and source of colluvial sediments at Vaihingen-Enz, Germany. Catena, 38(2), 89-107.

Leng, R., in prep. Das Frammersbacher Sechserbuch. Rechtswesen und Schriftlichkeit einer frühneuzeitlichen Spessartgemeinde. Mit einer Edition des Sechserbuches.

Leopold, L.B., Langbein, W.B., 1964. Quasi-equilibrium states in channel morphology. American Journal of Science, 262, 782-794.

Leopold, L.B., Wolman, M.G., Miller, J.P., 1964. Fluvial Processes in Geomorphology. W.H. Freeman and Co., San Francisco.

Ludemann, T., 2010. Past fuel wood exploitation and natural forest vegetation in the Black Forest, the Vosges and neighbouring regions in western Central Europe. Palaeogeography, Palaeoclimatology, Palaeoecology, 291(1-2), 154-165.

Luettig, G., 1960. Zur Gliederung des Auelehms im Flußgebiet der Weser. Eiszeitalter und Gegenwart, 11, 39-50.

Macklin, M.G., Benito, G., Gregory, K.J., Johnstone, E., Lewin, J., Michczynska, D.J., Soja, R., Starkel, L., Thorndycraft, V.R., 2006. Past hydrological events reflected in the Holocene fluvial record of Europe. Catena, 66(1-2), 145-154.

Macklin, M.G., Lewin, J., 2008. Alluvial responses to the changing Earth system. Earth Surface Processes and Landforms, 33(9), 1374-1395.

Mager, J., Meißner, G., Orf, W., 1989. Die Kulturgeschichte der Mühlen. Wasmuth, Tübingen.

Magny, M., 2004. Holocene climate variability as reflected by mid-European lake-level fluctuations and its probable impact on prehistoric human settlements. Quaternary International, 113(1), 65-79.

Montgomery, D.R., 2007. Soil erosion and agricultural sustainability. Proceedings of the National Academy of Sciences, 104(33), 13268-13272.

Montgomery, D.R., 2008. Dreams of Natural Streams. Science, 319(5861), 291-292.

Moore, I.D., Gessler, P.E., Nielsen, G.A., Peterson, G.A., 1993. Soil attribute prediction using terrain analysis. Soil Science Society of America Journal 57, 443-449.

Mück, W., 2010. Müller und Mühlen im Aischgrund und seinen Nachbartälern : vom Werden und Vergehen einer fast verschwundenen Welt. Darstellungen aus der fränkischen Geschichte, 9. Wiss. Kommissionsverlag, Würzburg.

Mueller, S., 2011. New insights about Pleistocene periglacial slope deposits and pedogenesis in the Hessian Spessart Mountains. PhD-thesis, Goethe University, Frankfurt, 230 pp.

Murray, A.S., Wintle, A.G., 2000. Luminescence dating of quartz using an improved single-aliquot regenerative-dose protocol. Radiation Measurements, 32(1), 57-73.

Nadeau, M.-J., Grootes, P.M., Schleicher, M., Hasselberg, P., Rieck, A., Bitterling, M., 1998. Sample throughput and data stability at the Leibniz–Labor AMS facility. Radiocarbon, 239(40).

Nadeau, M.-J., Schleicher, M., Grootes, P.M., Erlenkeuser, H., Gottdang, A., Mous, D.J.W., Sarnthein, J.M., Willkomm, H., 1997. The Leibniz–Labor AMS facility at the Christian–Albrechts–University, Kiel, Germany. Nuclear Instruments and Methods in Physics Research Section B, 123(22).

Nelle, O., 2003. Woodland history of the last 500 years revealed by anthracological studies of charcoal kiln sites in the Bavarian Forest, Germany. Phytocoenologia, 33(4), 667-682.

Niller, N.-P., 1998. Praehistorische Landschaften im Loessgebiet bei Regensburg - Kolluvien, Auenlehme und Boeden als Archive der Palaeoumwelt. . PhD, University of Regensburg, Regensburg, 429 pp.

Notebaert, B., Verstraeten, G., 2010. Sensitivity of West and Central European river systems to environmental changes during the Holocene: A review. Earth-Science Reviews, 103(3-4), 163-182.

Oberdorfer, E., Reich, A., 1990. Die Birkenberge im Bayrischen Wald. Der Bayerische Wald, 23(1), 12 - 19.

Panin, A.V., Fuzeina, J.N., Belyaev, V.R., 2009. Long-term development of Holocene and Pleistocene gullies in the Protva River basin, Central Russia. Geomorphology, 108(1-2), 71-91.

Pimentel, D., Harvey, C., Resosudarmo, P., Sinclair, K., Kurz, D., McNair, M., Crist, S., Shpritz, L., Fitton, L., Saffouri, R., Blair, R., 1995. Environmental and Economic Costs of Soil Erosion and Conservation Benefits. Science, 267(5201), 1117-1123.

Pizzuto, J., O'Neal, M., 2009. Increased mid-twentieth century riverbank erosion rates related to the demise of mill dams, South River, Virginia. Geology, 37(1), 19-22.

Poesen, J., Nachtergaele, J., Verstraeten, G., Valentin, C., 2003. Gully erosion and environmental change: importance and research needs. Catena, 50(2-4), 91-133.

Prescott, J.R., Hutton, J.T., 1988. Cosmic ray and gamma ray dosimetry for TL and ESR. International Journal of Radiation Applications and Instrumentation. Part D. Nuclear Tracks and Radiation Measurements, 14(1-2), 223-227.

Reid, L.M., Dunne, T., 2003. Sediment budgets as an organizing framework in fluvial geomorphology. In: G.M. Gondolf, H. Piègay (Eds.), Tools in Fluvial Geomorphology. John Wiley & Sons Ltd, Chichester.

Reimer, P.J.B., Mike G. L.; Bard, Edouard; Bayliss, Alex; Beck, J. Warren; Bertrand, Chanda J. H.; Blackwell, Paul G.; Buck, Caitlin E.; Burr, George S.; Cutler, Kirsten B.; Damon, Paul E.; Edwards, R. Lawrence; Fairbanks, Richard G.; Friedrich, Michael; Guilderson, Thomas P.; Hogg, Alan G.; Hughen, Konrad A.; Kromer,

Bernd; McCormac, Gerry; Manning, Sturt; Ramsey, C. Bronk; Reimer, Ron W.; Remmele, Sabine; Southon, John R.; Stuiver, Minze; Talamo, Sahra; Taylor, F. W.; van der Plicht, Johannes; Weyhenmeyer, Constanze E., 2004. IntCal04 terrestrial radiocarbon age calibration, 0-26 cal kyr BP. Radicarbon, 46, 1029-1058.

Ribeiro, P.J., Diggle, P., J., 2001. GeoR: A package for Geostatistical Analysis. R. news, 1, 15-18.

Roering, J.J., Almond, P., Tonkin, P., McKean, J., 2002. Soil transport driven by biological processes over millennial time scales. Geology, 30(12), 1115-1118.

Rommens, T., Verstraeten, G., Bogman, P., Peeters, I., Poesen, J., Govers, G., Van Rompaey, A., Lang, A., 2006. Holocene alluvial sediment storage in a small river catchment in the loess area of central Belgium. Geomorphology, 77(1-2), 187-201.

Schenk, E.R., Hupp, C.R., 2009. Legacy Effects of Colonial Millponds on Floodplain Sedimentation, Bank Erosion, and Channel Morphology, Mid-Atlantic, USA1. JAWRA Journal of the American Water Resources Association, 45(3), 597-606.

Schirmer, W., 1991. Breaks in the Late Quaternary river development of Middle Europe. Wetlands in Flanders, 6, 115 - 120.

Schirmer, W., 1995a. Valley bottoms in the late Quaternary. Zeitschrift für Geomorphologie Supplement, 100, 27-51.

Schirmer, W., 1995b. Valley bottoms in the late Quaternary. Zeitschrift für Geomorphologie N.F.(Suppl.-Bd. 100), 27–51.

Schirmer, W., 1997. Der Naturraum Main–Regnitz im ersten Jahrtausend n. Chr. Schriftenreihe des historischen Vereins Bamberg, 41, 46–60.

Schirmer, W., 2007. Der Naturraum Main-Regnitz im ersten Jahrtausend n. Chr. In: R. Bergemann, G. Dippold, J. Haberstroh (Eds.), Missionierung und Christianisierung im Regnitz- und Obermaingebiet.

Schlueter, O., 1952. Die Siedlungsräume Mitteleuropas in frühgeschichtlicher Zeit : 1:1 500 000. Zentralausschuß für deutsche Landeskunde und dem Amt für Landeskunde. Verlag des Amtes fuer Landeskunde, Hamburg.

Schmitt, A., Rodzik, J., Zglobicki, W., Russok, C., Dotterweich, M., Bork, H.-R., 2006. Time and scale of gully erosion in the Jedliczny Dol gully system, south-east Poland. CATENA, 68(2-3), 124-132.

Schunder, F., 1995. Die Rexroth-Geschichte, Mannesmann Verlag, Lohr.

Schweingruber, F.H., 1990. Anatomie europäischer Hölzer. Ein Atlas zur Bestimmung europäischer Baum-, Strauch- und Zwergstrauchhölzer. Verlag Paul Haupt, Bern.

Semmel, A., 1976. Die Beziehung zwischen Relief, Gestein und Böden in hessischen Buntsandsteinlandschaften. Zeitschrift für Geomorphologie N.F., Supplement-Band 24, 23-32.

Semmel, A., 2002. Die periglaziale Hauptlage – Genese, Alter und anthropogene Veränderungen. Terra Nostra, 2002/6, 342-348.

Smolska, E., 2007. Development of gullies and sediment fans in last-glacial areas on the example of the Suwalki Lakeland (NE Poland). Catena, 71(1), 122-131.

Stankoviansky, M., 2003. Historical evolution of permanent gullies in the Myjava Hill Land, Slovakia. CATENA, 51(3-4), 223-239.

Starkel, L., 2002. Change in the frequency of extreme events as the indicator of climatic change in the Holocene (in fluvial systems). Quaternary International, 91(1), 25-32.

Steenhuis, T., Ferreira, C.S., Tilahhun, S.A., Tarekegn, B.C., Elkamil, M., Easton, Z.M., Ferreira, A.D., 2011. Environmental tipping points in landscape interventions, EGU General Assembly. Geophysical Research Abstracts, Vienna.

Stolz, C., 2011. Budgeting soil erosion from floodplain sediments of the central Rhenish Slate Mountains (Westerwald), Germany. The Holocene, 21(3), 499-510.

Stuiver, M., Grootes, P.M., Braziunas, T.F., 1995. The GISP2 δ18O Climate Record of the Past 16,500 Years and the Role of the Sun, Ocean, and Volcanoes. Quaternary Research, 44(3), 341-354.

Stuiver, M., Polach, H.A., 1977. Discussion - Reporting of ^{14}C Data. Radicarbon, 19(3), 355 - 363.

Switalski, M., 2005. Landmüller und Industrialisierung : Sozialgeschichte fränkischer Mühlen im 19. Jahrhundert. PhD-thesis, Augsburg University, Augsburg, 278 pp.

Szmanda, J.B., Oczkowski, H.L., Przegietka, K.R., 2004. Age of the Vistula river overbank deposit in Torun. Geochronometria, 23, 35-38.

Temmerman, S., Bouma, T.J., Van de Koppel, J., Van der Wal, D., De Vries, M.B., Herman, P.M.J., 2007. Vegetation causes channel erosion in a tidal landscape. Geology, 35(7), 631-634.

Touflan, P., Talon, B., Walsh, K., 2010. Soil charcoal analysis: a reliable tool for spatially precise studies of past forest dynamics: a case study in the French southern Alps. The Holocene, 20(1), 45-52.

Trimble, S.W., 2008. Man-Induced Soil Erosion on the Southern Piedmont: 1700-1970, 2nd ed. Soil and Water Conservation Society, Ankeny, IA.

Trimble, S.W., 2009. Fluvial processes, morphology and sediment budgets in the Coon Creek Basin, WI, USA, 1975-1993. Geomorphology, 108(1-2), 8-23.

Trimble, S.W., Crosson, P., 2000. U.S. Soil Erosion Rates--Myth and Reality. Science, 289(5477), 248-250.

Valentin, C., Poesen, J., Li, Y., 2005. Gully erosion: Impacts, factors and control. CATENA, 63(2-3), 132-153.

Vanwalleghem, T., Bork, H.R., Poesen, J., Schmidtchen, G., Dotterweich, M., Nachtergaele, J., Bork, H., Deckers, J., Brüsch, B., Bungeneers, J., De Bie, M., 2005a. Rapid development and infilling of a buried gully under cropland, central Belgium. Catena, 63(2-3), 221-243.

Vanwalleghem, T., Poesen, J., Van Den Eeckhaut, M., Nachtergaele, J., Deckers, J., 2005b. Reconstructing rainfall and land-use conditions leading to the development of old gullies. The Holocene, 15(3), 378-386.

Vanwalleghem, T., Van Den Eeckhaut, M., Poesen, J., Deckers, J., Nachtergaele, J., Van Oost, K., Slenters, C., 2003. Characteristics and controlling factors of old gullies under forest in a temperate humid climate: a case study from the Meerdaal Forest (Central Belgium). Geomorphology, 56(1-2), 15-29.

Verachtert, E., Van Den Eeckhaut, M., Poesen, J., Deckers, J., 2010. Factors controlling the spatial distribution of soil piping erosion on loess-derived soils: A case study from central Belgium. Geomorphology, 118(3-4), 339-348.

Virchow, R., 1852. Die Noth im Spessart. Aus den Verhandlungen der physikalisch-medizinischen Gesellschaft in Würzburg, 3. Stahl`sche Buchhandlung, Würzburg.

Walentowski, H., 2001. Die Rolle der Birken in einheimischen Pflanzengesellschaften. In: Biodiversity (Ed.). Bayerische Landesanstalt für Wald- und Forstwirtschaft, München.

Walter, R.C., Merritts, D.J., 2008. Natural Streams and the Legacy of Water-Powered Mills. Science, 319(5861), 299-304.

Wildhagen, H., Meyer, B., 1972. Holozaene Bodenentwicklung, Sedimentbildung und Geomorphogenese im Flußauen-Bereich des Goettinger Leintal-Grabens. Goettinger Bodenkundliche Berichte, 21, 1-158.

Williams, M., 2000. Dark ages and dark areas: global deforestation in the deep past. Journal of Historical Geography, 26(1), 28-46.

Wintle, A.G., Murray, A.S., 2006. A review of quartz optically stimulated luminescence characteristics and their relevance in single-aliquot regeneration dating protocols. Radiation Measurements, 41(4), 369-391.

Zolitschka, B., 1998. A 14,000 year sediment yield record from western Germany based on annually laminated lake sediments. Geomorphology, 22(1), 1-17.

Zygmunt, E., 2009. Alluvial fans as an effect of long-term man-landscape interactions and moist climatic conditions: A case study from the Glubczyce Plateau, SW Poland. Geomorphology, 108(1-2), 58-70.

Table 1: OSL dating results

Sample	Lab code; selected/ measured aliquots	Depth [m]	Dose rate [Gy/ka]	Paleodose [Gy]				Rel. SD [%]	Over-dispersion [%]	OSL age [ka]	OSL age [a AD/BC]
				Mean ± SD	Median	CAM	MAM				
K1 OSL5	BT 564 (29/36)	1.45	3.13 ± 0.15	2.16 ± 0.29	2.10	2.14 ± 0.05	2.05 ± 0.09	13.4	**12.3**	0.65 ± 0.04	1360 ± 40 AD
K1 OSL4	BT 565 (29/36)	1.75	3.07 ± 0.15	2.34 ± 0.52	2.18	2.29 ± 0.08	2.10 ± 0.06	22.3	19.0	0.68 ± 0.04	1330 ± 40 AD
K1 OSL3	BT 566 (23/36)	2.05	3.12 ± 0.16	5.46 ± 2.25	4.99	5.1 ± 0.38	3.41 ± 0.29	41.3	35.3	1.09 ± 0.11	920 ± 110 AD
K1 OSL2	BT 567 (28/36)	2.55	2.54 ± 0.13	16.25 ± 6.37	14.54	15.19 ± 1.06	9.42 ± 0.76	39.2	36.4	3.71 ± 0.35	1700 ± 350 BC
K1 OSL1	BT 568 (32/36)	3.00	2.31 ± 0.11	42.17 ± 9.79	40.66	41.19 ± 1.59	31.89 ± 1.92	23.2	21.4	13.81 ± 1.06	
SIII_N OSL 1	BT 643 (18/24)	2.55	3.04 ± 0.16	61.17 ± 20.13	53.76	57.96 ± 4.22	44.53 ± 3.2	32.9	30.0	14.65 ± 1.3	
SIII_N OSL 2	BT 644 (8/24)	2.10	1.96 ± 0.10	141.72 ± 32.50	142.33	133.07 ± 10.22	113.12 ± 13.33	22.9	18.4	57.71 ± 7.41	
SIII_N OSL 3	BT 645 (10/24)	1.65	3.11 ± 0.16	31.51 ± 6.35	33.25	30.86 ± 1.78	26.21 ± 3.06	20.2	17.0	8.43 ± 1.08	
SIII_N OSL 4	BT 646 (14/24)	0.85	2.93 ± 0.15	8.56 ± 4.18	7.78	7.64 ± 1.0	3.32 ± 0.41	48.9	48.8	1.13 ± 0.15	880 ± 150 AD
SI_N OSL 1	BT 725 (20/24)	2.00	2.88 ± 0.14	38.33 ± 8.64	35.12	37.5 ± 1.69	33.68 ± 1.95	22.5	20.0	11.69 ± 0.88	
SI_N OSL 2	BT 726 (22/24)	1.30	3.45 ± 0.17	31.85 ± 4.54	30.35	31.55 ± 0.88	29.94 ± 1.4	14.3	**12.9**	8.68 ± 0.59	
SI_N OSL 3	BT 727 (24/25)	0.90	3.40 ± 0.17	8.23 ± 1.51	8.48	8.08 ± 0.32	6.31 ± 0.41	18.3	19.1	1.86 ± 0.15	160 ± 150 AD
HBKHN3-OSL1	HUB-0025 (12/12)	1.44	3.09 ± 0.17	92.55 ± 4.49	93.46	92.57 ± 1.27		4.9	1.6	29.97 ± 1.65	
HBKHN3-OSL2	HUB-0026 (12/12)	1.12	3.05 ± 0.17	91.03 ± 6.01	90.56	90.42 ± 1.58		6.6	3.8	29.65 ± 1.68	
HBKHN3-OSL3	HUB-0027 (24/27)	0.80	2.54 ± 0.13	3.13 ± 0.67	2.87	3.07 ± 0.11	2.81 ± 0.07	21.3	17.9	1.11 ± 0.06	900 ± 60 AD

HBKHN5-OSL1	HUB-0028 (24/24)	1.02	2.85 ± 0.15	32.8 ± 4.11	31.37	32.53 ± 0.79		12.5	11.3	11.43 ± 0.67	
HBKHN5-OSL2	HUB-0029 (23/24)	0.94	2.73 ± 0.15	14.65 ± 4.88	14.3	13.91 ± 0.93	8.89 ± 0.57	33.3	31.9	3.25 ± 0.27	1240 ± 270 BC
HBKHN5-OSL3	HUB-0030 (20/24)	1.34	2.88 ± 0.15	4.15 ± 1.0	4.2	4.04 ± 0.21	2.91 ± 0.19	24.1	23.2	1.01 ± 0.08	1000 ± 80 AD
HBKHN5-OSL4	HUB-0031 (15/24)	0.36	3.10 ± 0.16	1.01 ± 0.05	1.0	1.01 ± 0.01		5.4	1.3	0.33 ± 0.02	1680 ± 20 AD
HBK6-OSL1	HUB-0070 (39/42)	1.50	3.02 ± 0.15	51.78 ± 20.49	51.88	41.17 ± 3.53	13.56 ± 1.31	39.6	46.3	4.49 ± 0.49	2480 ± 490 BC
HBK6-OSL2	HUB-0071 (12/24)	1.20	2.88 ± 0.15	3.1 ± 0.83	3.0	2.98 ± 0.19	2.39 ± 0.22	26.9	20.8	0.82 ± 09	1190 ± 90 AD
HBK6HN6-OSL2	HUB-0072 (27/48)	0.90	3.19 ± 0.17	60.07 ± 20.31	60.41	55.7 ± 3.97	28.88 ± 2.22	34.6	35.7	9.06 ± 0.84	
HBK8-OSL3	HUB-0073 (18/30)	2.70	2.61 ± 0.14	10.83 ± 5.85	7.59	9.56 ± 1.08	4.93 ± 0.52	54.0	47.4	1.89 ± 0.22	120 ± 220 AD
HBK8-OSL4	HUB-0074 (10/24)	1.60	2.86 ± 0.14	5.81 ± 2.39	5.61	5.4 ± 0.67	3.37 ± 0.42	41.1	38.7	1.18 ± 0.16	830 ± 160 AD
HBK8-OSL6	HUB-0075 (24/30)	1.70	2.81 ± 0.14	1.35 ± 0.19	1.33	1.34 ± 0.04		14.1	13.1	0.48 ± 0.03	1530 ± 30 AD
HBK8-OSL8	HUB-0076 (13/24)	0.90	2.81 ± 0.14	1.33 ± 0.26	1.21	1.31 ± 0.07	1.17 ± 0.07	19.7	16.8	0.42 ± 0.03	1590 ± 30 AD
HBK8-OSL10	HUB-0077 (14/24)	0.60	3.08 ± 0.16	2.17 ± 0.68	2.04	2.05 ± 0.16	1.39 ± 0.14	31.4	26.8	0.45 ± 0.05	1560 ± 50 AD
HBHS-OSL1	HUB-0101 (22/30)	0.90	2.88 ± 0.15	5.24 ± 3.62	3.93	4.34 ± 0.56	1.72 ± 0.18	69.1	59.8	0.60 ± 0.07	1410 ± 70 AD
HBHS-OSL2	HUB-0102 (34/40)	0.80	3.09 ± 0.16	22.63 ± 8.31	22.69	20.8 ± 1.61	4.53 ± 0.44	36.7	45.0	1.47 ± 0.16	540 ± 160 AD
HBHS-OSL3	HUB-0103 (13/30)	0.40	2.96 ± 0.15	3.98 ± 1.13	3.62	3.85 ± 0.27	3.21 ± 0.26	28.5	24.8	1.08 ± 0.1	930 ± 100 AD
HBHS-OSL4	HUB-0104 (27/40)	0.40	3.24 ± 0.16	80.36 ± 9.35	70.41	79.77 ± 1.63		11.6	9.9	24.6 ± 1.32	
HBHN10-OSL1	HUB-0128 (20/30)	0.20	3.14 ± 0.16	2.21 ± 0.3	2.24	2.2 ± 0.07		13.4	11.9	0.7 ± 0.04	1310 ± 40 AD
HBHN10-OSL2	HUB-0129 (29/40)	0.80	3.10 ± 0.16	10.25 ± 5.46	9.28	9.02 ± 0.85	3.32 ± 0.31	53.3	50.6	1.07 ± 0.11	940 ± 110 AD

HBCBS10-OSL	HUB-0130 (25/40)	0.50	2.66 ± 0.14	3.95 ± 1.65	3.53	3.63 ± 0.3	1.44 ± 0.15	41.7	41.4	0.54 ± 0.06	1470 ± 60 AD
HBHW1-OSL1	HUB-0145 (18/24)	0.25	2.64 ± 0.12	1.35 ± 0.2	1.38	1.34 ± 0.05		14.5	13.6	0.51 ± 0.03	1500 ± 30 AD
HBHW1-OSL2	HUB-0146 (21/24)	1.03	2.48 ± 0.11	2.61 ± 0.32	2.61	2.59 ± 0.07		12.18	11.6	1.05 ± 0.06	960 ± 60 AD
HBSIII-OSLN1	HUB-0147 (17/24)	0.35	2.83 ± 0.14	2.92 ± 1.48	2.5	2.59 ± 0.31	0.99 ± 0.12	50.6	49.5	0.35 ± 0.05	1660 ± 50 AD
HBSIII-OSLN2	HUB-0148 (12/24)	0.70	2.77 ± 0.14	34.35 ± 17.96	31.84	29.83 ± 4.63	12.12 ± 1.6	52.3	53.3	4.38 ± 0.62	2370 ± 620 BC
HBSIII-OSLN3	HUB-0149 (20/24)	1.20	3.16 ± 0.16	34.02 ± 8.92	31.57	32.87 ± 1.67	27.45 ± 1.98	26.22	21.6	8.68 ± 0.76	
HBSIII-OSLN4	HUB-0150 (15/24)	1.35	3.10 ± 0.16	32.22 ± 7.57	29.68	31.46 ± 1.74	24.75 ± 2.1	23.5	20.3	7.97 ± 0.79	

red= very broad De distributions without any clear peaks at low paleodoses (not used for analysis)
green=De distribution with a peak

Table 2: Radiocarbon dates

Sample	lab code	δ13C (‰)	δ14C age (years BP +/- 1σ)	calibrated age (calBP 2σ-error bounds)	error [years]	calibrated age (calAD/B
HB K2 HK 21	KIA42950	-28.66 +/- 0.31	1390 +/- 35	1351 (1311) 1271	40	679 - 599 AD
HB SII HK 11	KIA42951	-25.95 +/- 0.20	6330 +/- 35	7326 (7246) 7167	80	5376 - 5217 BC
HB SII HK 1000	KIA37840	-25.31 +/- 0.22	9315 +/- 45	10661 (10481) 10302	180	8711 - 8352 BC
HB K1 Pr.13	KIA38522	-27.04 +/- 0.29	865 +/- 30	902 (800) 698	102	1048 - 1252 AD
HB K1 Pr.16	KIA38523	-24.48 +/- 0.25	1010 +/- 30	974 (887) 800	87	976 - 1150 AD
HB K1 Pr.18	KIA38524	-26.24 +/- 0.24	950 +/- 30	926 (860) 795	66	1024 - 1155 AD
HB SI/N Feuerstelle	KIA38525	-24.52 +/- 0.14	2440 +/- 25	2701 (2529) 2358	172	751 - 408 BC
HB HN 5 HK 3a	KIA43249	-22.62 +/- 0.19	1140 +/-25	1168 (1070) 972	98	782 - 978 AD
HB HN 5 HK (1m Tiefe)	KIA41464	-26.40 +/- 0.19	925 +/- 25	921 (851) 781	70	1029 - 1169 AD
HB HS 1 Meiler 1	KIA41463	-25.89 +/- 0.21	150 +/- 30	287 (143) 0	144	1667 - 1954 AD
HB K Knickpoint	KIA43689	-26,16 ± 0,17	985 ± 30	952 (874) 797	78	998 - 1153 AD